

PATRICIA BORIM

**EXPLORING METHODS TO SYNTHESIZE POLYMERS
WITH COMPLEX ARCHITECTURE BY RADICAL
POLYMERIZATION VIA A COMBINATION OF “CATALYST
FREE” RAFT AND ATRP**

Doctoral thesis presented to Institute of Chemistry of São Carlos of University of São Paulo as part of the requirements to obtain the title of Doctor in Sciences.

Concentration Area: Analytical and Inorganic Chemistry.

Advisor: Professor Dra. Carla Cristina Schmitt Cavalheiro.

Exemplar revisado

O exemplar original encontra-se em
acervo reservado na Biblioteca do IQSC-USP

São Carlos – SP
2021

Autorizo a reprodução e divulgação total ou parcial deste trabalho, por qualquer meio convencional ou eletrônico para fins de estudo e pesquisa, desde que citada a fonte.

Assinatura:

Data:

Ficha Catalográfica elaborada pela Seção de Referência e Atendimento ao Usuário do SBI/IQSC

Borim, Patricia

Exploring methods to synthesize polymers with complex architecture by radical polymerization via a combination of "catalyst free" RAFT and ATRP / Patricia Borim. — São Carlos, 2021.

104 f.

Tese (Doutorado em Química Analítica e Inorgânica) — Instituto de Química de São Carlos / Universidade de São Paulo, 2021.

Orientadora: Profa. Dra. Carla Cristina Schmitt Cavalheiro

1. RDRP. 2. ATRP. 3. RAFT. 4. Networks. 5. STEM gels. I. Título.

Wilneide do C. Marchi Maiorano - CRB: 3978/8



“Don’t ever let somebody tell you, you can’t do something. You got a dream, you gotta protect it, people can’t do something themselves, they wanna tell you, you can’t do it.

If you want something, go get it.

Forever trust who YOU are and nothing else matters”.

Acknowledgments

First and foremost, to my advisor from Institute of Chemistry of São Carlos – Sao Paulo University (IQSC – USP), Professor Carla Cristina Schmitt Cavalheiro for allowing me the opportunity to conduct research in her laboratory.

I would like to express my gratitude to Prof. Krzysztof (Kris) Matyjaszewski from Carnegie Mellon University (CMU) for allowing me the opportunity to work for six months in his laboratory, for sharing his knowledge, and for helping me think about how to improve my chemistry skills. Many thanks for this great opportunity. It was the best opportunity I have had in the last 4 years of my doctorate.

I am also very grateful to Dr. Jim Spanswick from CMU for his invaluable support throughout my six months at Carnegie Mellon, for the wise advice, and for encouraging me to follow my dreams and for being available to correct my monthly reports during my time in Pittsburgh and for contributing to the correction of my thesis.

A thank you to all the Maty Polymer Lab and especially to Michael Martinez and Julia Cuthbert for the great teamwork. Thank you very much for the discussions on polymer chemistry and for teaching me how to conduct different experiments. Also, I am grateful to Brenda Chambers for helping me with my arrival at CMU. A special thank you also goes to all my friends from “Maty Land”: Sylwia, Francesca, Marco, Mike, Adam, Julianna, Greg, Julian and Sajjad.

To the laboratory technicians and friends of Institute of Chemistry of Sao Carlos who always helped me, specially to Jennifer Chauca and Silmara Buchvieser.

To the technicians Priscila Cervini for TG analysis, Marcio de Paula and Carlos Bento for the SEM analysis, Sylvana Agostinho and André Tognon for NMR analysis, Aline Silva and Alessandra Poli for rheology analysis and Marcelo Calegario for X-Ray analysis.

I appreciate the collaboration of my lab-mates from the Photochemistry Lab at USP/IQSC.

Thank you kindly to my family and my friends: Alana Zulke, Jake Van Loon, Andressa Zawadzki, et al. for the assistance that allowed me to get to my present position.

I would also like to thank Dr Willy Glen Santos for helping me with the fluorescence analysis and for sharing your ideas and knowledge, thank you very much!

To Dr Marco Antonio Horn Jr. for making available all the reagents needed to continue my project in Brazil.

To CAPES Process 1706418 for the scholarship at Sao Paulo University (Brazil) and for the grant to support me at Carnegie Mellon University (USA) from November/2018 to April/2019 (Finance Code 001).

RESUMO

Inicialmente, seis diferentes monômeros foram estudados para Polimerização Radicalar via Adição Fragmentação Reversível (RAFT) fotoinduzida sob luz verde. Os monômeros utilizados foram: poli(etileno glicol) metacrilato de metil éter (PEG₃₀₀MA and PEG₅₅₀MA), metacrilato de butila (BMA), metacrilato de poldimetilsiloxano (PDMSMA), lauril metacrilato (LMA) e metacrilato de 2-(dimetilamino)etil (DMAEMA). A fotopolimerização de todos os monômeros, exceto para BMA e LMA, por RAFT sem catalisador sob luz verde mostrou-se descontrolada, enquanto BMA e LMA forneceram alta conversão e baixa polidispersividade: de 95%; 1,31 e 80%; 1,35, respectivamente. Em um segundo aspecto a tese investigou alguns agentes de transferência que foram adicionados à Polimerização por Radicais Livres (FRP) para permitir o cálculo do coeficiente de transferência do halogênio para a cadeia de propagação, a fim de determinar a rapidez com que ocorre e também para encontrar uma molécula ideal para fazer estruturas do tipo “*bottlebrush*”. Os melhores resultados foram obtidos com etilbromo- α -isobutirato (EBiB) onde foi determinado um coeficiente de transferência (Cs) igual a 0,0162. Além disso, estruturas de polímeros em rede foram sintetizadas por FRP e estruturas funcionalizadas foram preparadas usando RAFT e Polimerização Radicalar por Transferência de Átomo (ATRP). Observou-se que redes altamente reticuladas podem ser frágeis, mas a preparação de géis com estruturas macromoleculares projetados e estruturados (STEM) altamente sintonizáveis podem ser preparados por procedimentos de polimerização radicalar de desativação reversível (RDRP). Esses polímeros de rede foram caracterizados por testes de inchamento. Em um último momento da pesquisa, novas redes poliméricas com diferentes funcionalidades foram sintetizadas por FRP, onde a cadeia principal é composta por metacrilato de metila (MMA) e, PEG₅₅₀DMA foi utilizado como agente de reticulação (crosslinking), enquanto LMA, 1-pirenometil metacrilato e 2-cloridrato de metacrilato de aminoetila foram utilizados para funcionalizar esses polímeros. Eles foram caracterizados por reologia, análise termogravimétrica (TG/DTA), UV-vis e Fluorescência.

Palavras-Chave: RDRP, ATRP, RAFT, Redes Poliméricas, STEM gels.

ABSTRACT

Initially, six different monomers were examined for Reversible Addition Fragmentation chain-Transfer Polymerization (RAFT) photoinduced polymerization under green light. The monomers used were: poly(ethylene glycol) methyl ether methacrylate (PEG₃₀₀MA and PEG₅₀₀MA), butyl methacrylate (BMA), poly(dimethylsiloxane) methacrylate (PDMSMA), lauryl methacrylate (LMA) and 2-(dimethylamino)ethyl methacrylate (DMAEMA). Photo polymerization of all monomers, except for BMA and LMA, by catalyst free RAFT under green light appeared to be very uncontrolled while BMA and LMA provided high conversion and low dispersity of 95%; 1.31 and 80 %; 1.35, respectively. In a second aspect of the research program, some transfer agents were added to Free Radical Polymerizations (FRP) in order to allow calculation of the transfer coefficient from the halogen to propagating chain in order to determine how fast it occurs and also to find a good molecule to make bottlebrushes structures. The best results were obtained with ethylbromo- α -isobutyrate (EBiB) where we determined a transfer coefficient (C_s) equal 0.0162. Also, network polymers structures were synthesized by FRP and functionalized structures were prepared by using RAFT and Atom Transfer Radical Polymerization (ATRP). It was observed that highly crosslinked networks can be brittle but the preparation of highly tunable Structurally Tailored and Engineered Macromolecular (STEM) gels could be prepared by Reversible Deactivation Radical Polymerization (RDRP) procedures. These network polymers were characterized by swelling tests. In the last aspect of the research, novel polymer networks with different functionalities were synthesized by FRP, where the main chain is composed of methyl methacrylate (MMA), and PEG₅₅₀DMA was used as crosslink agent, while LMA, 1-pyrenemethyl methacrylate and 2- aminoethyl methacrylate hydrochloride were used to functionalize these polymers. They were characterized by rheology, thermogravimetric analysis (TG/DTA), UV-vis and Fluorescence.

Key-words: RDRP, ATRP, RAFT, Networks, STEM gels.

LIST OF FIGURES

Figure 1 – Propagation steps for radical polymerization.....	21
Figure 2 – Activation-deactivation mechanism for free radical propagation.....	23
Figure 3 – Proposed mechanism for an ATRP reaction.....	24
Figure 4 – Mechanism reported for RAFT by Rizzardo and collaborators.....	26
Figure 5 – Topology, composition and functionality of polymers.....	27
Figure 6 – Linear, branched and crosslinked polymers.....	29
Figure 7 – System used for photo polymerization by RAFT.....	33
Figure 8 – Structure of PEG ₃₀₀ MA.....	37
Figure 9 – Kinetic spectra of ¹ H NMR for PEG ₃₀₀ MA Catalyst Free RAFT Polymerization, conversion: Calculated by ¹ H NMR, solvent: DMSO-d ⁶	38
Figure 10 – Graphs A, B, C, D - Conditions: (PEG ₃₀₀ MA): (CDTPA) = 200: 1. All samples irradiated by Green LED lights. Measured by Chloroform GPC calibrated to PMMA standards, solvent: water.....	39
Figure 11 – Structure of BMA.....	40
Figure 12 – Kinetic spectra of ¹ H NMR for BMA Catalyst Free RAFT Polymerization conversion: Calculated by ¹ H NMR, solvent: DMSO-d ⁶	41
Figure 13 – Graphs A, B, C, D - Conditions: (BMA) : (CDTPA) = 200 : 1. All samples irradiated by Green LED lights . Measured by Chloroform GPC calibrated to PMMA standards, solvent: THF.....	42
Figure 14 – Structure of PDMSMA.....	43
Figure 15 – Kinetic spectra of ¹ H NMR for PDMSMA Catalyst Free RAFT Polymerization conversion: Calculated by ¹ H NMR, solvent: DMSO-d ⁶	43
Figure 16 – Conversion over time for PDMSMA. Conditions: (PDMSMA):(CDTPA) = 200:1. All samples irradiated by Green LED lights. Measured by Chloroform GPC calibrated to PMMA standards, solvent for GPC: CHCl ₃	44
Figure 17 – Structure of LMA.....	45
Figure 18 – Kinetic spectra of ¹ H NMR for LMA Catalyst Free RAFT Polymerization conversion: Calculated by ¹ H NMR, solvent: CHCl ₃	45

Figure 19 – Graphs A, B, C, D - Conditions: (LMA):(CDTPA) = 200:1. All samples irradiated by Green LED lights. Measured by Chloroform GPC calibrated to PMMA standards, solvent: THF.	46
Figure 20 – Structure of PEG ₂ MA	47
Figure 21 – Kinetic spectra of ¹ H NMR for PEG ₂ MA Catalyst Free RAFT Polymerization conversion: Calculated by ¹ H NMR, solvent: DMSO-d ⁶	47
Figure 22 – Graphs A, B, C, D - Conditions: (PEG ₂ MA):(CDTPA) = 200:1. All samples irradiated by Green LED lights . Measured by Chloroform GPC calibrated to PMMA standards, solvent: DMF.....	48
Figure 23 – Structure of DMAEMA	49
Figure 24 – Kinetic spectra of ¹ H NMR for PEG ₂ MA Catalyst Free RAFT Polymerization conversion: Calculated by ¹ H NMR, solvent: CDCl ₃	49
Figure 25 – Graphs A, B, C, D - Conditions: (DMAEMA):(CDTPA) = 200:1. All samples irradiated by Green LED lights. Measured by Chloroform GPC calibrated to PMMA standards, solvent: DMF.....	50
Figure 26 – Kinetic spectra of ¹ H NMR for PEG ₃₀₀ MA photo ATRP Polymerization. Solvent: CDCl ₃	51
Figure 27 – Graph of conversion over time. Conditions: (PEG ₃₀₀ MA):(EBiB) = 50:1. All samples irradiated by UV light (365 nm).	52
Figure 28 – Structures of different transfer agents used by FRP.....	55
Figure 29 – Example of transfer to EBiB.	56
Figure 30 – ¹ H NMR spectra for Butyl Acrylate (BA).....	58
Figure 31 – ¹ H NMR spectra for Anisole in the time zero of the reaction.	59
Figure 32 – Kinetics of FRP by ¹ H NMR spectra for BA with different EBiB ratio (round 1). ...	60
Figure 33 – Graphs of Conversion, Ln, M _n and C _s for BA.....	61
Figure 34 – GPC curves for BA Round 1.....	62
Figure 35 – Kinetics of FRP by ¹ H NMR spectra for BA with different EBiB ratio (round 2)...	63
Figure 36 – Conversion of polymer for BA.	64
Figure 37 – Kinetics of FRP by ¹ H NMR spectra for MMA with different EBiB ratio and without EBiB.	65
Figure 38 - Graphs of conversion, GPC data and C _s calculation for MMA.	66

Figure 39 - GPC curves for FRP by MMA.	67
Figure 40 – Transfer Coefficient for MMA and EBiB in the Dark.	68
Figure 41 – GPC traces for polymerization by FRP with MMA and EBiB in the dark.	69
Figure 42 – Transfer Coefficient for MMA and Et-Cl-Prop - Ambient Light.	69
Figure 43 – GPC traces for polymerization by FRP with MMA and Et-Cl-Prop - ambient light.	70
Figure 44 – Transfer Coefficient for MMA and Me-Br-Prop – Ambient Light.	71
Figure 45 – GPC traces for polymerization by FRP with MMA and Me-Br-Prop – ambient light.	71
Figure 46 – Transfer coefficient for EbiB, Et-Cl-Prop and Me-Br-Prop.	72
Figure 47 - ¹ H NMR for polymerization of MMA by FRP without transfer agent (TA) at 60 °C for 45 minutes of reaction - Repetition 1.	74
Figure 48 – ¹ H NMR for polymerization of MMA by FRP without transfer agent (TA) at 60 °C for 45 minutes of reaction - Repetition 2.	75
Figure 49 – GPC traces for polymerization of MMA by FRP without transfer agent (TA) at 60 °C for 45 minutes of reaction - Repetitions 1 and 2.	76
Figure 50 – Structure of the monomer PEG ₇₅₀ DMA and an ideal network.	77
Figure 51 – Steps for checking swelling for GS-Matrix	78
Figure 52 – GS-Matrix made by FRP.	80
Figure 53 – Process of Synthesis of Inimer.	83
Figure 54 – Flow chart to exemplify how the STEM -Gels were characterized by swelling ratio.	85
Figure 55 – Characterization of inimer-Br molecule by ¹ H NMR.	87
Figure 56 – ¹ H NMR spectrum of inimer-Cl before purification	88
Figure 57 – STEM -0 and STEM -1 by RAFT and ATRP.	89
Figure 58 – TGA curves of samples 2, 3, 4, 5, 7 and 8.	91
Figure 59 – Storage modulus (G') and loss modulus (G'') of samples 1, 2, 3, 4, 5 and 7.	93
Figure 60 – Tan δ of samples 1, 2, 3, 4, 5 and 7.	94
Figure 61 – UV-vis absorption spectra of sample 2	95
Figure 62 – Fluorescence spectra of samples 2, 3, 4, 5, 6, 7 and 8.	96

LIST OF TABLES

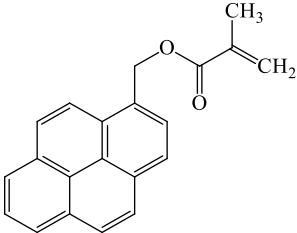
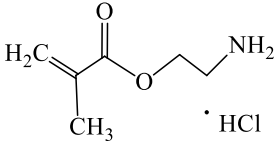
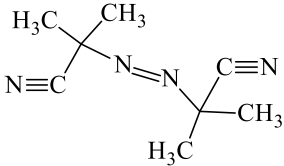
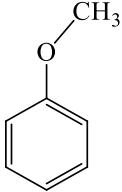
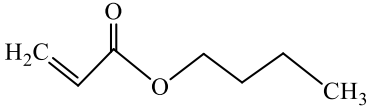
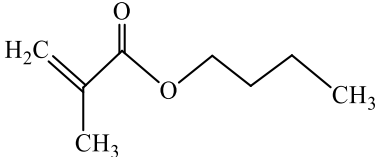
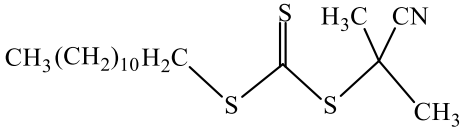
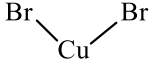
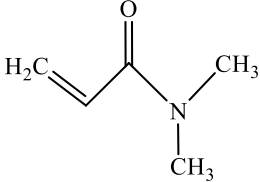
Table 1 – General conditions for Catalyst Free RAFT polymerization of PEG ₃₀₀ MA.	34
Table 2 – General conditions for Catalyst Free RAFT polymerization with BMA.	34
Table 3 – General conditions and results for Catalyst Free RAFT polymerization with PDMSMA	35
Table 4 – General conditions for Catalyst Free RAFT polymerization with LMA.	35
Table 5 – General conditions for Catalyst Free RAFT polymerization with PEG ₂ MA.	35
Table 6 – General conditions for Catalyst Free RAFT polymerization with DMAEMA.	36
Table 7 – General conditions for photo ATRP with PEG ₃₀₀ MA.	36
Table 8 – Conditions used in FRP of BA using EBiB ratio 100	54
Table 9 – Conditions used in FRP of BA using an EBiB ratio of 150	54
Table 10 – Conditions used in FRP of BA using an EBiB ratio of 200	54
Table 11 – Conditions used for determination of the Transfer Coefficient for three different Transfer Agents: EBiB, Et-Cl-Prop and Me-Br-Prop.	56
Table 12 – Conditions used for polymerization by FRP without Transfer Agent (TA).....	57
Table 13 – Results for Transfer Coefficient for three different Transfer Agents: EBiB, Et-Cl-Prop and Me-Br-Prop.....	68
Table 14 – Results for Transfer Coefficient for three different Transfer Agents: EBiB, Et-Cl-Prop and Me-Br-Prop.....	73
Table 15 – Conditions used for GS-Matrix synthesis.	77
Table 16 – Data yields and steps for checking the swelling.....	79
Table 17 – Data swelling for GS-Matrix.	81
Table 18 – Data swelling and yields for GS-Matrix.....	82
Table 19 – Conditions used for synthesis of STEM -0 by RAFT.	85
Table 20 – Conditions used for synthesis of STEM -1 by photo ATRP using UV-Light for 6 hours.	86
Table 21 – Degree of Swelling calculated for STEM -0 and STEM -1 (A and B)	89
Table 22 – Conditions used in functionalized networks with PEG ₅₅₀ DMA	90
Table 23 – Quantitative results from TG curves. Including temperature range, mass loss percentages and residues for sample analyzed.	92

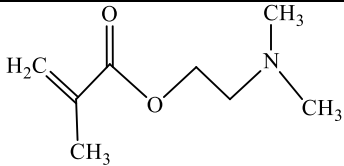
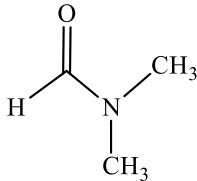
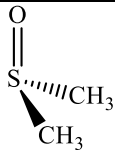
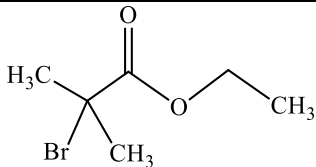
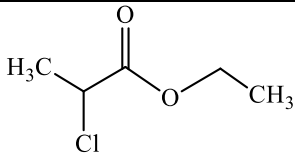
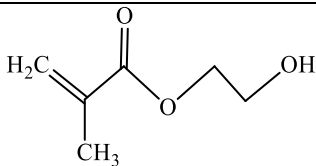
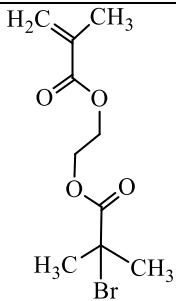
LIST OF ABBREVIATIONS

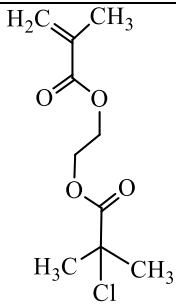
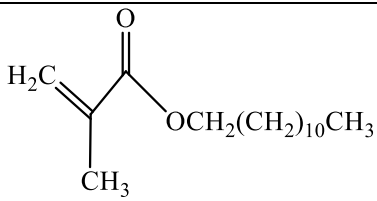
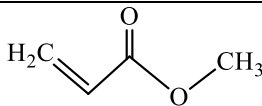
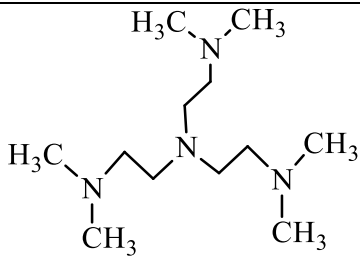
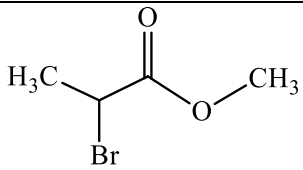
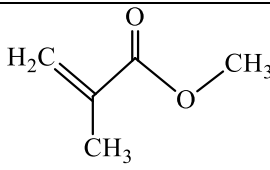
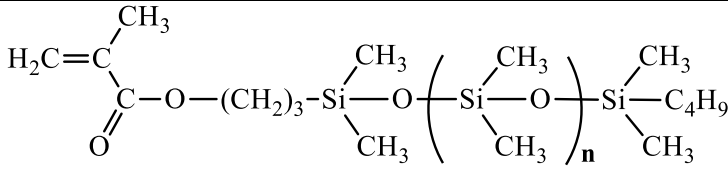
- ¹H NMR** – Proton nuclear magnetic resonance
- 1-PyM** - 1-pyrenemethyl methacrylate
- 2-Amino** - 2-aminoethyl methacrylate hydrochloride
- AIBN** - 2,2'-Azobis(2-methylpropionitrile)
- ATRP** – Atom Transfer Radical Polymerization
- BA** – Butyl Acrylate
- BMA** – Butyl Methacrylate
- CPDTA** - 2-Cyano-2-propyl dodecyl trithiocarbonate
- CuBr₂** – Copper (II) bromide
- Cs** – Transfer Coefficient
- DMA** – N,N- Dimethylacrylamide
- DMAEMA** - 2-(Dimethylamino)ethyl methacrylate
- DMF** - N,N-Dimethylmethanamide
- DMSO** - Dimethyl sulfoxide
- PDI** – Polydispersity Index
- EBiB** – Ethyl α -bromoisobutyrate
- Et-Cl- Prop** - Ethyl 2-chloropropionate
- FRP** – Free Radical Polymerization
- HEMA** - (Hydroxyethyl)methacrylate
- HEMA-iBBr or Inimer-Br** – inimer molecule functionalized with bromine
- HEMA-iBCl or Inimer-Cl** – inimer molecule functionalized with chlorine.
- LMA** – Lauryl Methacrylate
- MA** – Methyl Acrylate
- Me₆TREN** – Tris(2-(dimethylamino)ethyl)amine.
- Me-Br-Prop** – Methyl 2-bromopropionate
- MMA** – Methyl Methacrylate
- NMR** – Nuclear Magnetic Resonance
- PDMSMA** – Polydimethylsiloxane methyl acrylate
- PEG₂MA** – Poly(ethylene glycol) methacrylate average Mn 2

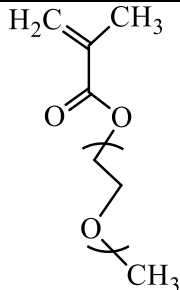
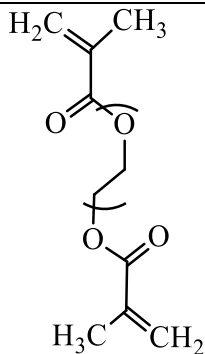
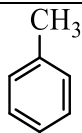
PEG₃₀₀MA - Poly(ethylene glycol) methacrylate average Mn 300
PEG₅₅₀DMA - Poly(ethylene glycol) dimethacrylate average Mn 550
PEG₇₅₀DMA - Poly(ethylene glycol) dimethacrylate average Mn 750
PEO₇₅₀DMA – Poly(ethylene oxide) dimethacrylate average Mn 750
RAFT - Reversible addition-fragmentation chain-transfer polymerization
RDRP – Reversible Deactivation Radical Polymerization.
SEM – Scanning Electron Microscopy.
STEM - Structurally Tailored & Engineered Macromolecular
TG/DTA – Thermogravimetric Analysis
THF – Tetrahydrofuran
GPC/SEC - Gel permeation chromatography via size exclusion chromatography

LIST OF STRUCTURES

<p>1-pyrenemethyl methacrylate</p>	
<p>2-aminoethyl methacrylate hydrochloride</p>	
<p>AIBN</p>	
<p>Anisole</p>	
<p>BA</p>	
<p>BMA</p>	
<p>CPDTA</p>	
<p>CuBr₂</p>	
<p>DMA</p>	

DMAEMA	
DMF	
DMSO	
EBiB	
Et-Cl-Prop	
HEMA	
HEMA-iBBr (Inimer-Br)	

<p>HEMA-iBCl (Inimer-Cl)</p>	
<p>LMA</p>	
<p>MA</p>	
<p>Me₆TREN</p>	
<p>Me-Br-Prop</p>	
<p>MMA</p>	
<p>PDMSMA</p>	

<p>PEG_xMA</p>	
<p>PEG_xDMA</p>	
<p>Toluene</p>	

SUMMARY

1	CHAPTER 1 – INTRODUCTION	20
1.1	STATE OF ART	20
1.2	RDRP and FRP	21
1.2.1	Reversible Deactivation Radical Polymerization (RDRP)	22
1.2.2	Propagation of free radicals via activation-deactivation	23
1.3	ATRP and RAFT	24
1.3.1	Atom Transfer Radical Polymerization (ATRP)	24
1.3.2	Reversible Addition-Fragmentation chain-Transfer Polymerization (RAFT)	26
1.4	POLYMERS ARCHITECTURE	27
2	CHAPTER 2 – OBJECTIVES	32
3	CHAPTER 3 - DEVELOPMENT	33
3.1	CATALYST FREE RAFT POLYMERIZATION	33
3.1.1	Experimental Procedures	33
3.1.2	Results and discussion	37
3.2	EXPERIMENTS FOR CALCULATION OF TRANSFER COEFFICIENT	53
3.2.1	Experimental Procedures and calculations of Cs for FRP	53
3.2.2	Results and discussion	57
3.3	SYNTHESIS of GS-MATRIX USING PEG ₇₅₀ DMA by FRP	76
3.3.1	Experimental Procedures	76
3.3.2	Results and discussion	80
3.4	STEM GELS by RAFT and PHOTO ATRP	82
3.4.1	Experimental Procedures	82
3.4.2	Results and discussion	86
3.5	NEW FUNCTIONALIZED NETWORKS WITH PEG ₅₅₀ DMA	89

3.5.1	Experimental Procedures	90
3.5.2	Results and discussion	90
4	CHAPTER 4 - CONCLUSION	98
5	REFERENCES.....	99
6	Curriculum vitae.....	103

1 CHAPTER 1 – INTRODUCTION

1.1 STATE OF ART

Reversible deactivation radical polymerization (RDRP) techniques, such as RAFT and ATRP, have been utilized to prepare polymers of well-defined structure and architecture [1-3]. Recent reports have investigated the orthogonality of dual-RDRP systems to prepare materials capable of undergoing post-synthetic modifications by a second RDRP reaction (i.e. RAFT of a precursor, then ATRP). The dual-RDRP approach relies on the incorporation of procedurally inert functional groups onto a pre-polymer, which could be activated in the presence of external stimuli, or catalysts, to graft chains from the pre-polymer by the second RDRP procedure. Dual RDRP approaches have been already used to obtain polymers with complex architectures including bottlebrush polymers [4], star polymers [5], multiblock copolymers, and polymer networks [6].

The dual-RDRP approach was used to prepare structurally tailored and engineered macromolecular (STEM) networks [7]. STEM networks are crosslinked materials functionalized with latent RAFT chain transfer agents, or ATRP initiators, capable of grafting sidechains from the backbone precursor.

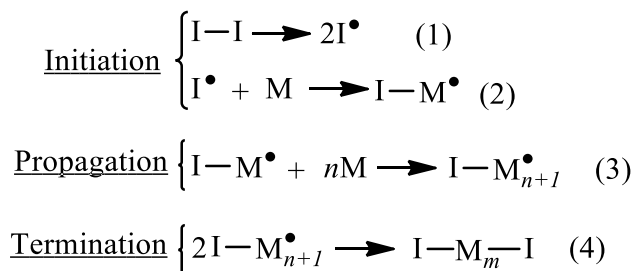
The first STEM networks were prepared by conventional free radical polymerization (FRP) of (meth)acrylate monomers with ATRP inimers which subsequently could be used to graft chains from inside the network upon exposure to UV light [8]. The same principle was extended to a dual RDRP approach by synthesizing the primary network by RAFT polymerization [7]. The advent of photoiniferter, or “catalyst-free”, RAFT polymerization has allowed for post-polymerization modifications to be conducted using selective activation under visible wavelengths of light. The effectiveness of STEM gel modifications relies on both the lack of compatibility of the RDRP technique and inimer used to make the precursor network (STEM-0) as well as the quality of graft polymerization conducted inside of a STEM precursor network (STEM-1). Poor orthogonality would yield materials of poorly defined topology, while good orthogonality yields materials of well-defined structure. Unfortunately, synthetic limitations and lack of definitive methods of characterization of polymer networks has prevented effective assessment of control over polymerizations performed inside the interior of STEM-0 networks. In

this work, we compare the mechanical properties of STEM-1 networks prepared by both RAFT then ATRP and ATRP then RAFT polymerizations as routes to compare internal structure. The contribution of this work to the current literature was to explore multi-RDRP techniques for the synthesis of polymers networks and bottlebrushes polymers, in addition, new materials comprising functionalized polymers networks structures were characterized by different techniques.

1.2 RDRP and FRP

Free radical polymerization has been one of the most extensively used methods for the synthesis of polymeric materials, especially in industry. This is a versatile method that can be applied to several vinyl monomers, with $\text{CH}_2=\text{CR}_1\text{R}_2$ structure (in which, R_1 and R_2 are various functional groups) [9]. In addition, radical polymerization requires simple experimental conditions and can be used over a wide temperature range. Radical polymerization does not require high pressures or other conditions of greater care: except the removal of oxygen and impurities from the system, which could capture free radicals and inhibit polymerization. Thus, radical polymerization offers the possibility of preparing polymers on a large scale with a huge variety of properties. Despite these advantages, conventional polymerization via free radicals presents limitations in relation to the control of polymer characteristics, such as molar mass and polydispersity (PDI or \mathcal{D}). In this mechanism, the propagation and termination steps occur rapidly compared to the initiation step. These factors contribute to the low level of control over the final characteristics of the polymer [9]. The reaction mechanism for a standard radical polymerization is exemplified by three steps, which are represented in Figure 1:

Figure 1 – Propagation steps for radical polymerization



Where, “I” corresponds to the initiator structure and “M” to the monomer selected for the reaction. The steps can be explained separately below:

- ❖ Initiation: In this process, the decomposition of the reaction initiator (1) results in the formation of two radical species. A radical species must react with the first monomer unit forming the first monomeric radical (2), this second formed species is an active species in the reaction.
- ❖ Propagation: At this stage, the first formed monomer radical (2) should react with the second monomer unit initiating propagation (3), the propagating chain is in its active state, so it is the active species of the reaction, and can also be called a macroinitiator because it is a polymeric molecule in the active state.
- ❖ Termination: In the last stage of free radical chain polymerization, chain propagation can be stopped by secondary reactions, such as coupling between two radicals, forming an inactive chain.

1.2.1 Reversible Deactivation Radical Polymerization (RDRP)

Radical Polymerization proved relevant to the polymer industry in the 20th century, and in recent decades there has been considerable progress in the research and development of controlled and/or "living" radical polymerization procedures (CRP/LRP Controlled/Living Radical Polymerization) [9]. Controlled Radical Polymerization (CRP) or simply Living Radical Polymerization, was thus named by chemist Michael Szwarc, who had studied Anionic Polymerization [10] from its discovery, which was characterized by its "living" character. Therefore, the term "Living Polymerization", was introduced in the 1950s to describe a Controlled Polymerization. It is worth clarifying here that the term "alive" is, by definition, one in which the growth of the polymer chain occurs continuously in the absence of irreversible chain transfer or termination reactions [11]. A "living" polymerization allows control of the macromolecular characteristics of the prepared polymer, which is a prerequisite for defining the macroscopic properties of polymers that are to be used in the following areas: nanotechnology (electronics, computer science), and materials technology (compatibilizers, adhesives, dispersal agents, and thermoplastic elastomers, among others) [9].

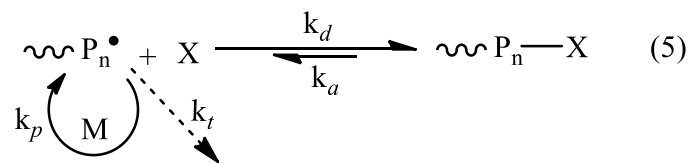
Within this context, the term "alive" served to characterize a radical that propagates free from termination reactions, therefore, it can be said that the theoretical M_n ($M_{n,th}$) of the polymer should be equal to, or very close to, the obtained polymer M_n ($M_{n,exp}$), where M_n refers to the average numerical molar mass of the polymer, consequently, an efficiency factor close to 1, can indicate the living character of a polymerization reaction, the efficiency factor (f) is calculated by the ratio between: $M_{n,th}/M_{n,exp}$.

The commonly used term Controlled Radical Polymerization (CRP) is permitted, but controlled Reversible Deactivation Radical Polymerization (RDRP) is recommended.

1.2.2 Propagation of free radicals via activation-deactivation

The propagation of the free radical in a RDRP can occur through an activation-deactivation process, in this mechanism, there is the establishment of a dynamic balance between the active species and the dormant (or also called inactive) species. This balance occurs by an activation constant for the formation of the radical (active) species and the return to the dormant (inactive) state, which occurs with a deactivation constant; this mechanism is shown in Figure 2 below.

Figure 2 – Activation-deactivation mechanism for free radical propagation.



The radical propagation that occurs by the activation-deactivation mechanism is based on the Persistent Radical Effect (PRE); this characteristic is capable to provide a self-regulatory effect on some RDRP systems. This mechanism is predominant, especially in ATRP reactions. The propagation of radicals can be deactivated by species X (halogen) with a deactivation constant (k_d). Rapid exchange between active and dormant species is necessary for good control of molecular weight, polydispersity and architecture of polymer chains in all systems that make up RDRP procedures.

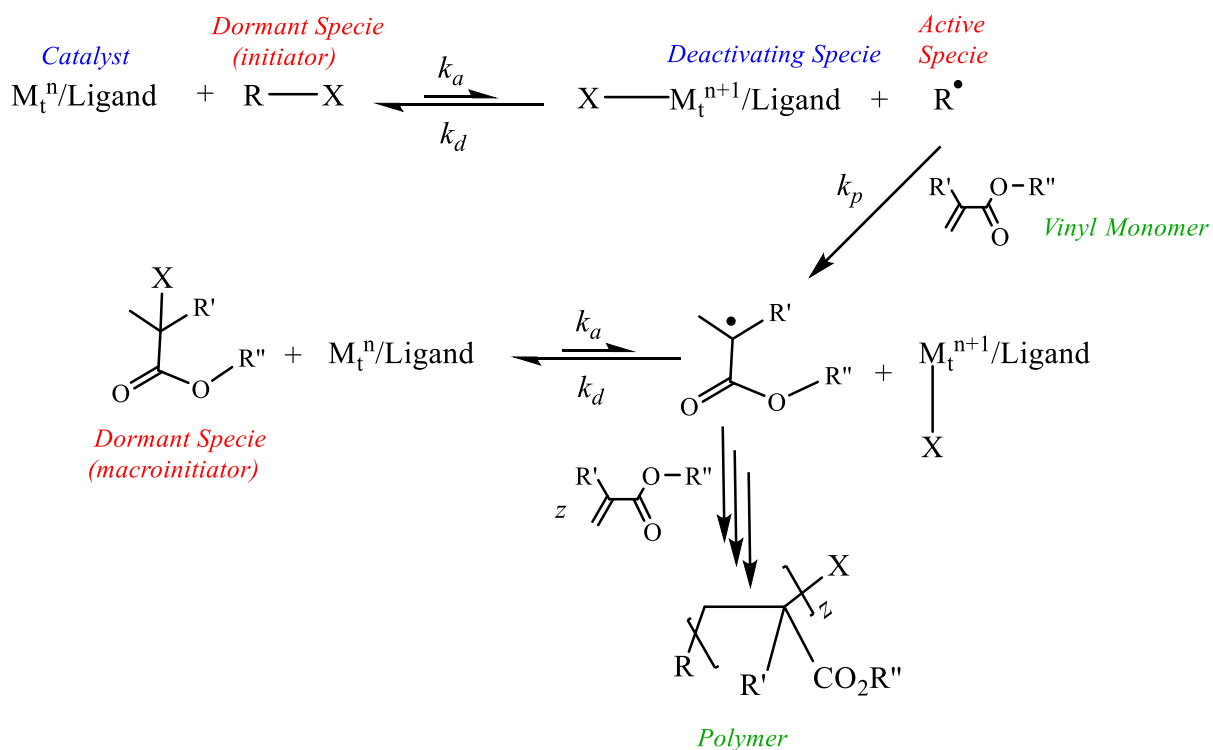
1.3 ATRP and RAFT

1.3.1 Atom Transfer Radical Polymerization (ATRP)

ATRP is a very simple synthetic route and is suitable for obtaining polymers with complex architectures, as well as preparation of organic or bio conjugated hybrid materials. In addition, ATRP makes it possible to incorporate functional groups into the polymer extremities or along polymer chain backbones [12,13].

The mechanism of ATRP consists of the interaction of a catalyst and an initiator (alkyl halide), the latter is also called the dormant species. The monomer is added to the reaction medium and stabilizes the radical species (or active species) which is the species generated by the initiator, forming the first polymeric unit (monomer radical). The catalyst in turn is oxidized by addition of the radical halide forming a disabled species. The mechanism that exemplifies this reaction is shown in Figure 3 below.

Figure 3 – Proposed mechanism for an ATRP reaction.



The free radical originates from the homolytic cleavage of the covalent carbon - halogen bond (RX). This cleavage corresponds to the activation step. In an ATRP, activation is promoted by a transition metal complex, which has a coordinated ligand to form an active transition metal complex that is soluble in the reaction medium. The halogen on the initiator coordinates the metal center in the M^n oxidation state causing the cleavage. Thus, the organic compound becomes a free radical, that is, the active species of the polymerization. The formed complex, on the other hand, undergoes oxidation, forming a M^{n+1} unit. Thus, the free radical initiates the propagation, whose growth is interrupted as soon as the active species finds a M^{n+1} complex. The oxidized complex is called a deactivating species, as it disrupts the growth of the chain, turning it again into a dormant species. In this case, the complex undergoes a reduction, returning to the lower oxidation state M^n (or activating species) [14-16]. In order to attain good control over the molar mass in an ATRP, it is necessary that the deactivation constant (k_d) is greater than the activation constant (k_a), that is, there must be a dynamic equilibrium favoring the formation of the dormant species [17].

The chemical equilibrium involved in this mechanism should be directed at the objective of maintaining a minimum concentration of radical species in the reaction medium, thus eliminating possible termination reactions, allowing control of the molar mass of the polymer. On the other hand, such terminations cannot be completely avoided in ATRP, because when they occur at the beginning of a polymerization, they lead to an accumulation of the concentration of deactivating species (i.e., M^{n+1}/Ligand). Consequently, equilibrium will self-adjust “setting up” reaction conditions that result in formation of a desired concentration of the deactivating species and the concentration of radicals will be reduced, allowing polymerization to occur, therefore, in a sense, self-regulation of the polymerization procedure [12]. Consequently, control over the ATRP reaction can be improved by adding small amounts of the deactivating species, which result in fast attainment of the final equilibrium concentrations between deactivator and dormant species.

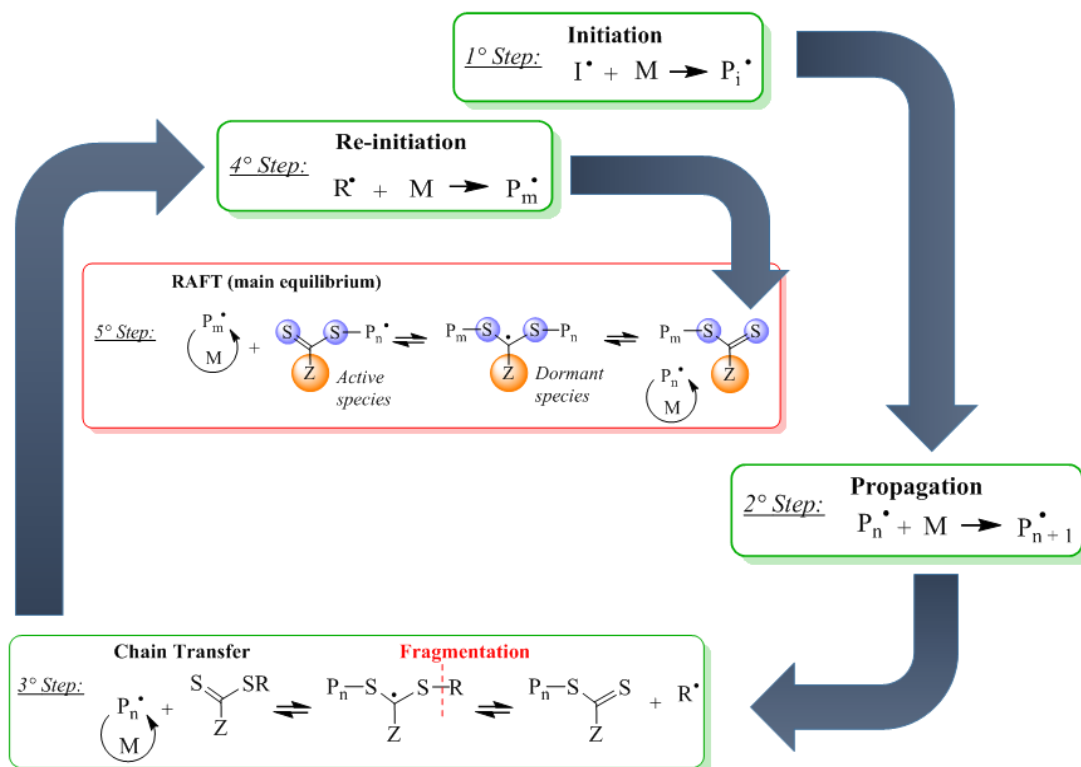
Several different transition metals, including copper, iron, cobalt, ruthenium and nickel (usually in the form of chlorine, bromine or iodine salts), have been used in conjunction with various complex forming ATRP ligands, predominately including nitrogen and structures based on phosphines [13]. The most commonly used transition metal is copper, largely due to its low

cost and versatility. The function of the ligand is to solubilize the metal ion, which also affects the potential for reducing the transition metal ion. Alkyl chlorides, bromides and iodides are typically used as initiators [18].

1.3.2 Reversible Addition-Fragmentation chain-Transfer Polymerization (RAFT)

The RAFT-mediated polymerization reaction was first reported in 1998 by Rizzardo and collaborators [19-21]. For a RAFT-mediated reaction, it is necessary to use vinyl monomers, an initiator (e.g., AIBN) and the RAFT agent (dithioester). The species that make up this reversible transfer mechanism are activated based on their structures. The vinyl monomer will suffer a radical attack on a sp^3 carbon that composes the vinyl group's double bond, thereby forming a tertiary carbon radical, which is stable and will spread in the polymerization reaction medium. The AIBN initiator is a source of radicals and can be activated thermally, and the use of UV radiation has already been reported [19,22,23]. It should be noted that in this RAFT mechanism the necessary "RAFT agent", can also be called a chain transfer agent (CTA). The function of each molecule present will be discussed later in the discussion elucidating the mechanism proposed by Rizzardo et al. [19, 23-24] for RAFT that is represented in Figure 4.

Figure 4 – Mechanism reported for RAFT by Rizzardo and collaborators.



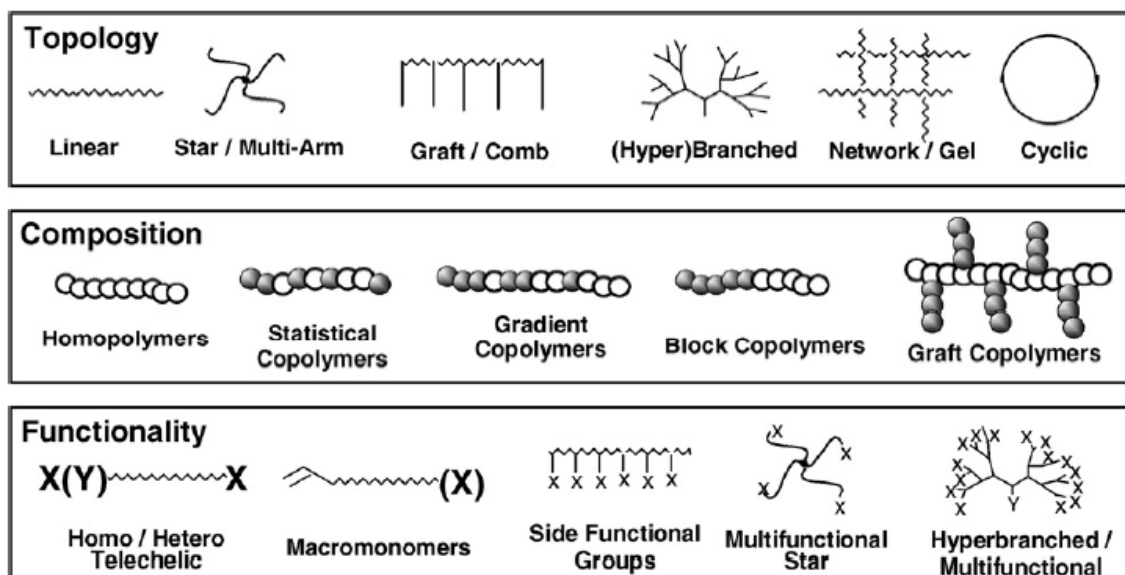
As illustrated in the Figure 4, in the first step there is formation of a monomeric radical, derived from the initiator reacting with a monomer. In the second step, a polymer radical will be responsible for the propagation of the polymerization of the monomer forming a designated polymer chain (P_{n+1}), which would be a macro radical. In the third step, the added CTA, forms an intermediate radical in combination with the growing polymer chain and the fragmentation of the intermediate radical produces a new R radical group, this R output group can restart polymerization (Step 4 - Re-initiation) by chain transfer.

The balance between chains composed of active and dormant species (Step 5) provide the main equilibrium of the mechanism. In this step, control of polymerization is formed with a dynamic exchange between the radical of the active and dormant/inactive polymer chains, keeping most chains in the dormant state. In this sense, RAFT has proved to be a robust technique and has been used for RDRP with a diversity of vinyl monomers [18].

1.4 POLYMERS ARCHITECTURE

Polymer architecture is attained by a combination of topology, composition and functionality. RDRP procedures are suitable for the preparation of polymers with controlled architecture [25]. Figure 5 shows these classifications.

Figure 5 – Topology, composition and functionality of polymers.



Source: Reference 25.

RDRP is very well suited for the preparation of (co)polymers with controlled topologies, including star- and comb-like polymers as well as branched, hyperbranched, dendritic, network, and cyclic type structures.

RDRP processes can be used to significantly improve network uniformity over structures prepared by FRP [26]. Well-defined polymers with crosslinkable pendant moieties can be prepared to form microgel networks. Degradable gels can be prepared with disulfide linkages [27]. Additionally, it is possible to use crosslinkers which can be reversibly cleaved that subsequently lead to the formation of reversible gels [28].

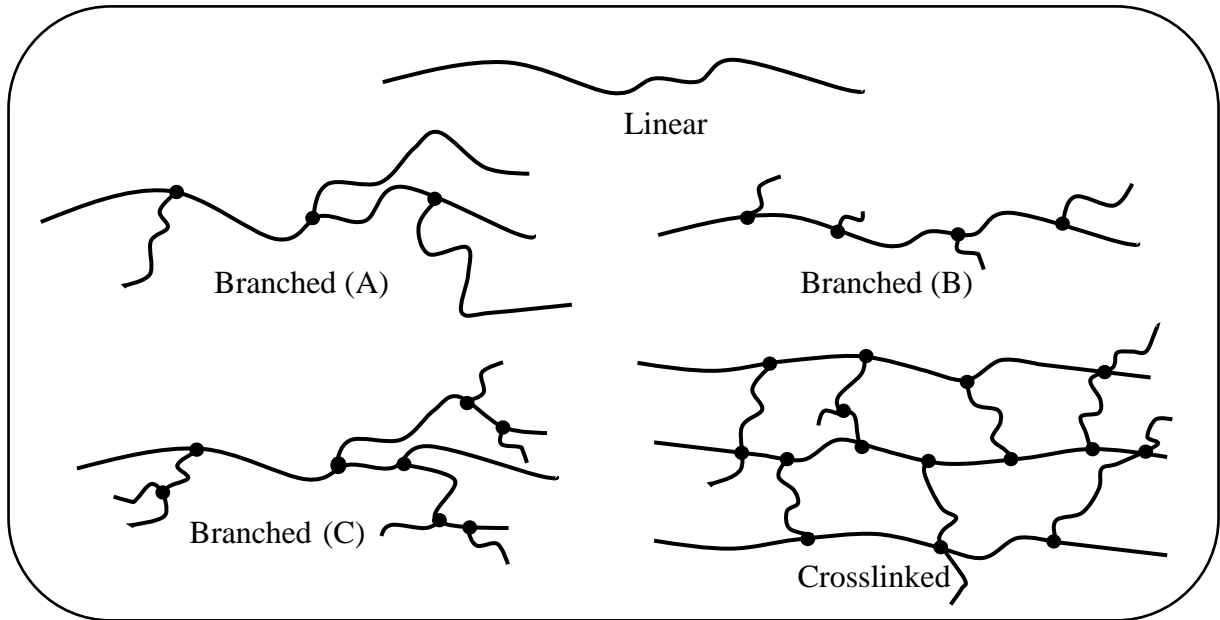
The tolerance that CRP processes show toward functional groups allows for the prolific production of a vast array of statistical, segmented (blocks and graft), periodic (mostly alternating), and gradient copolymers. In addition to materials prepared by one specific CRP technique, many segmented copolymers are prepared by a combination of radical polymerization and other techniques.

Finally, in the case of functionality, it can be introduced to specific parts of a macromolecule. This includes incorporation of side functional groups directly to a polymer backbone [26] or in a protected form [29].

On the other hand, polymers can be classified as *linear*, *branched*, or *crosslinked* polymers depending on their structure.

Linear polymers have monomer molecules linked together in one continuous length to form the polymer molecule. Branched polymers are those in which there are side branches of linked monomer molecules protruding from various central branch points along the main polymer chain [30]. The difference between linear, branched and crosslinked polymers are represented in Figure 6.

Figure 6 – Linear, branched and crosslinked polymers.



Source: Reference 30.

The branched polymers can be comb-like in structure with either long (A) or short (B) branches while extensive branching can form a dendritic structure in which there are branches protruding from other branches, that is, branched branches (C).

It is very important to understand that when there are branches in the structure of the polymers this has an effect on the polymer properties, among them, the most important change is to decrease the crystallinity of the solid polymer. Branched polymers do not pack as easily into a crystal lattice as do linear polymers [30].

The third structure is the result of crosslinking and it is formed by chains that are linked at points other than their chain-ends and this can occur during the polymerization process by the use of appropriate monomers. One can also vary the number of crosslinks in order to obtain lightly or highly crosslinked polymers. When the number of crosslinks is sufficiently high, a three-dimensional or space network polymer is produced in which all the polymer chains in a sample have been linked together to form one giant molecule. Light crosslinking is used to impart good recovery (elastic) properties to polymers to be used as rubbers. Higher degrees of crosslinking are used to impart high rigidity and dimensional stability (under conditions of heat and stress) to polymers such as industrial phenol-formaldehyde and urea-formaldehyde polymers [30]. The crosslink number tends to increase T_g , increases the strength and hardness of the material.

On the other hand, a gel can be formed by a polymer network and a good definition is provided below:

A gel is a material composed of subunits that are able to bond with each other in such a way that one obtains a network of macroscopic dimensions, in which all the subunits are connected by bonds.... A gel has the mechanical properties characteristic of a solid, even though it is structurally disordered and indeed may contain a high volume fraction of liquid solvent [31].

Gels behave like networks of polymer molecules, where each molecule may be visualized as a spring. The entropy of the spring increases when it is stretched, providing a restoring force.

With the development of the so-called “living” radical polymerization procedures, currently known as RDRP, the synthesis of polymers with specific architectures has become increasingly easy. Polymers of complex architecture can be synthesized from specially adapted starting compounds or simply by first synthesizing linear chains that undergo additional reactions to inter-connect later forming the desired structures.

In general, a polymer chain becomes more compact as the degree of branching increases. In this way, branching also affects the entanglement of chains and the ability of the chains to slide over each other, this effect will influence the physical properties of the material. Long chain branches can increase polymer strength, toughness and glass transition temperature (t_g) due to the increase in the number of tangles per chain. On the other hand, a short branch can reduce the strength of the polymer due to the interruption of the chains' ability to interact with each other and crystallize. Polyethylene can serve as an example, in this case; high density polyethylene (HDPE), has a very low degree of branching and is relatively rigid which allows its use in applications such as bulletproof vests while low density polyethylene (LDPE) has a significant number of long and short branches, resulting in it being relatively flexible and finds application in materials like plastic films.

Dendrimers are a special case of branched polymers, where each unit of monomer is also a branching point. This tends to reduce intermolecular chain entanglement and crystallization. A related architecture, a dendritic polymer, is not perfectly branched, but shares properties similar to dendrimers due to its high degree of branching.

The degree of branching that occurs during polymerization can be influenced by the functionality of the monomers used [30]. For example, in a free radical polymerization of styrene,

the addition of divinylbenzene, which has a functionality of 2, will result in the formation of a branched polymer.

2 CHAPTER 2 – OBJECTIVES

In Reversible Addition Fragmentation chain-Transfer Polymerization (RAFT) photoinduced polymerization under green light, the objective was to change the bounding group to methyl acrylate to verify the influence of the electronic synergism coming from each ligand in the polymerization.

Transfer agents were added to Free Radical Polymerizations (FRP) to calculate the transfer coefficient from halogen to the propagation chain and determine which initiator was more efficient in the polymerization.

Synthesize Macromolecular Networks Structurally Adapted and Engineered Macromolecular Gels (STEM) functionalized with latent RAFT chain transfer agents, or ATRP primers, capable of grafting spinal precursor side chains.

Prepare GS-matrix type gels, using a pure crosslinker, PEG₇₅₀DMA.

Use PEG₅₅₀DMA in the functionalization of new networks and evaluate the influence of 2-amino and LMA monomers in the synthesis of functionalized networks.

3 CHAPTER 3 - DEVELOPMENT

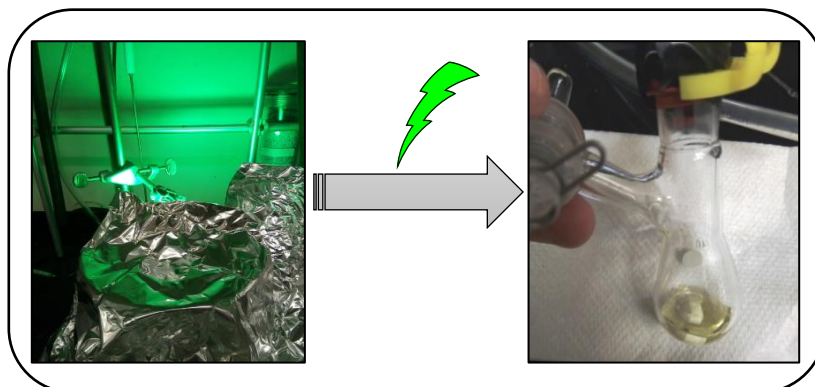
3.1 CATALYST FREE RAFT POLYMERIZATION

3.1.1 Experimental Procedures

3.1.1.1 Characterization of polymers (GPC/SEC)

All experiments were conducted under green light and six different alkyl methacrylate monomers with different substituents were used in the experiments. Figure 7 shows this system of photo-induced polymerization.

Figure 7 – System used for photo polymerization by RAFT.



^1H NMR analysis (Nuclear Magnetic Resonance of Hydrogen) was performed for the characterization of the polymers, and to prove that the polymerization was successful and Size Exclusion Chromatography (SEC) was employed to determine the molecular weight and polydispersity of the polymers obtained. All conditions used for the different polymers which have been studied are provided in the following segment:

a) **PEG₃₀₀MA**: Poly(ethyleneglycol)methyl ether methacrylate M_n 300.

DMSO was used as a solvent for polymerization and the ^1H NMR and GPC spectral analysis were carried out in DMSO- d^6 and water, respectively. All conditions are described in Table 1.

Table 1 – General conditions for Catalyst Free RAFT polymerization of PEG₃₀₀MA.

Materials	Density (g/mL)	MW (g/mol)	n (mol)	Mass (g)	Vol (mL)	Ratio
PEG ₃₀₀ MA	1.05	300.00	0.005	1.4864	1.56	200.00
CDTPA		403.67	2.48×10^{-5}	0.0100		1.00
DMSO	1.1	78.13	0.022	1.7167	1.56	
DMF (IS)	0.944			0.0472	0.0500	

b) BMA: Butyl Methacrylate.

DMSO was used as a solvent for the polymerization and the ^1H NMR and GPC was conducted in DMSO- d^6 and THF, respectively. All conditions and results are described in Table 2.

Table 2 – General conditions for Catalyst Free RAFT polymerization with BMA.

Materials	Density (g/mL)	MW (g/mol)	n (mol)	Mass (g)	Vol (mL)	Ratio
BMA	0.894	142.20	0.005	0.7045	0.63	200.00
CDTPA		403.67	2.48×10^{-5}	0.0100		1.00
DMSO	1.1	78.13	0.0089	0.6928	0.63	
DMF (IS)	0.944			0.0472	0.0500	

c) PDMSMA: Monomethacryloxypropyl terminated polydimethylsiloxane.

Dioxane was the solvent for the polymerization and analysis by ^1H NMR and GPC used DMSO- d^6 and CHCl_3 , respectively. All conditions are described in Table 3, as this monomer is expensive, reaction conditions used only 2.38 ml of 50% v/v, for monomer and solvent.

Table 3 – General conditions and results for Catalyst Free RAFT polymerization with PDMSMA

Materials	Density (g/mL)	MW (g/mol)	n (mol)	Mass (g)	Vol (mL)	Ratio
PDMSMA	0.96	1000.00	0.005	4.9545	4.76	200.00
CDTPA		403.67	2.48×10^{-5}	0.0100		1.00
dioxane	1.033	88.11	0.055763481	4.9133	4.76	
DMF (IS)	0.944			0.0472	0.0500	

d) LMA: Lauryl Methacrylate

In this experiment dioxane was used as a solvent for the polymerization and CDCl_3 and THF were used for ^1H NMR and GPC, respectively. All conditions are described in Table 4.

Table 4 – General conditions for Catalyst Free RAFT polymerization with LMA.

Materials	Density (g/mL)	MW (g/mol)	n (mol)	Mass (g)	Vol (mL)	Ratio
LMA	0.868	254.41	0.005	1.2605	1.09	200.00
CDTPA		403.67	2.48×10^{-5}	0.0100		1.00
dioxane	1.033	88.11	0.012827	1.1302	1.09	
DMF (IS)	0.944			0.0472	0.0500	

e) PEG₂MA:

DMSO was used as the solvent for polymerization and DMSO-d^6 and DMF were used for ^1H NMR and GPC, respectively. All conditions and results are described in Table 5.

Table 5 – General conditions for Catalyst Free RAFT polymerization with PEG₂MA.

Materials	Density (g/mL)	MW (g/mol)	n (mol)	Mass (g)	Vol (mL)	Ratio
PEG ₂ MA	1.02	188.22	0.005	0.9325	0.95	200.00
CDTPA		403.67	2.48×10^{-5}	0.0100		1.00
DMSO	1.1	78.13	0.013391966	1.0463	0.95	
DMF (IS)	0.944			0.0472	0.0500	

f) DMAEMA:

DMSO was also used as a solvent for polymerization; while CDCl_3 and DMF were used for ^1H NMR and GPC, respectively. All conditions are described in Table 6.

Table 6 – General conditions for Catalyst Free RAFT polymerization with DMAEMA.

Materials	Density (g/mL)	MW (g/mol)	n (mol)	Mass (g)	Vol (mL)	Ratio
DMAEMA	0.933	157.21	0.005	0.7789	0.73	200.00
CDTPA		403.67	2.48×10^{-5}	0.0100		1.00
DMSO	1.1	78.13	0.013391966	0.7994	0.73	
DMF (IS)	0.944			0.0472	0.0500	

g) Photo ATRP of PEG₃₀₀MA:

The work on photo ATRP employed a photo UV (365 nm) at 5.3 mW/cm^2 . For this experiment ^1H NMR was carried out in CDCl_3 and all samples were injected into water GPC. All conditions used for the experiments are described in Table 7.

Table 7 – General conditions for photo ATRP with PEG₃₀₀MA.

Materials	Density (g/mL)	MW (g/mol)	n (mol)	Mass (g)	Vol (mL)	Ratio
PEG ₃₀₀ MA	1.05	300	0.0064	1.9226	1.8310	50.00
EBiB	1.329	195.05	1.28×10^{-4}	0.0250	0.0188	1.00
CuBr ₂ (6 mg/mL in DMF)		223.37	2.56×10^{-6}	5.70×10^{-4}	0.09543	0.02
Me6TREN (39 mg/mL) in DMF	0.847	230.39	1.54×10^{-5}	0.0035	0.0042	0.12
DMF	0.944	73.09		5.1855	5.4931	

3.1.2 Results and discussion

a) **PEG₃₀₀MA**: Poly(ethyleneglycol)methyl ether methacrylate M_n300.

Figure 8 presents the structure of the monomer PEG₃₀₀MA.

Figure 8 – Structure of PEG₃₀₀MA.

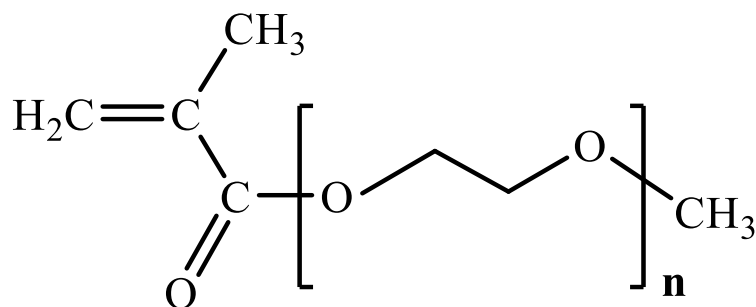


Figure 9 shows the ¹H NMR spectrum for Catalyst Free RAFT Polymerization using PEG₃₀₀MA and Figure 10 shows the data obtained by GPC.

Figure 9 – Kinetic spectra of ^1H NMR for PEG₃₀₀MA Catalyst Free RAFT Polymerization, conversion: Calculated by ^1H NMR, solvent: DMSO- d_6

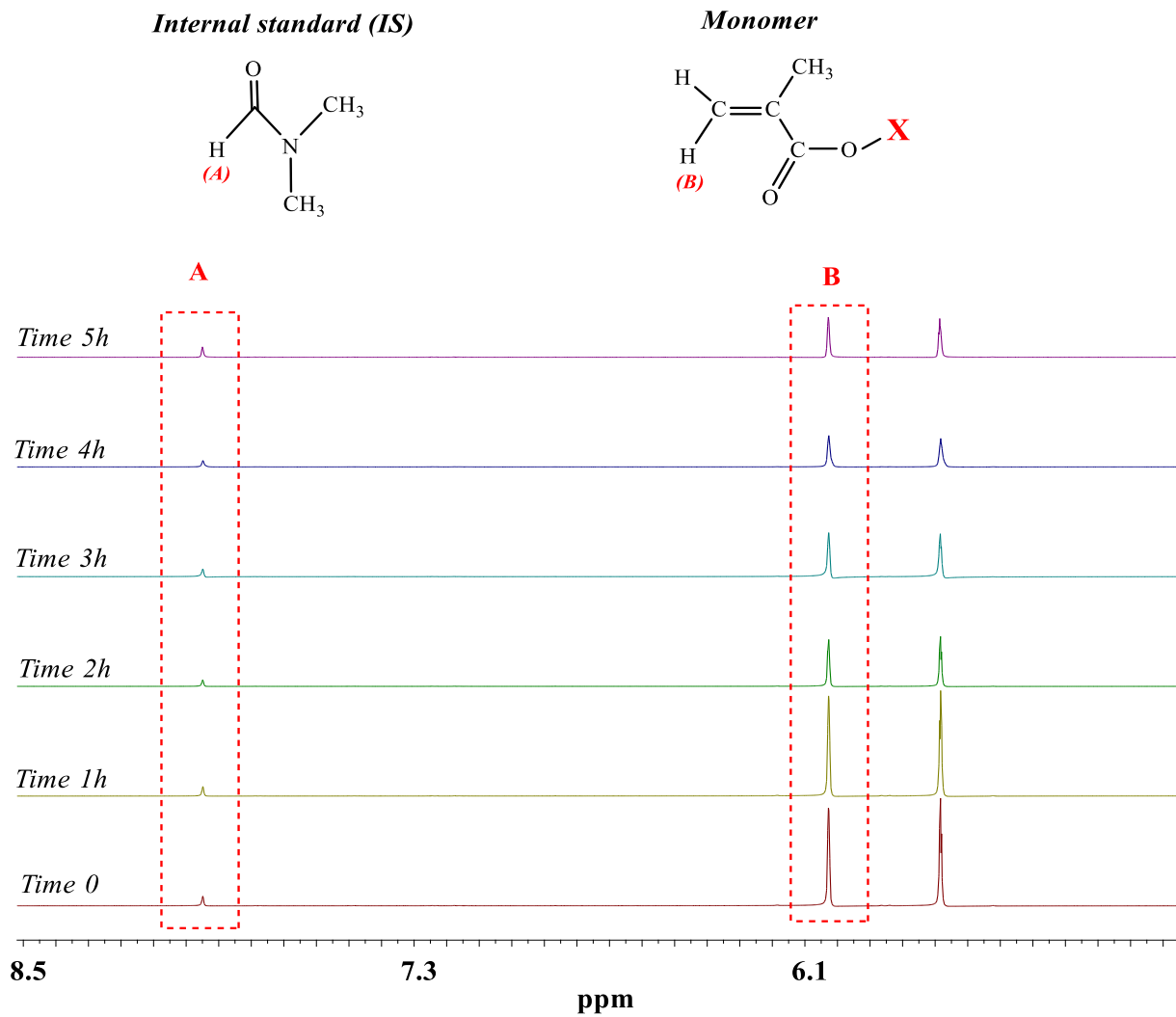
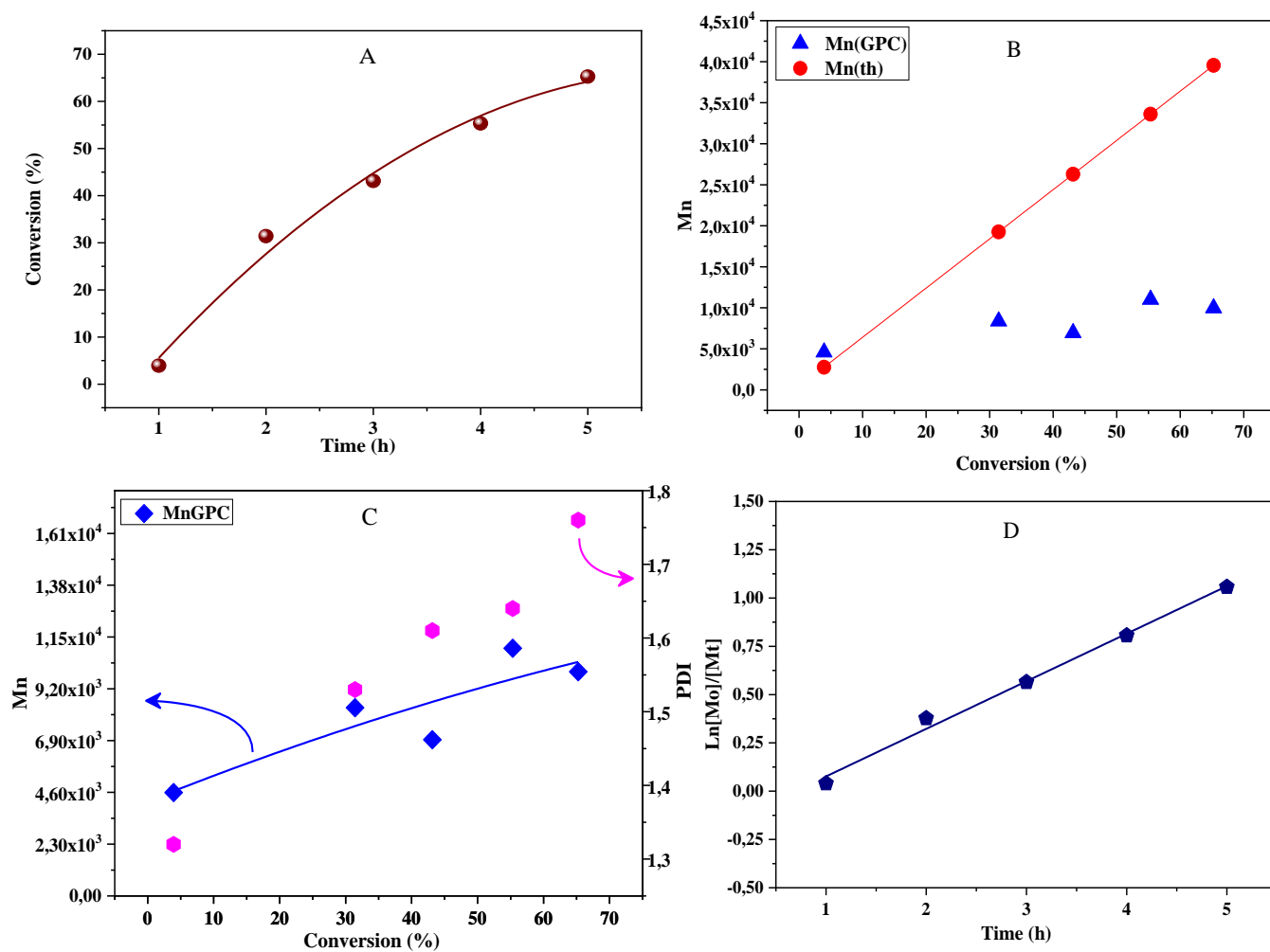


Figure 10 – Graphs A, B, C, D - Conditions: (PEG₃₀₀MA): (CDTPA) = 200: 1. All samples irradiated by Green LED lights. Measured by Chloroform GPC calibrated to PMMA standards, solvent: water.



Through the ¹H NMR spectrum shown in Figure 9, it can be seen that the peak intensity for proton A of the internal standard remains constant throughout the 5 hours of polymerization, while the proton B of the monomer decreases in intensity, showing that the polymerization reaction was successful. Another fact, also observed from graph A in Figure 10, is that a longer polymerization time leads to a higher polymer yield, reaching 65% at the end of 5 h of reaction, a similar result also observed by Heindenrich and Puskas (2008) [32], for the RAFT polymerization.

The closer the polymer MW values approximate linearity, to the theoretical MW values, the more the polymerization reaction was controlled. Figure 10B reveals that MW increases linearly as a function of conversion, but the polydispersity (PDI) was between 1.3 and 1.8, that is, the polymer chains formed have varied molecular weights (Figure 10C).

b) BMA: Butyl Methacrylate.

Figure 11 presents the structure of the monomer BMA.

Figure 11 – Structure of BMA

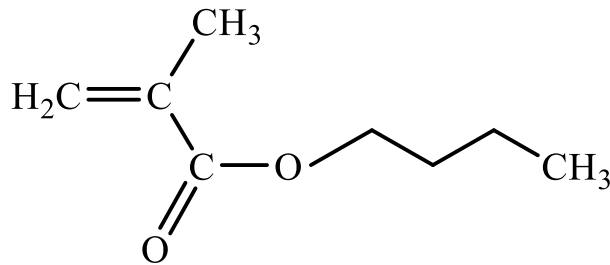


Figure 12 shows the ^1H NMR spectrum for Catalyst Free RAFT Polymerization using BMA and Figure 13 shows all data obtained by GPC.

Figure 12 – Kinetic spectra of ^1H NMR for BMA Catalyst Free RAFT Polymerization conversion: Calculated by ^1H NMR, solvent: DMSO-d^6 .

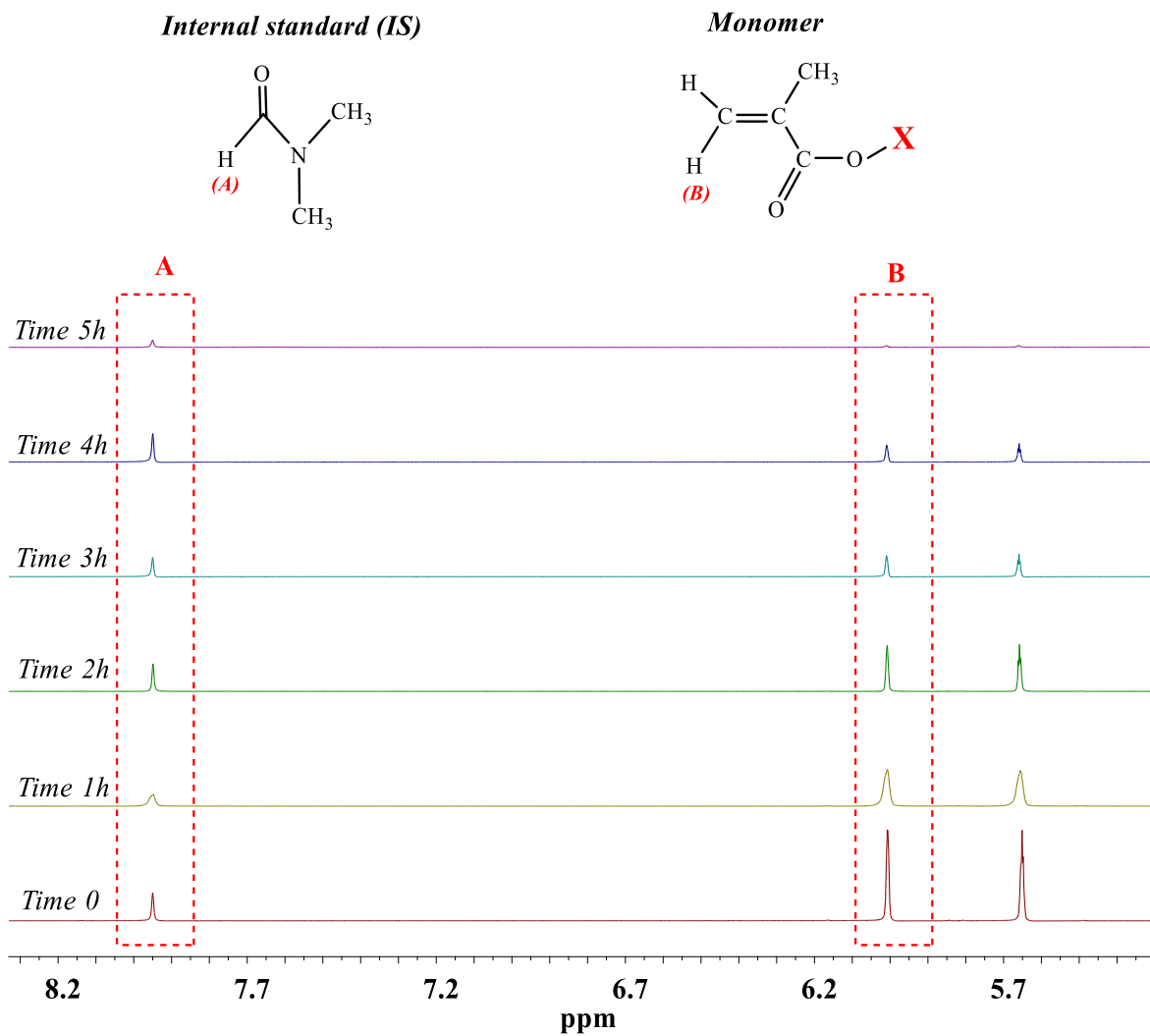
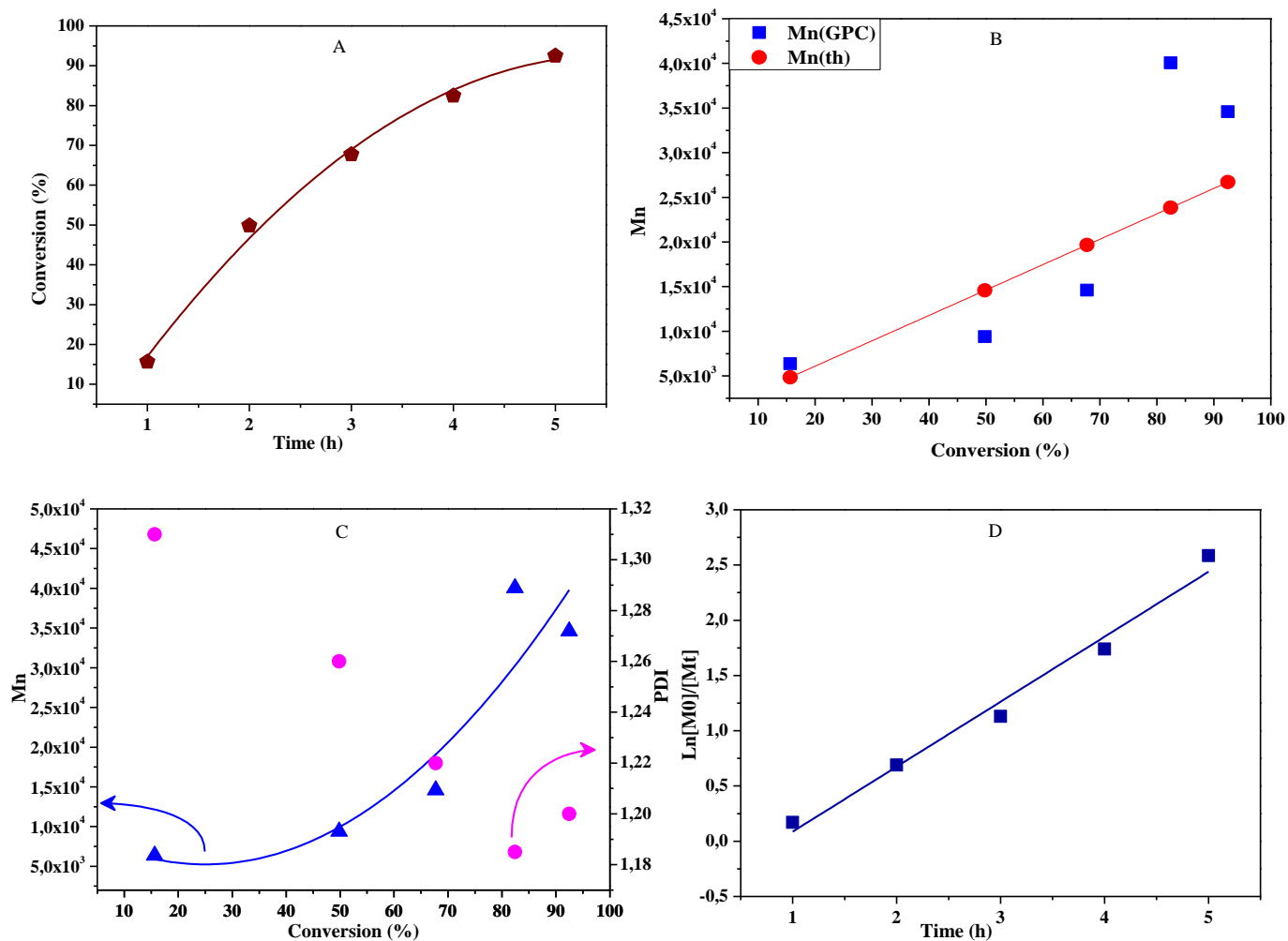


Figure 13 – Graphs A, B, C, D - Conditions: (BMA) : (CDTPA) = 200 : 1. All samples irradiated by Green LED lights . Measured by Chloroform GPC calibrated to PMMA standards, solvent: THF.



Unlike the polymerization in which PEG₃₀₀MA was used as a monomer, when using BMA, the RAFT agent attached more easily to the ends of the polymer chain, which can be verified by the decrease in peak intensity by 8.0 ppm, attributed to aromatic protons of the agent RAFT and also of the peak at 6.0 ppm referring to the vinylic protons of the BMA, showing that the entire monomer reacted (Figure 12). This can be proven by the high yield of the reaction, around 95% conversion (Figure 13A).

Over the reaction time, the polydispersity (PDI) decreases, reaching a narrow value of 1.2, which indicates the controlled nature of the polymerization (Figure 13C), and is also observed through graph B, in which the polymer MW values obtained approach the theoretical MW.

c) **PDMSMA**: Monomethacryloxypropyl terminated polydimethylsiloxane.

Figure 14 presents the structure of the monomer PDMSMA.

Figure 14 – Structure of PDMSMA

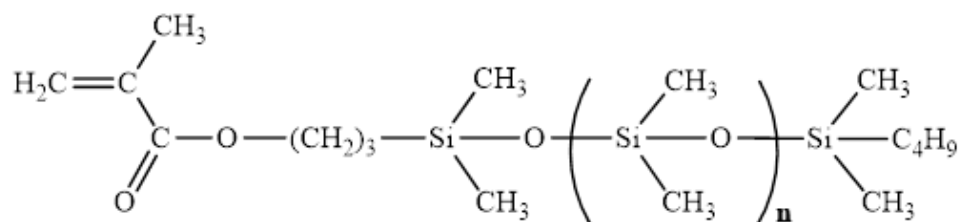


Figure 15 shows the ^1H NMR spectrum for Catalyst Free RAFT Polymerization using PDMSMA and Figure 16 shows the conversion over time and the data obtained by GPC after 42 hours.

Figure 15 – Kinetic spectra of ^1H NMR for PDMSMA Catalyst Free RAFT Polymerization conversion: Calculated by ^1H NMR, solvent: DMSO-d^6 .

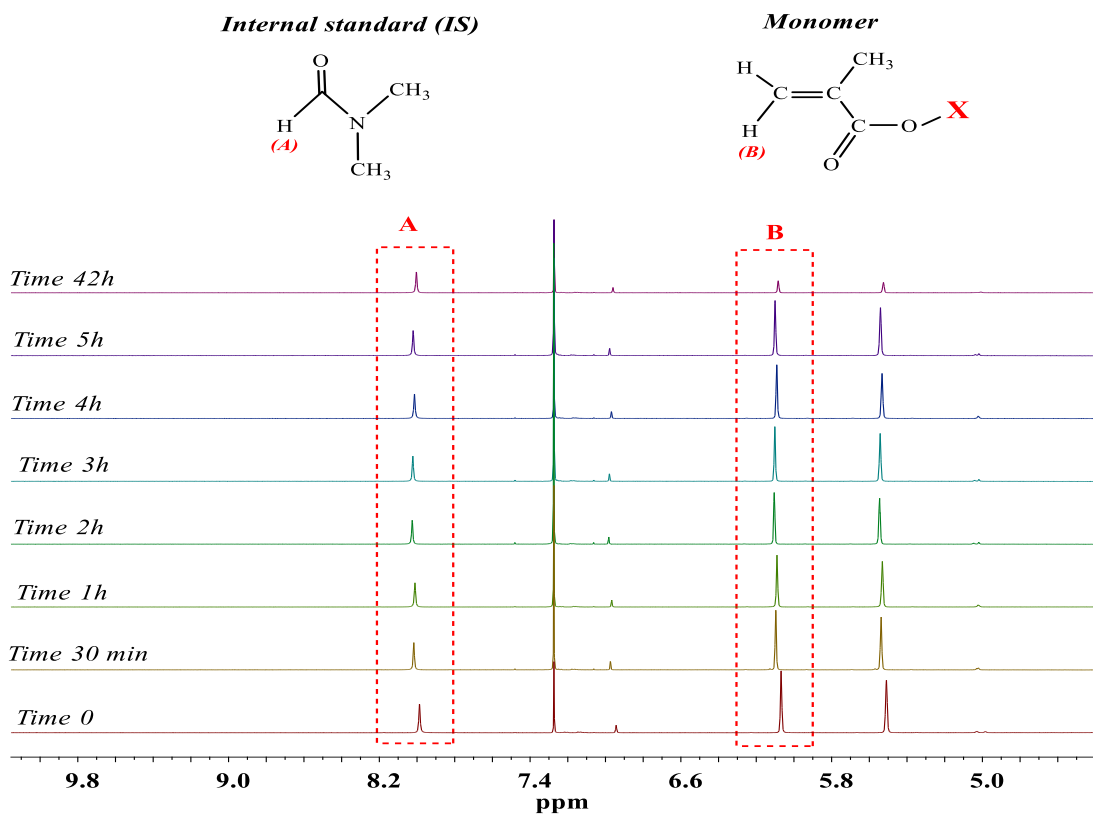
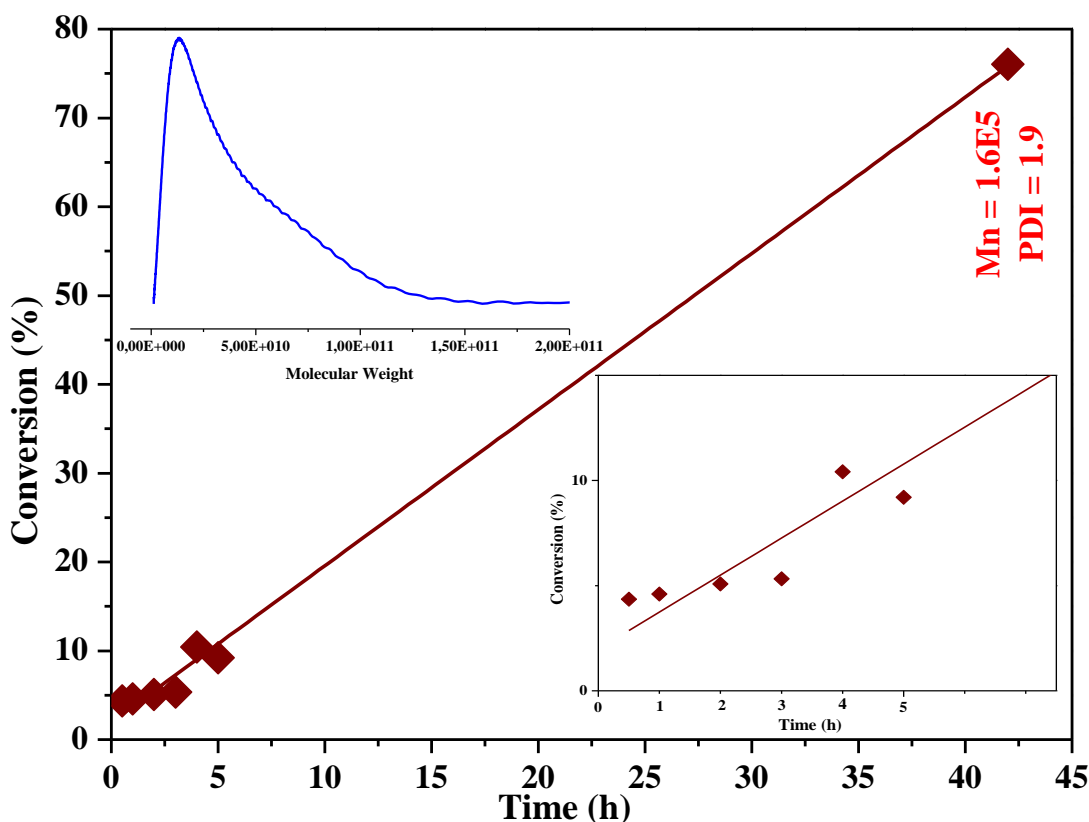


Figure 16 – Conversion over time for PDMSMA. Conditions: (PDMSMA):(CDTPA) = 200:1. All samples irradiated by Green LED lights. Measured by Chloroform GPC calibrated to PMMA standards, solvent for GPC: CHCl_3 .



In this case, the polymerization was very slow and we could not see any increase in the GPC curve from 1h until 5h, however, this reaction was allowed to continue for 42 hours and the conversion obtained was 76 %, so it was possible to observe this increase in MW in the curve on GPC for this time and we have determined $\bar{M}_n = 1.9$. Figure 16 shows the conversion obtained by ^1H NMR and data from GPC for 42 hours.

d) LMA: Lauryl Methacrylate

Figure 17 presents the structure of the monomer LMA.

Figure 17 – Structure of LMA

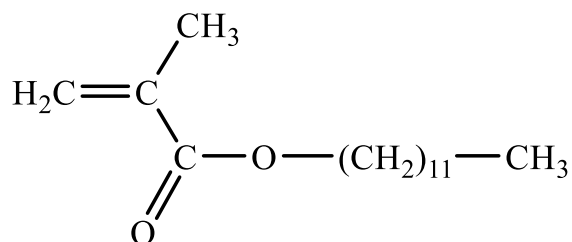


Figure 18 shows the ^1H NMR spectrum for Catalyst Free RAFT Polymerization using LMA and Figure 19 show all data obtained by GPC for this monomer.

Figure 18 – Kinetic spectra of ^1H NMR for LMA Catalyst Free RAFT Polymerization conversion: Calculated by ^1H NMR, solvent: CHCl_3 .

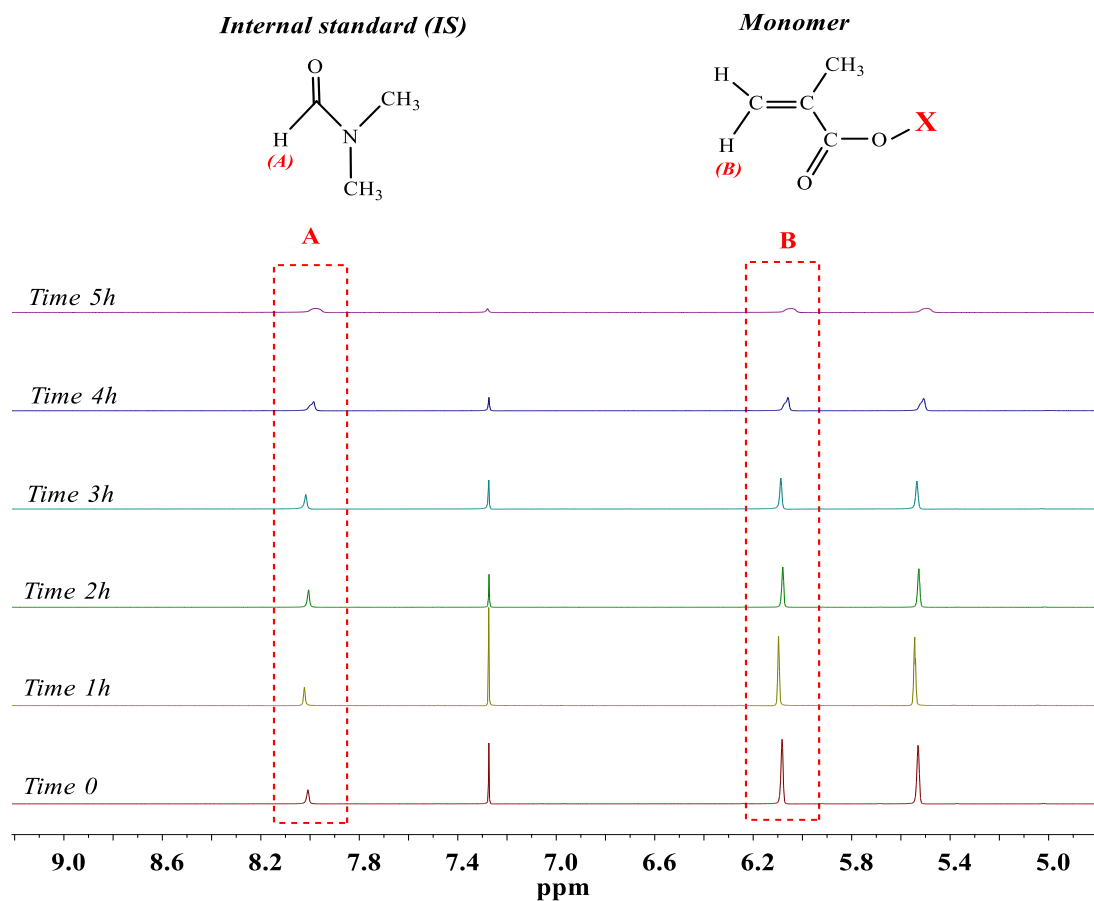
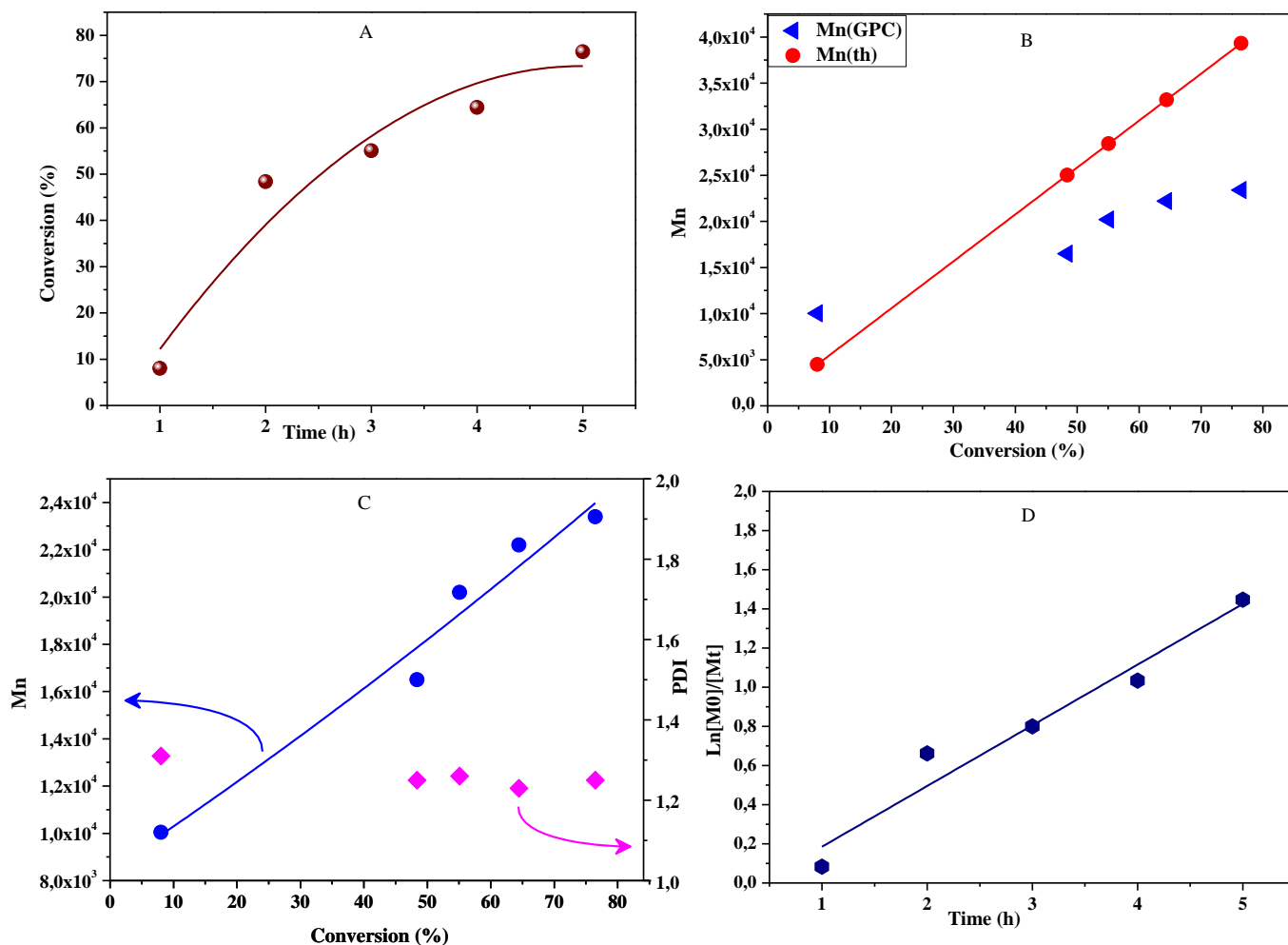


Figure 19 – Graphs A, B, C, D - Conditions: (LMA):(CDTPA) = 200:1. All samples irradiated by Green LED lights. Measured by Chloroform GPC calibrated to PMMA standards, solvent: THF.



Conversion by ¹H NMR (Figure 18) shows that, in this polymerization using LMA, the RAFT agent easily attached to the polymer chain, which reacts almost completely, with 75% conversion (Figure 19A).

The polymer MW values were close to linearity (theoretical MW) and the $D = 1.25$, showing the constancy of the growth of polymer chains formed, without variations in their molecular weights.

e) PEG₂MA:

Figure 20 presents the structure of the monomer PEG₂MA.

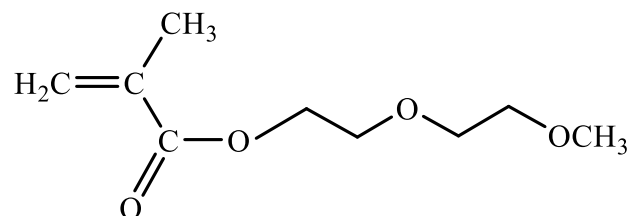
Figure 20 – Structure of PEG₂MA

Figure 21 shows the ¹H NMR spectrum for Catalyst Free RAFT Polymerization using PEG₂MA and Figure 22 shows all data obtained by GPC in graphs A, B, C and D.

Figure 21 – Kinetic spectra of ¹H NMR for PEG₂MA Catalyst Free RAFT Polymerization conversion: Calculated by ¹H NMR, solvent: DMSO-d⁶.

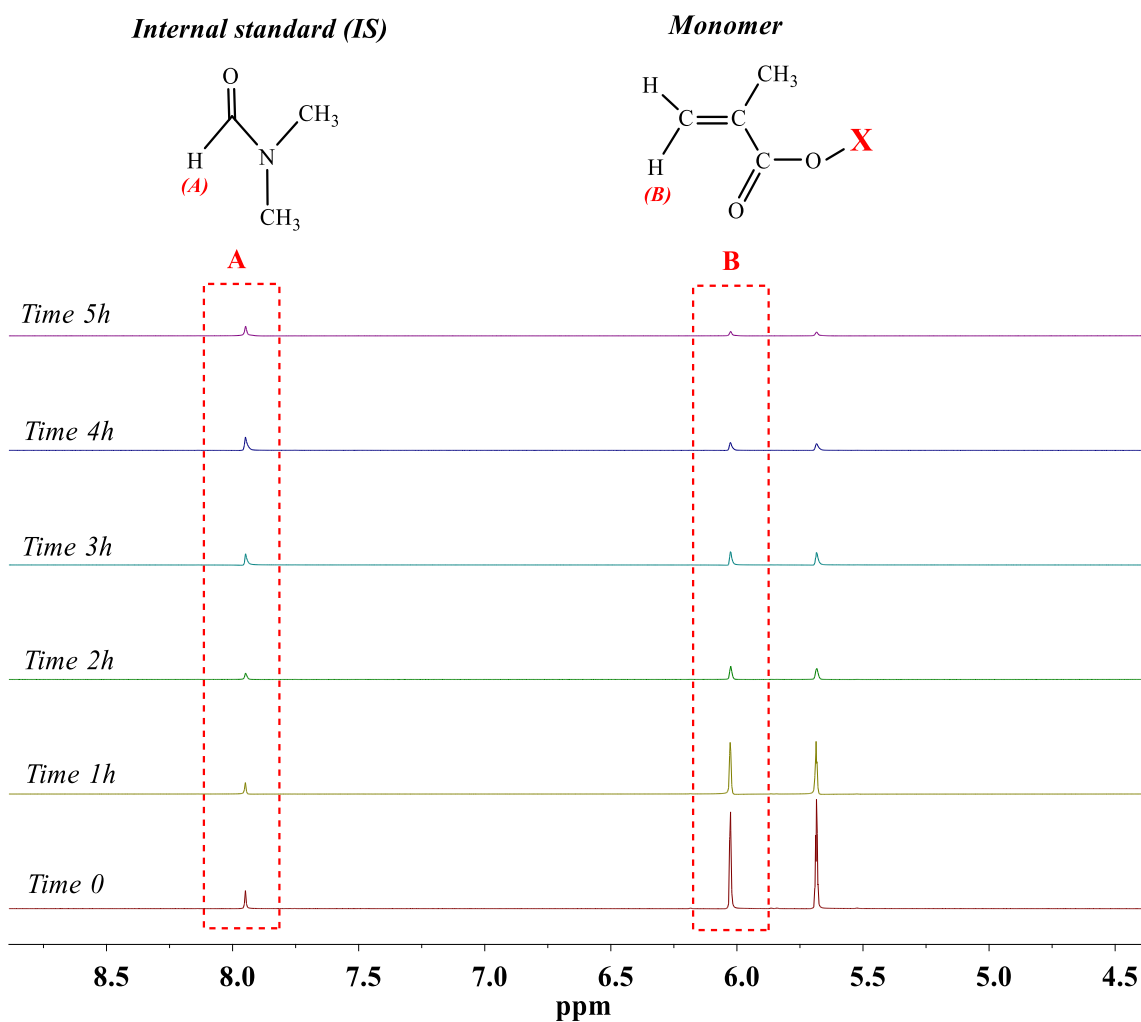
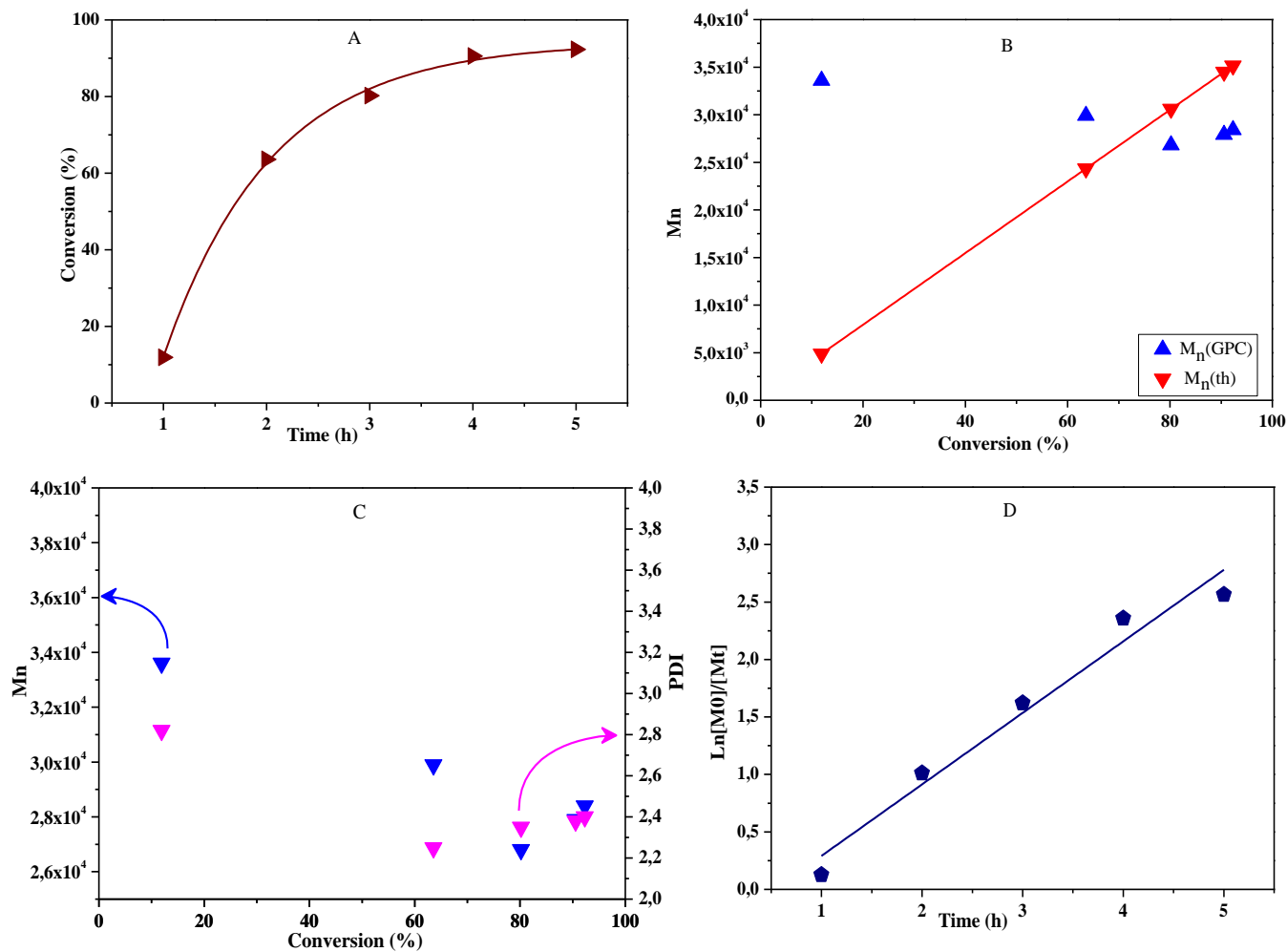


Figure 22 – Graphs A, B, C, D - Conditions: (PEG₂MA):(CDTPA) = 200:1. All samples irradiated by Green LED lights . Measured by Chloroform GPC calibrated to PMMA standards, solvent: DMF.



The polymerization reaction using PEG₂MA had a high conversion rate, 95%, as shown in graph A and can be seen by the kinetic spectra of ¹H NMR, by the decreasing peaks for both the proton A of the internal standard and proton B of the monomer.

Despite the high reaction yield, the change in the MW of the polymers obtained during the reaction were not close to linearity and, as a result, the polydispersity reached 2.4, indicating many polymer chains with different molecular weights.

f) DMAEMA:

Figure 23 presents the structure of the monomer DMAEMA.

Figure 23 – Structure of DMAEMA

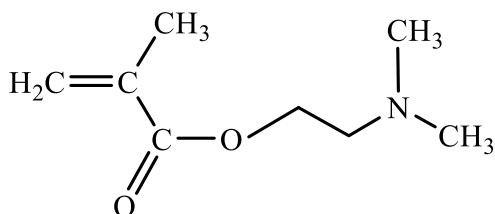


Figure 24 shows the ^1H NMR spectrum for Catalyst Free RAFT Polymerization using DMAEMA and Figure 25 shows all the data obtained by GPC.

Figure 24 – Kinetic spectra of ^1H NMR for PEG₂MA Catalyst Free RAFT Polymerization conversion: Calculated by ^1H NMR, solvent: CDCl_3 .

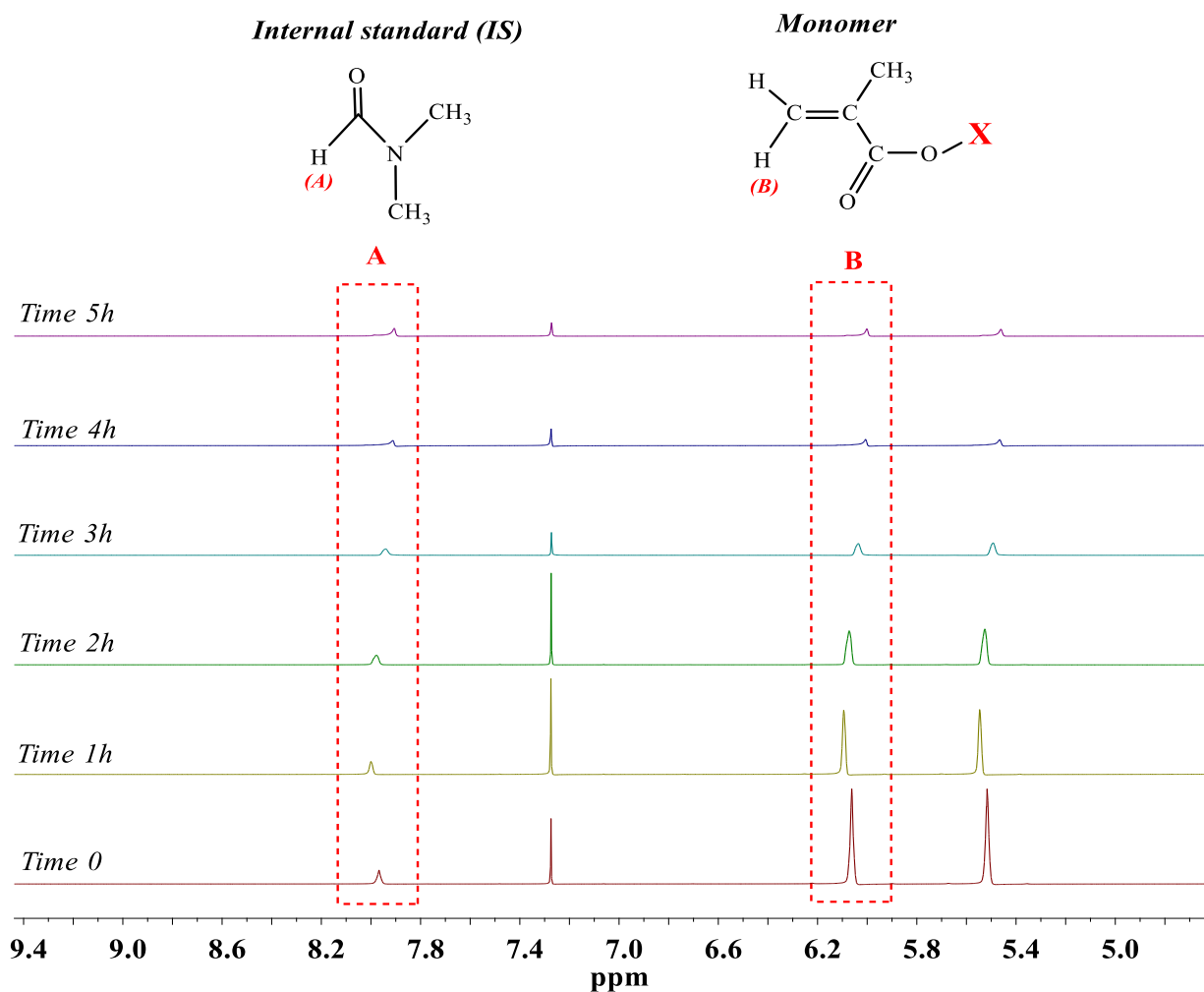
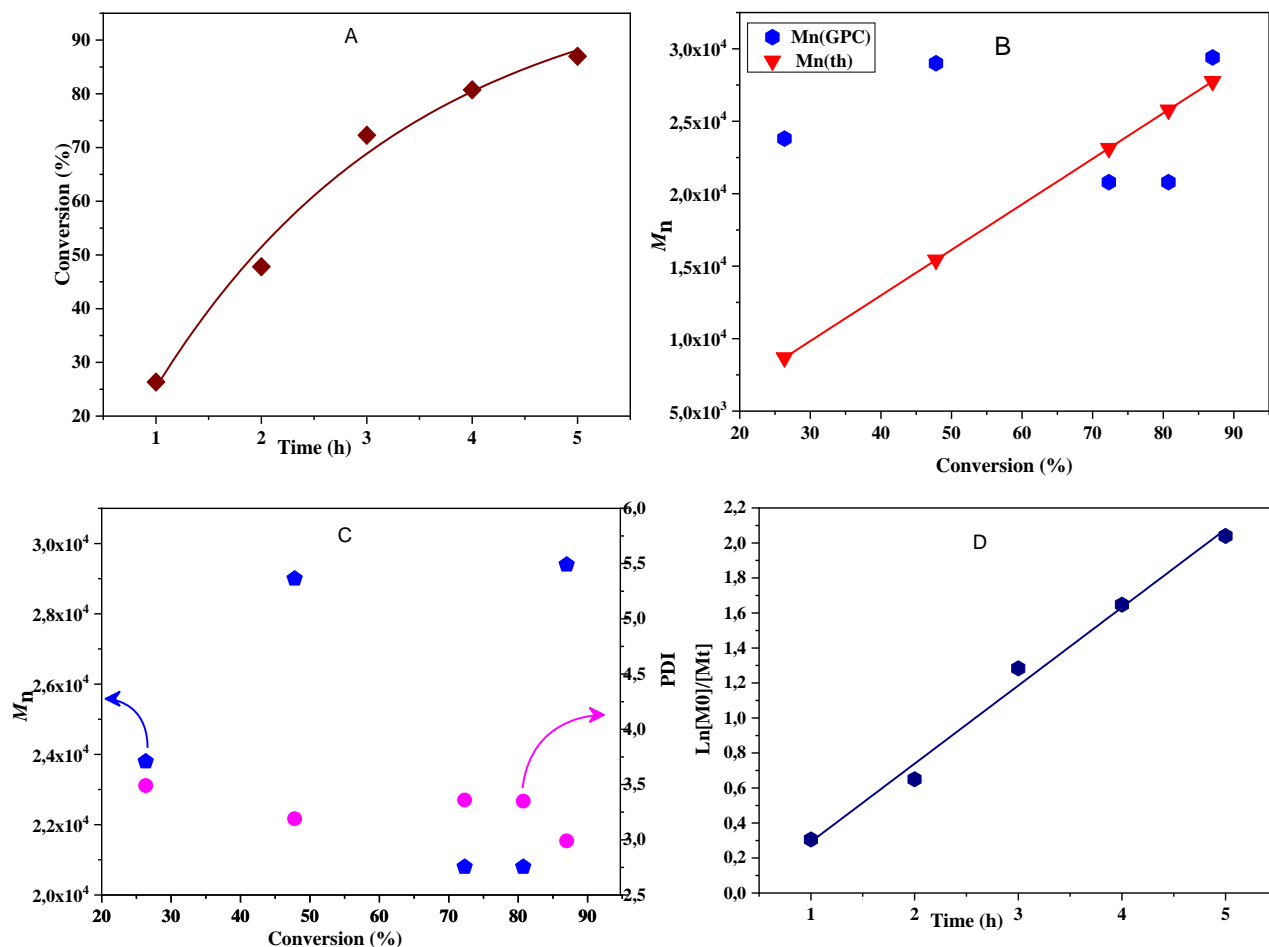


Figure 25 – Graphs A, B, C, D - Conditions: (DMAEMA):(CDTPA) = 200:1. All samples irradiated by Green LED lights. Measured by Chloroform GPC calibrated to PMMA standards, solvent: DMF.



As in polymerization reactions using PEG₂MA and BMA, the use of DMAEMA monomer resulted in a high conversion, 85%. The conversion by NMR, Figure 24, shows the decrease in peak intensity for the aromatic proton of RAFT at 8.0 ppm and the vinyl proton of DMAEMA at 6.0 ppm.

Even with attaining a high yield in this reaction, it was not possible to obtain polymers with similar molecular weight, which can be proven by the linearity deviation of the MW values

in relation to the theoretical MW (Figure 25B), in addition to the high polydispersity value, $D = 3.0$, observed for the final polymer.

g) Photo ATRP of PEG₃₀₀MA

Figure 26 shows the kinetic spectrum as measured by ¹H NMR and Figure 27 shows the system that I have used for this experiment and the first data obtained for conversion over time.

Figure 26 – Kinetic spectra of ¹H NMR for PEG₃₀₀MA photo ATRP Polymerization. Solvent: CDCl₃.

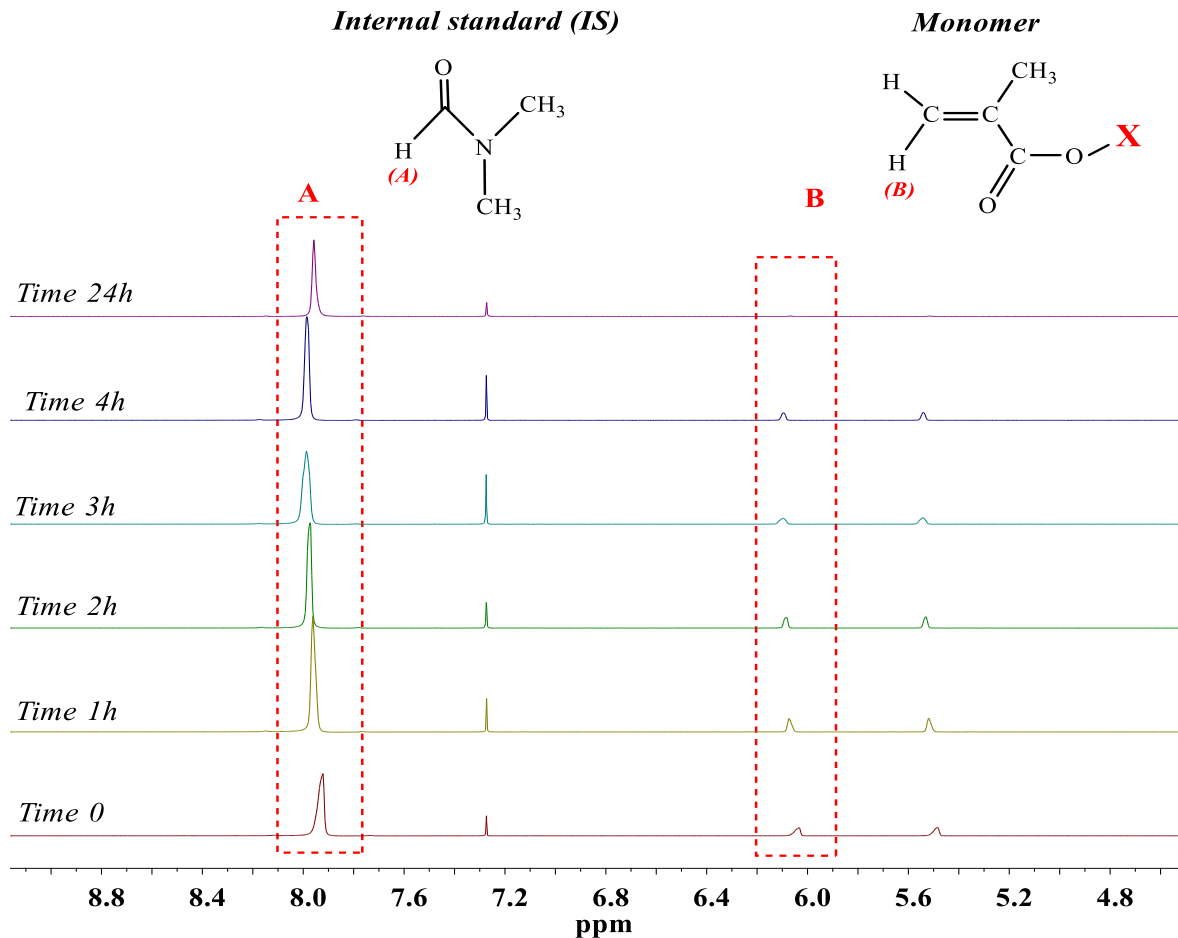
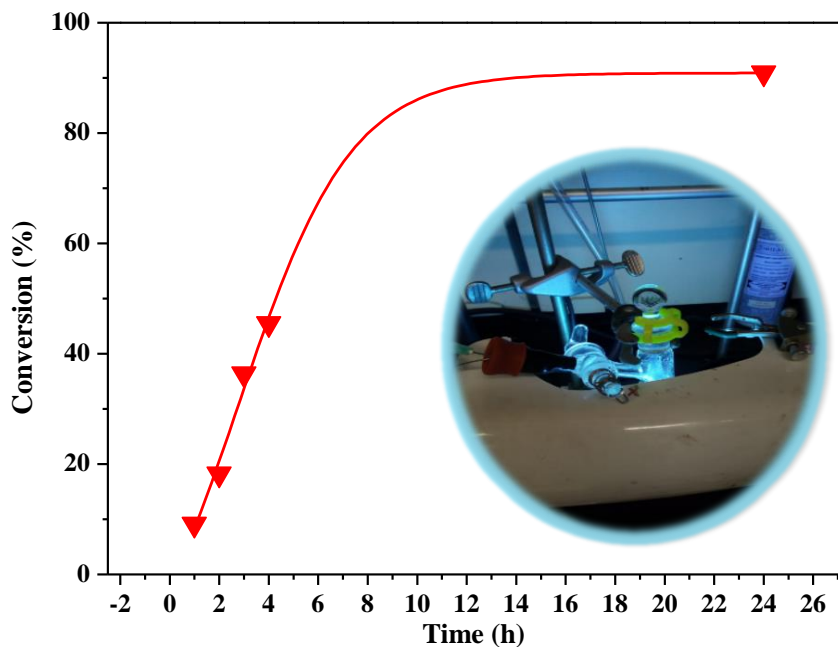


Figure 27 – Graph of conversion over time. Conditions: (PEG₃₀₀MA):(EBiB) = 50:1. All samples irradiated by UV light (365 nm).



The kinetic study for PEG₃₀₀MA photo ATRP Polymerization revealed a distinct profile of the PEG₃₀₀MA by RAFT polymerization kinetics. In the reaction in question, the reaction was initially fast up to 4 h of reaction and ended after 24 h, with a final conversion of 90%. However, after 4 h of reaction, the polymerization begins to deviate from linearity, indicating a varied concentration of radical species.

The PEG₃₀₀MA photo ATRP polymerization reaction, despite taking a longer time to finish, proved to be more efficient reaction compared to the PEG₃₀₀MA by RAFT polymerization because, in addition to the high yield, at the end of the reaction all the monomer was consumed.

3.2 EXPERIMENTS FOR CALCULATION OF TRANSFER COEFFICIENT

3.2.1 Experimental Procedures and calculations of Cs for FRP

All experiments were conducted under green light and six different methacrylate monomers with different substituents were used. The experiments with BA were repeated several times in order to obtain polymers with low conversion, however, due to the reaction rate being very fast, this was not possible. Since then, an experiment has been carried out using the proportion of EBiB = 10, but the conversion of monomer to polymer was not observed and, because of this, the proportion was increased with time and three different proportions of EBiB = 100, 150 and 200 were used for FRP. The experiments were called Round 1 and Round 2 and follow the procedures detailed below:

- Round 1: BA monomer, internal standard (anisole) and AIBN were placed in a Schlenk flask and the frozen solution was degassed for 1 hour, after which EBiB was added and the reaction started by heating the flask to 60 °C for five hours.

- Round 2: The solution was prepared using all reagents (monomer, IS, AIBN and EBiB) and, unlike Round 1, the freeze pump cycle was carried out four times and the reaction started at 60 °C. This same experiment was also performed without using EBiB to check if AIBN was initiating the reaction.

A third experiment was carried out using the same conditions as in Round 2, but using MMA as the monomer.

3.2.1.1 Experiments for Butyl Acrylate (BA - Round 1)

All conditions used in these experiments are described in the Tables 8, 9 and 10.

Table 8 – Conditions used in FRP of BA using EBiB ratio 100

Materials	Eq	mol	Mn	Mass (g)	ρ stock (g/mL)	V (mL)	V_{total}	Concentration (mol/L)
Butyl Acrylate	1500	0.027404	128.17	3.512362	0.894	3.9288	19.6441	1.3950
AIBN	1	1.83E-05	164.21	0.003				0.000917
EBiB	100	0.001827	195	0.356251	1.33E+00	2.68E-01		0.09175
Anisole	v/v %	78.92303				15.7153		

Table 9 – Conditions used in FRP of BA using an EBiB ratio of 150

Materials	Eq	mol	Mn	Mass (g)	ρ stock (g/mL)	V (mL)	V_{total}	Concentration (mol/L)
Butyl Acrylate	1500	0.027404	128.17	3.512362	0.894	3.9288	19.6441	1.39502
AIBN	1	1.83E-05	164.21	0.003				0.000911
EBiB	150	0.00274	195	0.534377	1.33E+00	4.02E-01		0.136704
Anisole	v/v %	78.39535				15.7153		

Table 10 – Conditions used in FRP of BA using an EBiB ratio of 200

Materials	Eq	mol	Mn	Mass (g)	ρ stock (g/mL)	V (mL)	V_{total}	Concentration (mol/L)
Butyl Acrylate	1500	0.027404	128.17	3.512362	0.894	3.9288	19.6441	1.3950
AIBN	1	1.83E-05	164.21	0.003				0.000905
EBiB	200	0.003654	195	0.712502	1.33E+00	5.36E-01		0.181062
Anisole	v/v %	77.87467				15.7153		

3.2.1.2 Experiments for Butyl Acrylate (BA - Round 2)

In this second experiment, the same conditions as in BA- Round 1 were used. Also, in this case, an additional experiment was carried out where EBiB was not added in order to check if AIBN was initiating the reaction.

3.2.1.3 Experiments for Methyl Methacrylate (MMA)

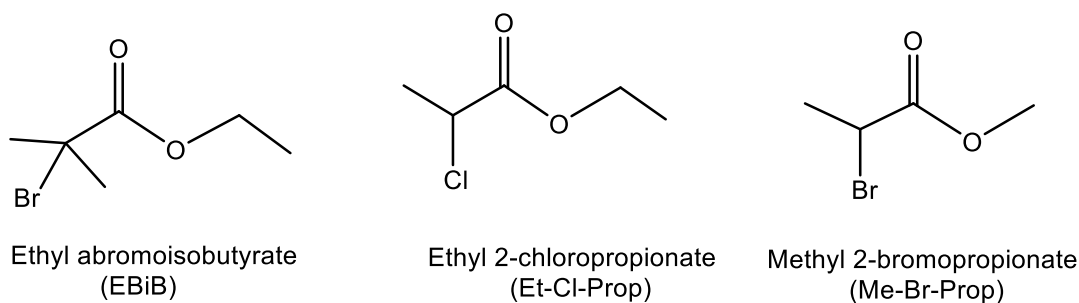
In this experiment, the same conditions as in BA-Round 2 were used, the reaction ran in the same way.

3.2.1.3.1 Calculation of Transfer Coefficient for different transfer agents: EBiB, Et-Cl-Prop and Me-Br-Prop.

Polymerizations of MMA by FRP were carried out to calculate the transfer coefficient of ATRP initiators. The values for transfer coefficients were 0.0163, 0.0277 and 0.0321 for tertiary radical (EBiB) and secondary radical with Cl and Br (Et-Cl-Prop and Me-Br-Prop), respectively, which were used to compare how fast these types of radical transfer/polymerization reaction occurred. It was not possible to obtain any polymer in the reaction carried out under ambient light with EBiB, so for these experiments a foil was used, but the opposite happened for both Et-Cl-Prop and Me-Br-Prop, in the dark there were some oligomers, but under ambient light there was the presence of the polymer.

The structures for both transfer agents in FRP are showed below in Figure 28.

Figure 28 – Structures of different transfer agents used by FRP.



The tertiary radical, should be more stable than a secondary radical. The secondary radical is more unstable and cannot "live" for a long time in the reaction, so it must be more reactive with the monomer because the radical does not survive for a long time in the reaction medium, which causes the reaction to occur more quickly

The transfer mechanism for agent transfers can be observed in Figure 29.

Figure 29 – Example of transfer to EBiB.

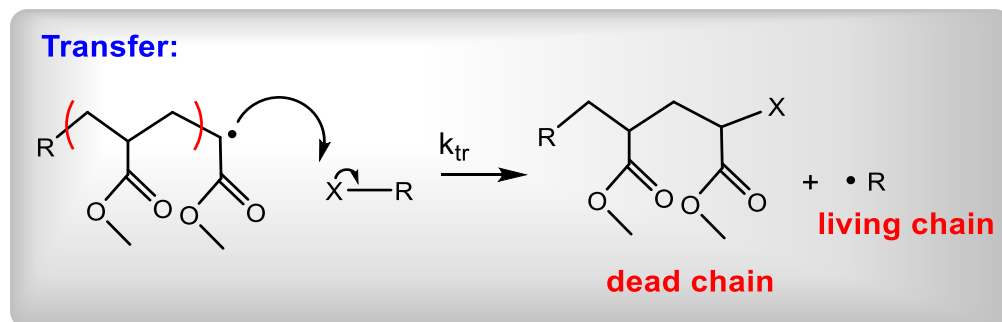


Table 11 shows the conditions used for all experiments.

Table 11 – Conditions used for determination of the Transfer Coefficient for three different Transfer Agents: EBiB, Et-Cl-Prop and Me-Br-Prop.

	Transfer Agent (TA)								
	EBiB			Et-Cl-Prop			Me-Br-Prop		
(MMA/TA)	30	150	-	30	150	-	15	150	-
(MMA)	1.88	1.88	1.88	1.88	1.88	1.88	1.88	1.88	1.88
(TA)	0.062	0.012	-	0.062	0.012	-	0.123	0.012	-
TA Ratio (X)	50	10	-	50	10	-	100	10	-

* All experiments were conducted for 45 minutes in 60 °C by FRP, IS=Anisole ~ 80%, Initiator: AIBN, Monomer MMA - AIBN:MMA:TA - 1:1500:X.

3.2.1.3.2 Calculation of Transfer Coefficient by FRP without TA

Polymerizations of MMA by FRP were carried out to calculate the transfer coefficient of ATRP initiators without transfer agent. This experiment was repeated twice to check the reproducibility of the preparation of polymers without a transfer agent. Table 12 shows the conditions that were used.

Table 12 – Conditions used for polymerization by FRP without Transfer Agent (TA)

45 min	Transfer Agent (TA)								
60 °C	EBiB			Et-Cl-Prop			Me-Br-Prop		
(MMA/TA)	30	150	-	30	150	-	15	150	-
(MMA)	1.88	1.88	1.88	1.88	1.88	1.88	1.88	1.88	1.88
(TA)	0.062	0.012	-	0.062	0.012	-	0.123	0.012	-
Anisole (mL)	3.8								
MMA (mL)	0.97								

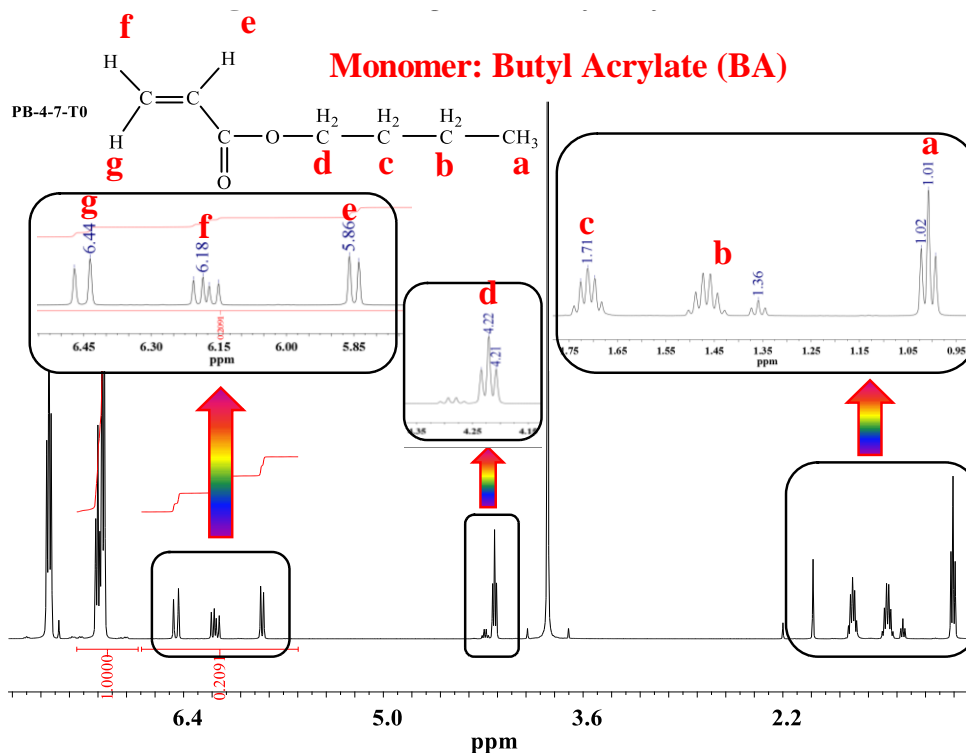
* All experiments were conducted for 45 minutes in 60 °C by FRP, IS=Anisole ~ 80%, Initiator: AIBN, Monomer MMA - AIBN:MMA:TA - 1:1500:0/ 1 mg: 0.97 mL.

3.2.2 Results and discussion

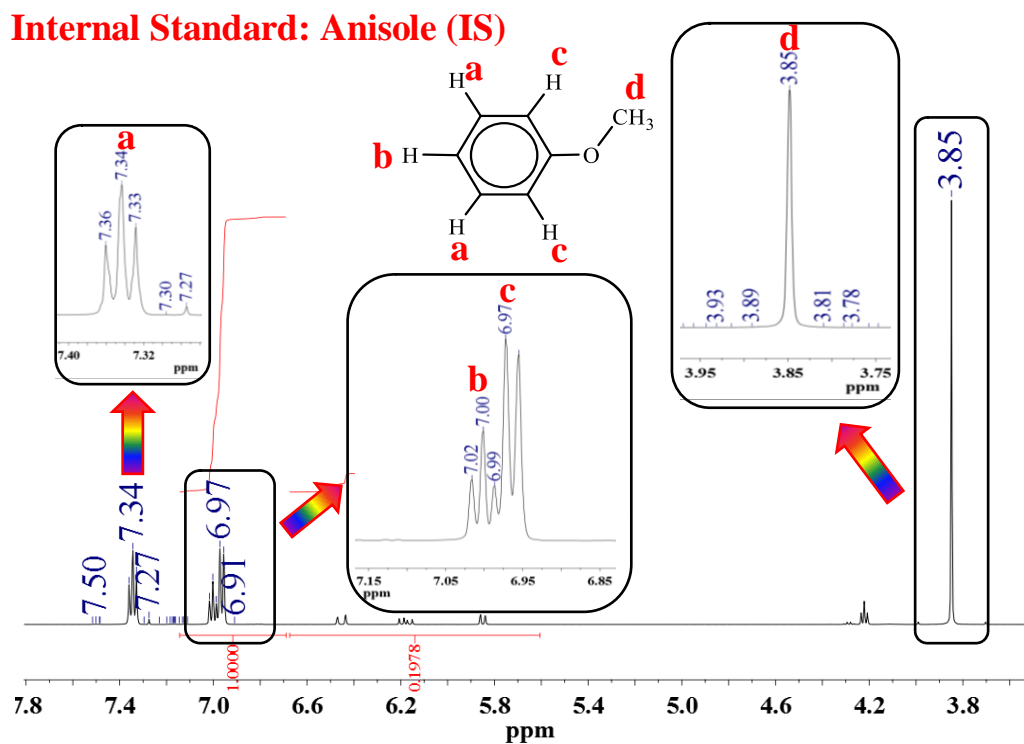
All results obtained for this series of experiments are shown below. In addition, some ¹H NMR spectra are shown in order to demonstrate how the conversion was calculated by the NMR ratio of the internal standard and the monomer. The conversion plots as well as GPC data and Cs calculations are also shown below.

3.2.2.1 Experiments for Butyl Acrylate (BA - Round 1)

Figure 30 shows the ¹H NMR spectrum obtained from butyl acrylate.

Figure 30 – ^1H NMR spectra for Butyl Acrylate (BA).

In the spectrum of monomer BA, the signals referring to protons **a**, **b** and **c** are at 1.01, 1.36 and 1.71 ppm, respectively, and are more shielded in relation to the **d** proton, at 4.21 ppm of the CH_2 group bonded to oxygen, which causes deshielding, and which is more accentuated in protons **e**, **f** and **g** in 5.86, 6.18 and 6.44 ppm because they suffer the steric effect of the neighboring groups. On the other hand, it is important to note that the movement of pi electrons is capable of promoting the anisotropy effect. Furthermore, it should be noted that the chemical shift does not depend on the steric effect, but on the electron-donating and electron-withdrawing effect. Note that for D group, the donor effect can activate the ortho and para positions as the D group does not donate electrons to the meta position.

Figure 31 – ^1H NMR spectra for Anisole in the time zero of the reaction.

In the case of the anisole molecule (Figure 31), the internal standard, the inductive effect of the $-\text{OCH}_3$ group prevails over the mesomeric effect, that is, oxygen removes electronic density from the aromatic ring and, therefore, the protons of this group (**d**) are more shielded and protons **a** and **b** are deshielded. The protons **a** undergo greater shift due to the high steric effect of the surrounding groups.

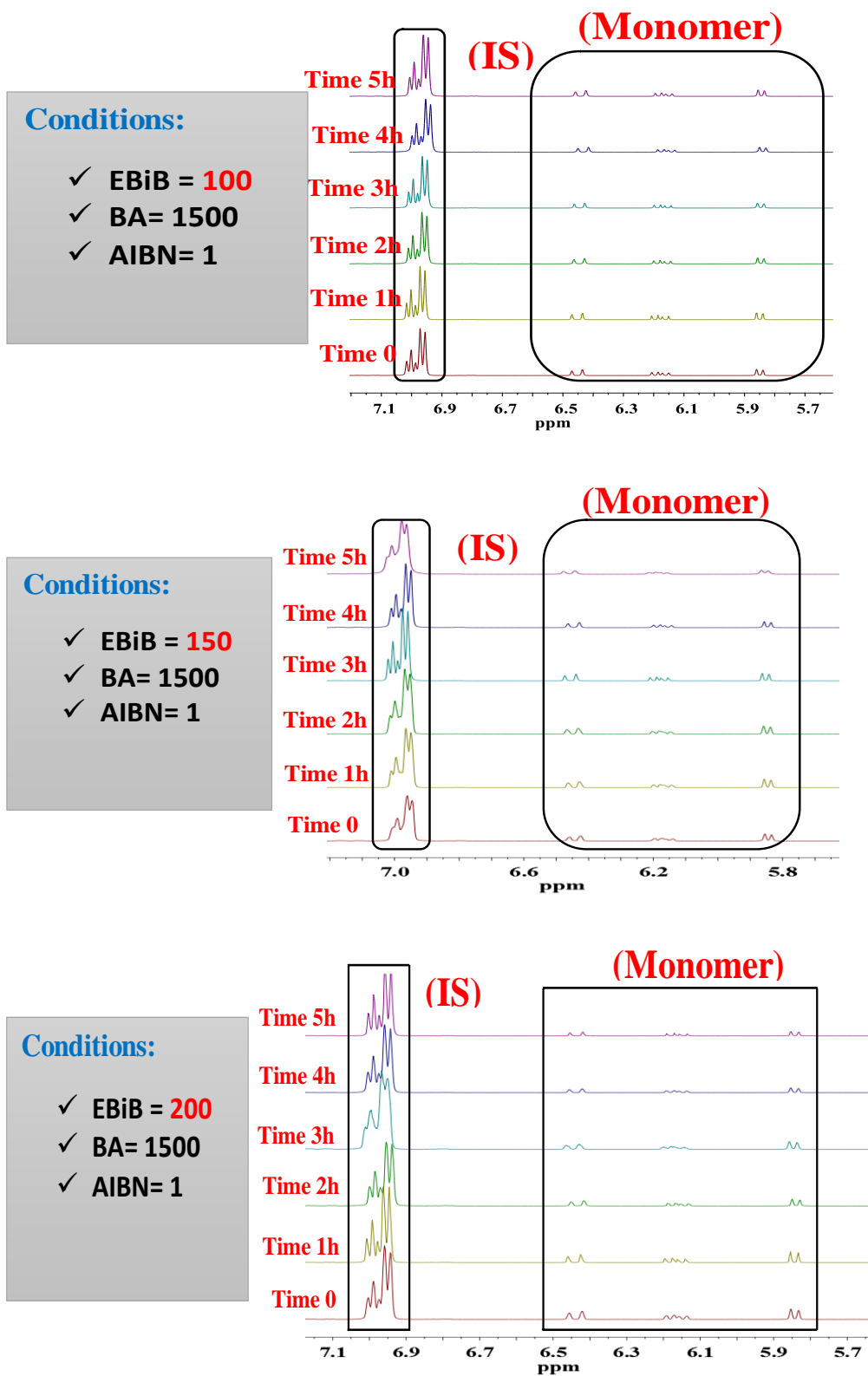
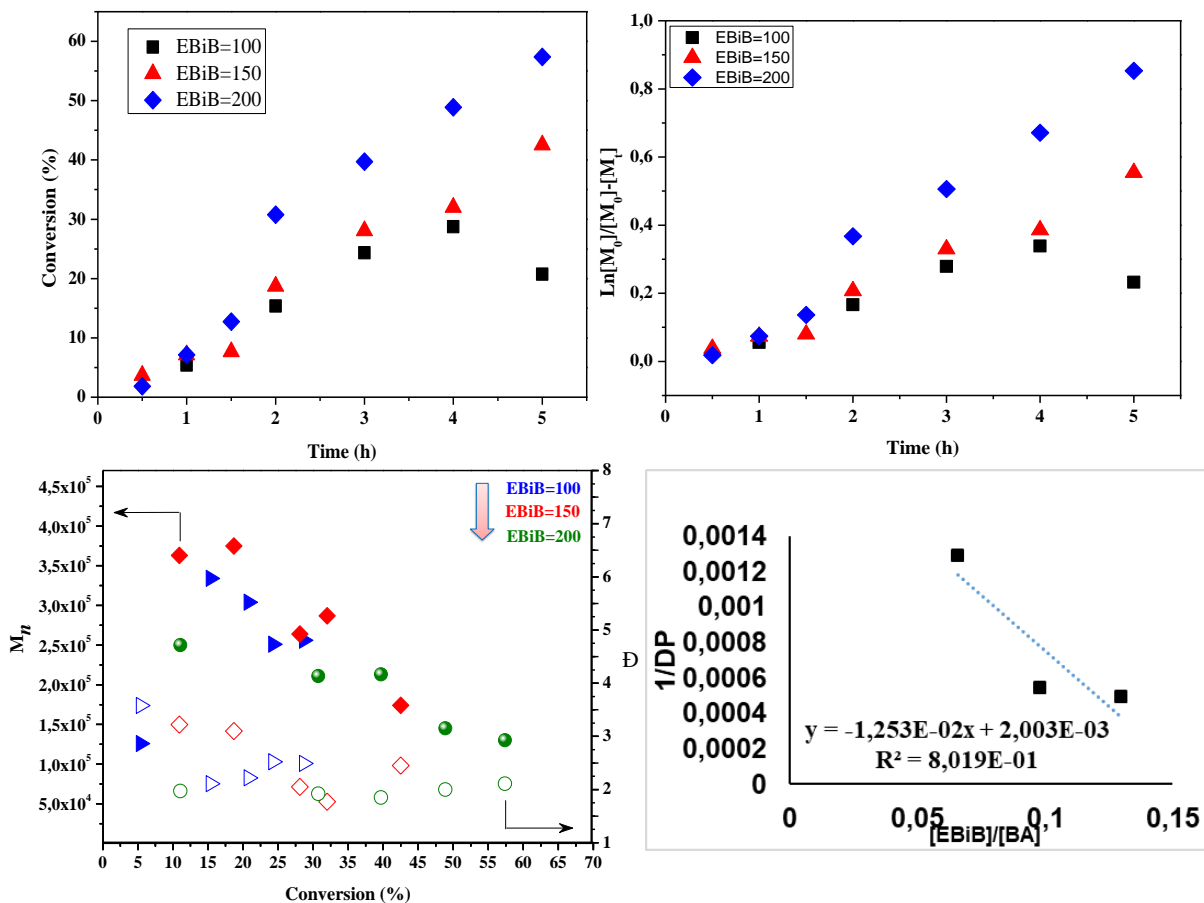
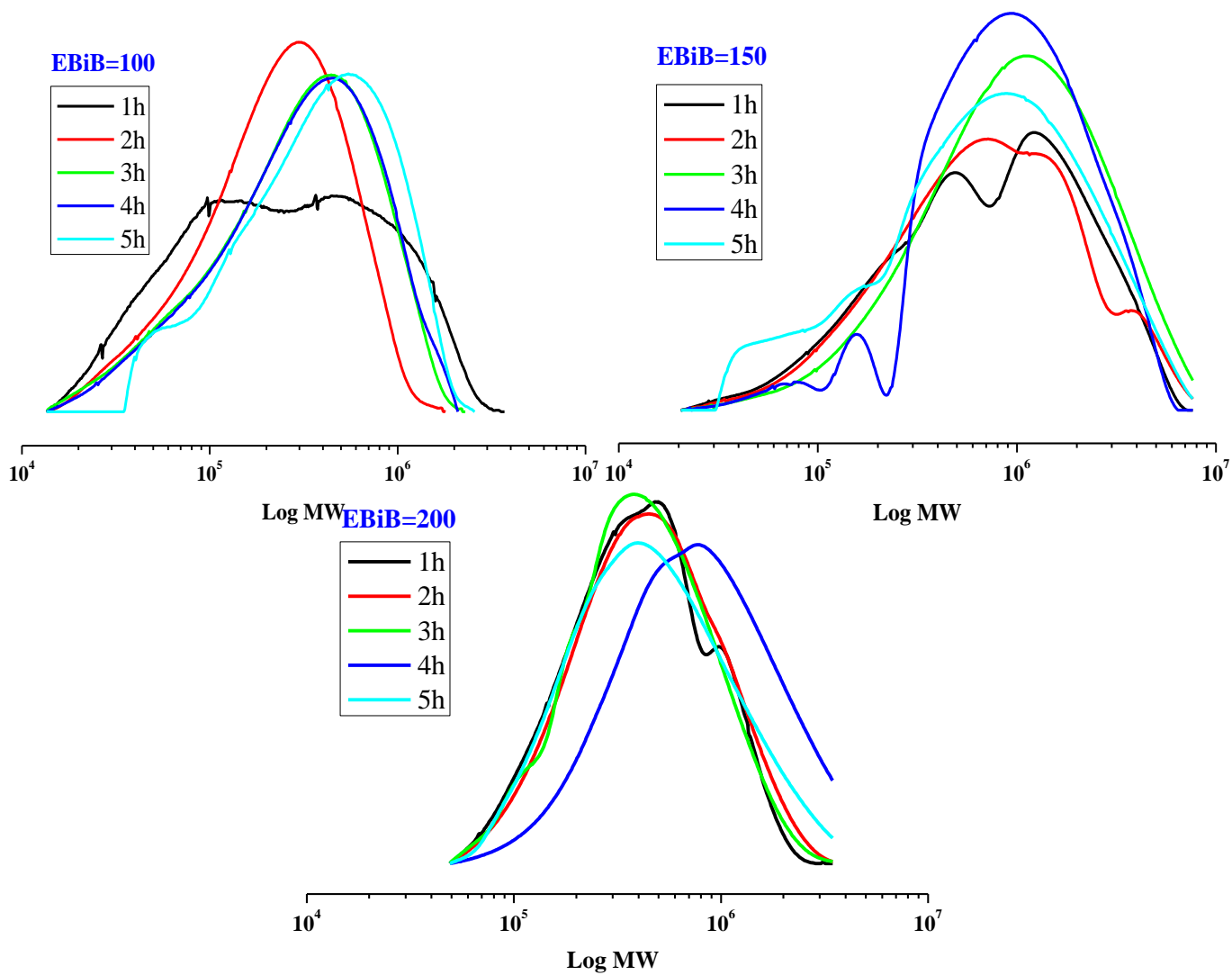
Figure 32 – Kinetics of FRP by ^1H NMR spectra for BA with different EBiB ratio (round 1).

Figure 33 – Graphs of Conversion, Ln, M_n and Cs for BA.

In the first case, the conversion increased with ratio of EBiB and a non-linear behavior in the graph of Ln indicates that there was an increase in the concentration of radical species, thus, slow initiation. In the other hand, it would be expected that the opposite behavior would be presented for the concentration behavior since an increase of the number of radical species would generate an increase of termination reactions, thus, low conversion due to high concentrations of EBiB. Then, this experiment was repeated and it was possible get better results in Round 2 which are presented in the next topic. The GPC curves for these experiments are presented in Figure 34.

Figure 34 – GPC curves for BA Round 1.



2.2.2.2 Experiments for Butyl Acrylate (BA - Round 2)

Figure 35 presents the kinetics of FRP for second experiment (Round 2).

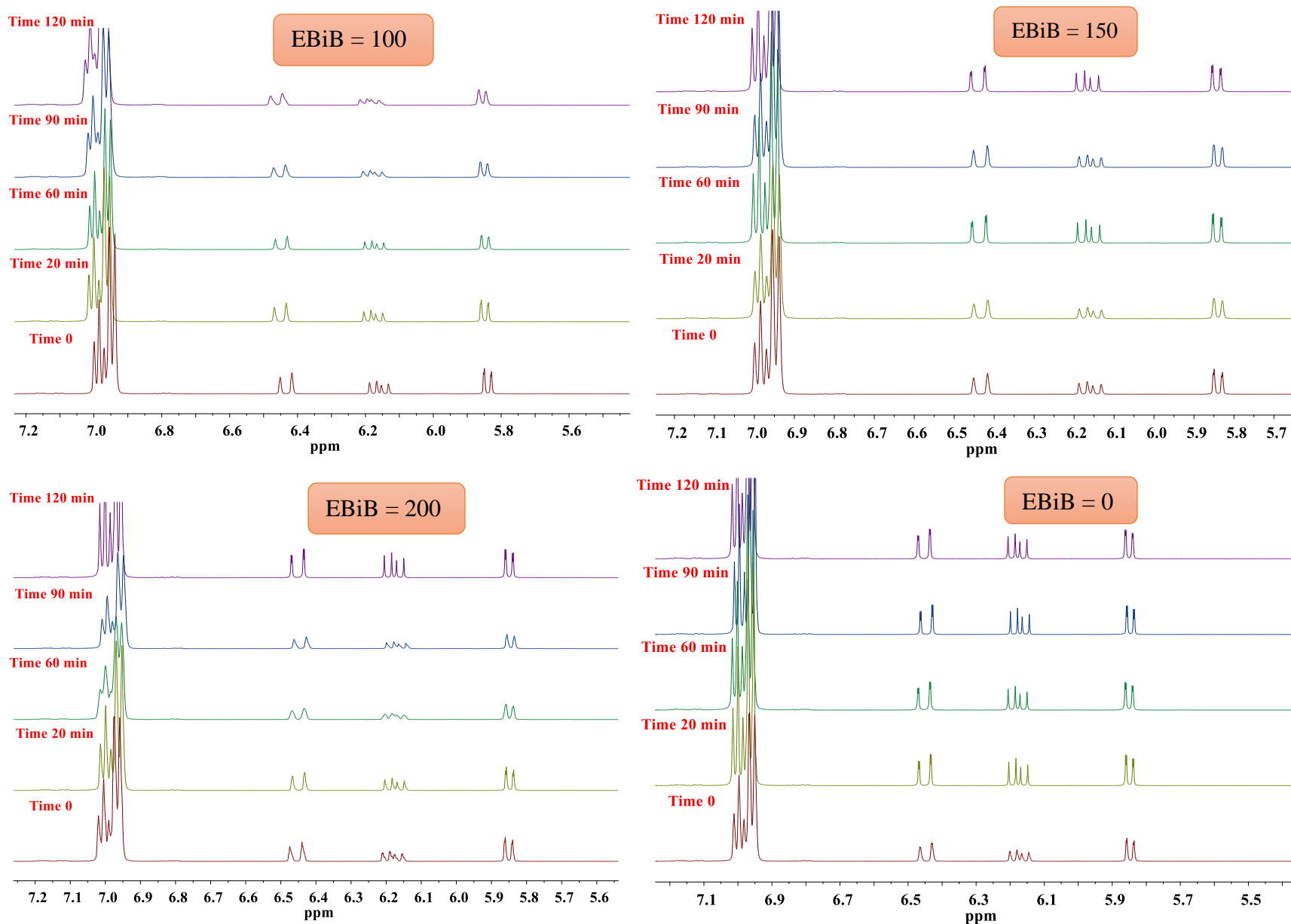
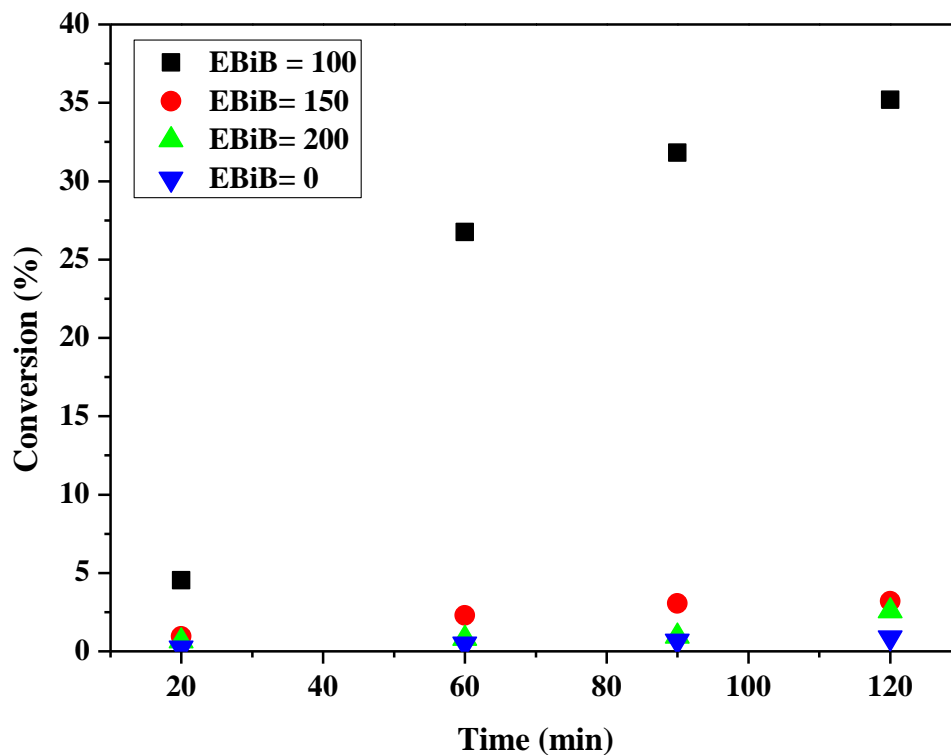
Figure 35 – Kinetics of FRP by ^1H NMR spectra for BA with different EBiB ratio (round 2).

Figure 36 shows the conversion over time for all experiments with different EBiB ratios and without EBiB.

Figure 36 – Conversion of polymer for BA.

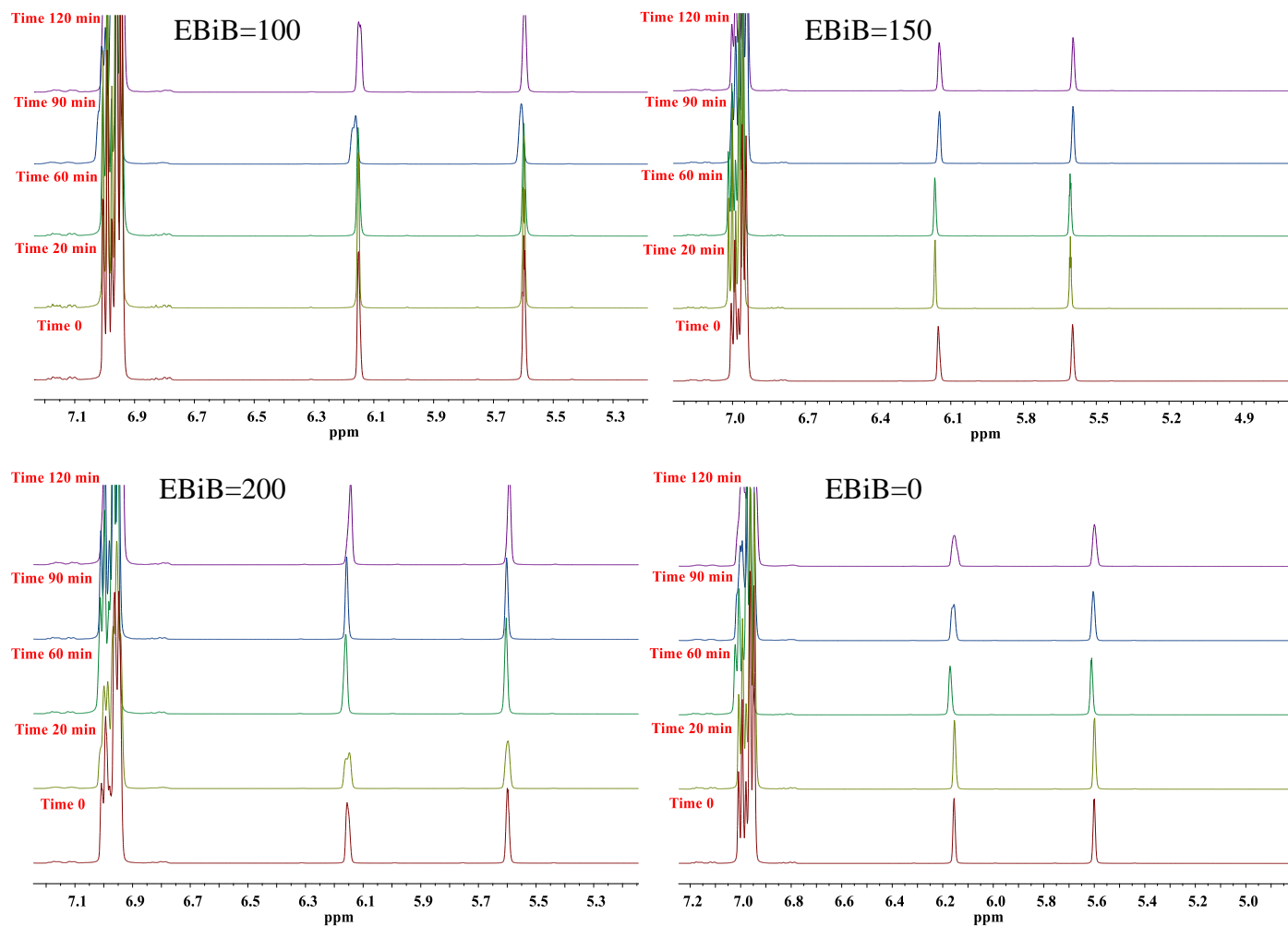


The result obtained was expected, and in fact a lower concentration of radicals decreased termination reactions which favored the increase of conversion for EbiB = 100. It is also observed that the AIBN does in fact initiate the reaction, it seems that the reaction became more homogeneous when it was added EBiB and the other reagents at the same time.

3.2.2.1.1 Experiments for Methyl Methacrylate (MMA)

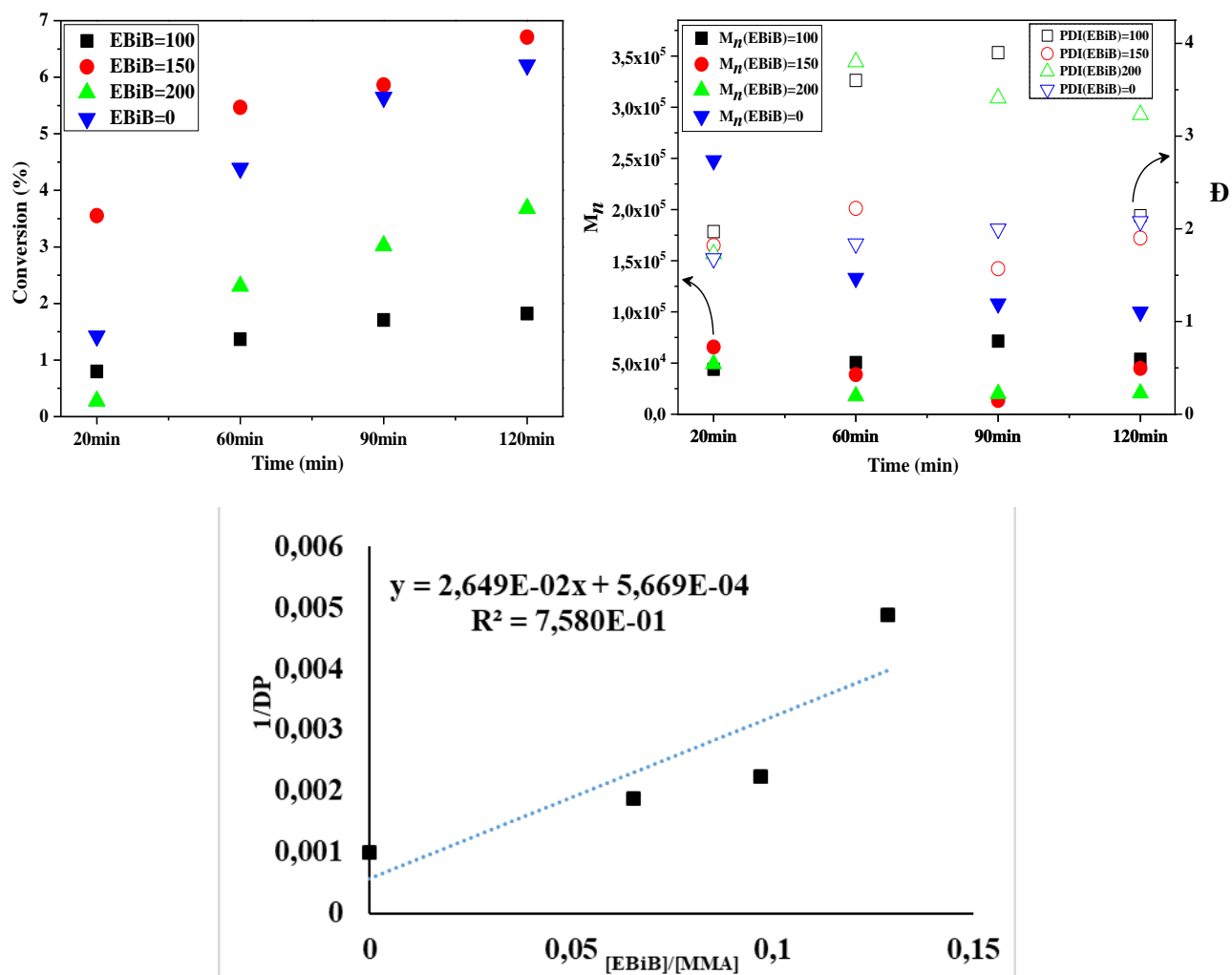
The Figure 37 shows the ^1H NMR spectra for this experiment.

Figure 37 – Kinetics of FRP by ^1H NMR spectra for MMA with different EBiB ratio and without EBiB.



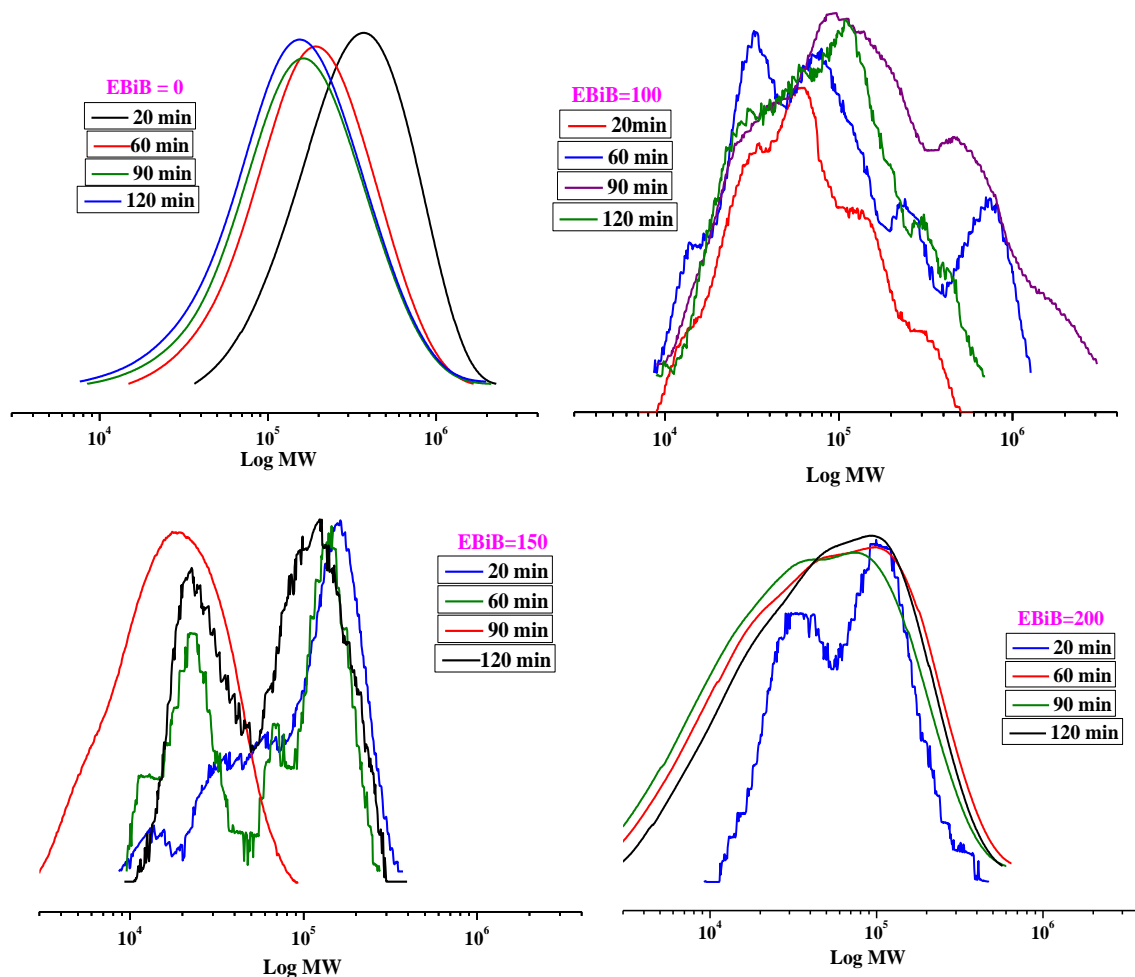
The Figure 38 shows the graphs for conversion and GPC data for this experiment.

Figure 38 - Graphs of conversion, GPC data and Cs calculation for MMA.



All polymers were injected into GPC and the Figure 39 shows the GPC curves to this data.

Figure 39 - GPC curves for FRP by MMA.



3.2.2.1.2 Calculation of Transfer Coefficient for different transfer agents: EBiB, Et-Cl-Prop and Me-Br-Prop.

All results of polymerization are showed in the Table 13.

Table 13 – Results for Transfer Coefficient for three different Transfer Agents: EBiB, Et-Cl-Prop and Me-Br-Prop

	Transfer Agent (TA)								
	EBiB			Et-Cl-Prop			Me-Br-Prop		
(MMA/TA)	30	150	-	30	150	-	15	150	-
Mol Wt x 10 ⁵	1.05	1.82	2.48	7.67	1.88	2.48	0.4	2.23	2.48
% C	4	3.5	1.4	1.1	1.6	1.4	2.2	2.1	1.4
Transfer Coefficient (Cs)	0.01626			0.02774			0.03209		

In the first case, for EBiB the $C_s = 0.0163$, it seems that for each transfer, which seems quite high since for each 60 monomer chain there is a transfer of Br. Also, it corresponds pretty well with C_s of 0.00147 for MA under UV.

This reaction was also carried out in the dark since it was not possible to get good results in the presence of light, it was observed high conversion and formation of oligomers under ambient light. Thus, EBiB was purified and maintained under foil for 45 minutes of reaction. All initiators were purified by passing them through a basic alumina plug before use. Figure 40 shows the C_s plot for EBiB and Figure 41 shows GPC traces for the polymerizations.

Figure 40 – Transfer Coefficient for MMA and EBiB in the Dark.

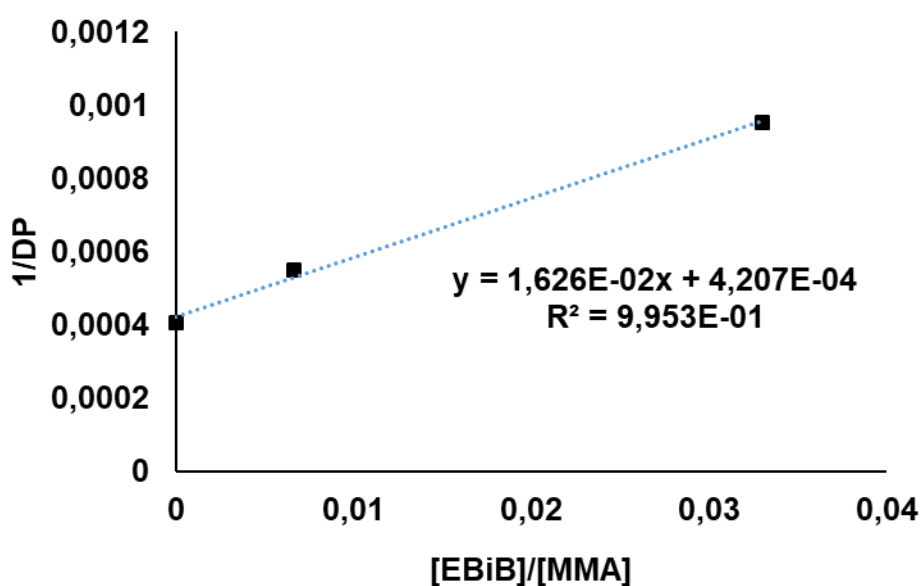
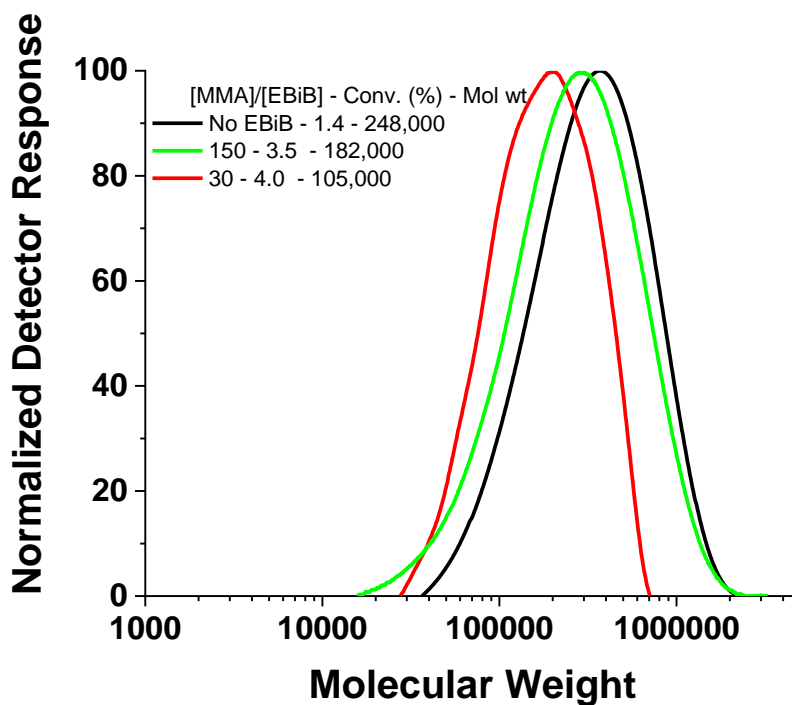


Figure 41 – GPC traces for polymerization by FRP with MMA and EBiB in the dark.



For Et-Cl-Prop ($C_s = 0.0277$) a higher value for C_s should be expected since it was worked on a secondary radical, this should be less stable than EBiB and maybe this implies a greater reactivity with the monomer for a short time. In this case, it seems that for each 36 monomer chains there is a transfer of Cl from a secondary radical.

Figure 42 shows the slope for Et-Cl-Prop and Figure 43 shows GPC traces for the polymerizations.

Figure 42 – Transfer Coefficient for MMA and Et-Cl-Prop - Ambient Light.

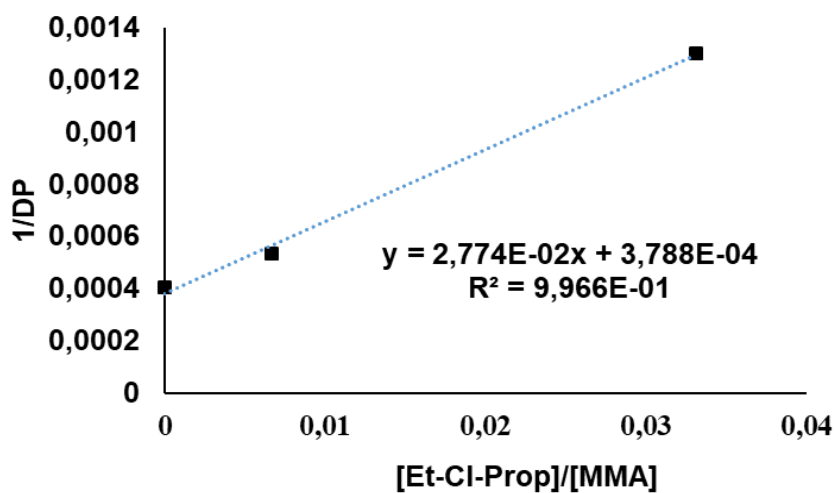
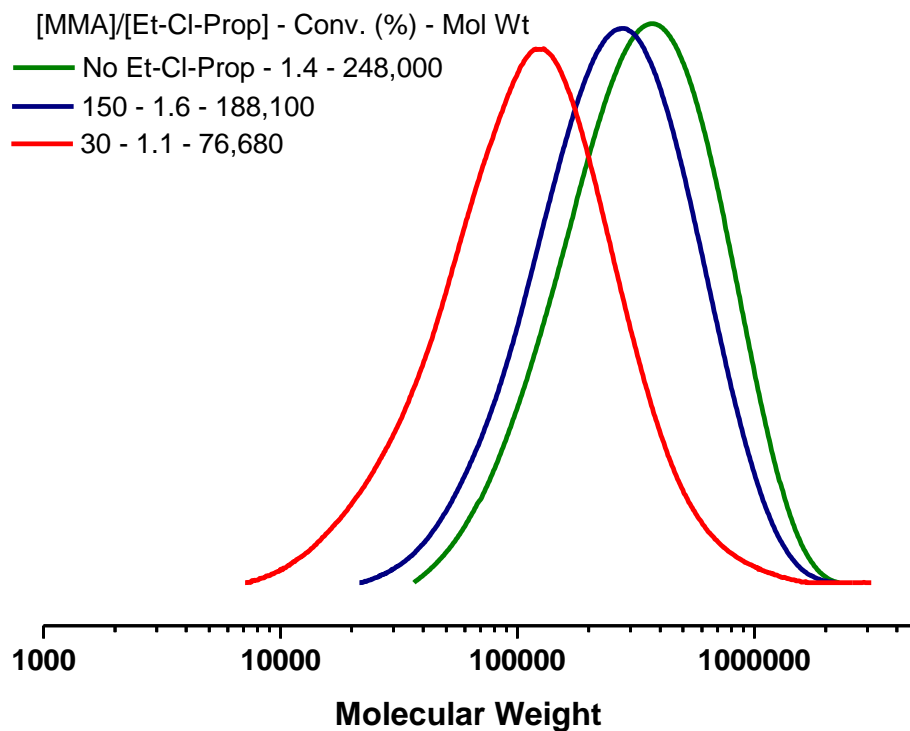


Figure 43 – GPC traces for polymerization by FRP with MMA and Et-Cl-Prop - ambient light.



The value calculated for Me-Br-Prop was $C_s = 0.03209$. Since it was worked on a secondary CTA this should be less stable than EbiB. In this case, it seems that for each 31 monomer chains there is a transfer of -Br from a secondary radical.

Figure 44 shows the slope for Et-Cl-Prop and Figure 45 shows GPC traces for polymerizations.

Figure 44 – Transfer Coefficient for MMA and Me-Br-Prop – Ambient Light.

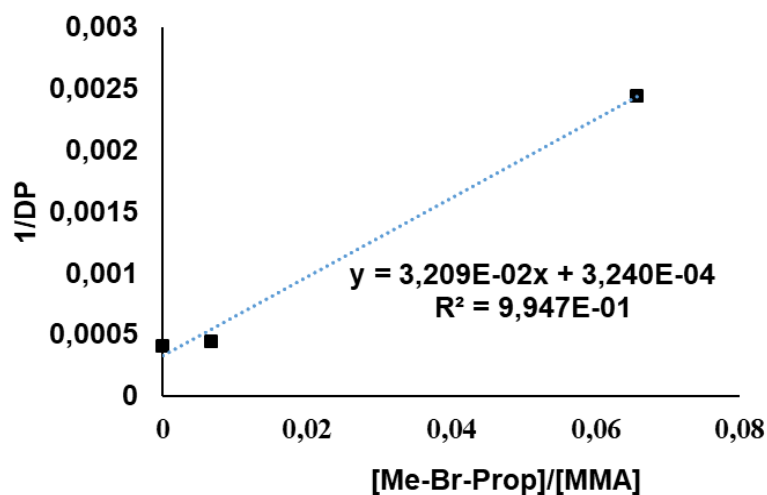


Figure 45 – GPC traces for polymerization by FRP with MMA and Me-Br-Prop – ambient light.

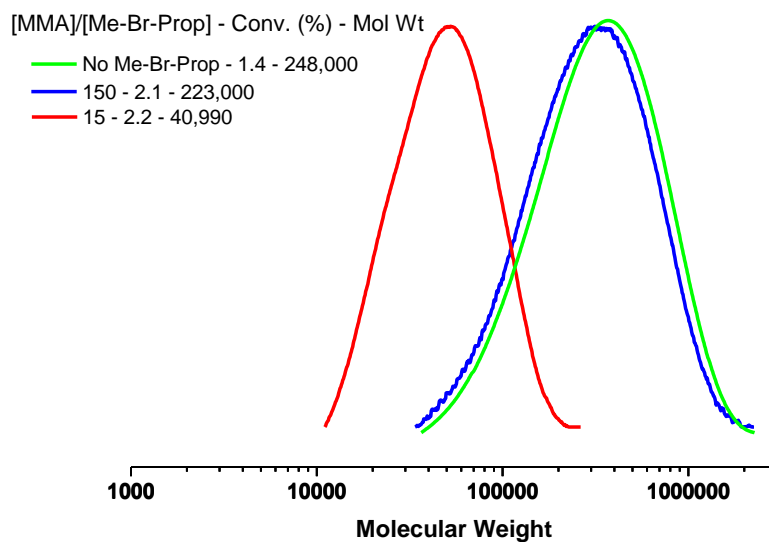
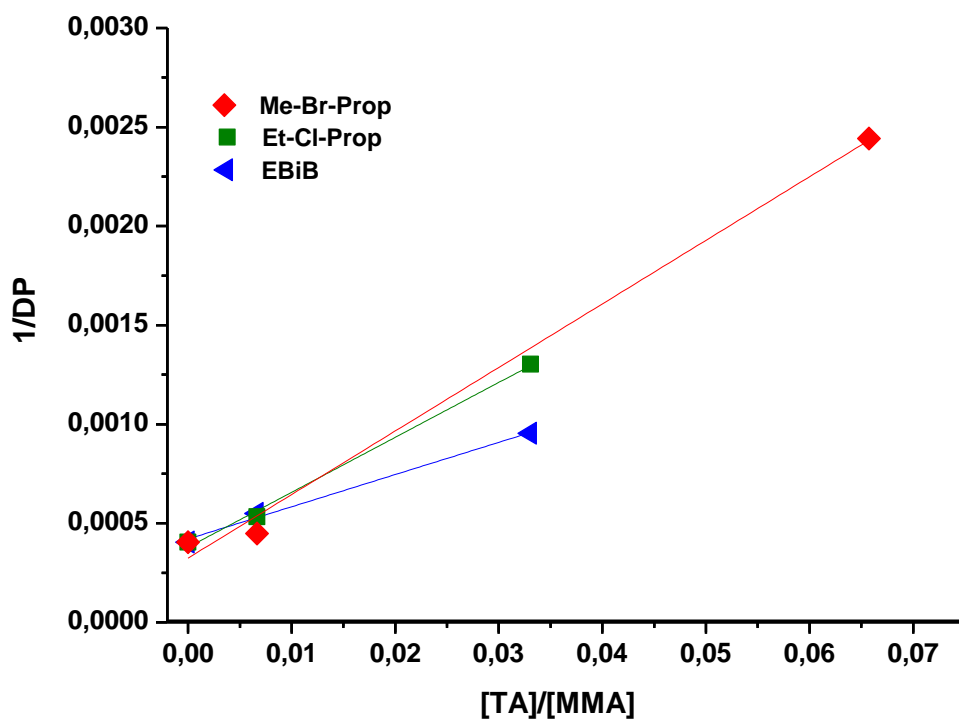


Figure 47 shows the comparison between the different transfer coefficients.

Figure 46 – Transfer coefficient for EbiB, Et-Cl-Prop and Me-Br-Prop.



3.2.2.1.3 Calculation of Transfer Coefficient by FRP without TA

Table 14 shows the results obtained for these experiments.

Table 14 – Results for Transfer Coefficient for three different Transfer Agents: EBiB, Et-Cl-Prop and Me-Br-Prop.

	Transfer Agent (TA)								
	EBiB			Et-Cl-Prop			Me-Br-Prop		
(MMA/TA)	30	150	-	30	150	-	15	150	-
Mol Wt x 10 ⁵	1.05	1.82	2.48	7.67	1.88	2.48	0.4	2.23	2.48
% C	4	3.5	1.4	1.1	1.6	1.4	2.2	2.1	1.4
Mol Wt x 10 ⁵									
Essay 1	0.79								
% C	5.5								
Essay 1									
Mol Wt x 10 ⁵									
Essay 2	1.12								
% C	5.3								
Essay 2									
Transfer Coefficient (Cs)	0.01626			0.02774			0.03209		

Figure 47 shows the conversion of monomer (MMA) to polymer (pMMA) for the first experiment and Figure 48 shows the conversion from monomer to polymer for the second repetition.

Figure 47 - ^1H NMR for polymerization of MMA by FRP without transfer agent (TA) at $60\text{ }^\circ\text{C}$ for 45 minutes of reaction - Repetition 1.

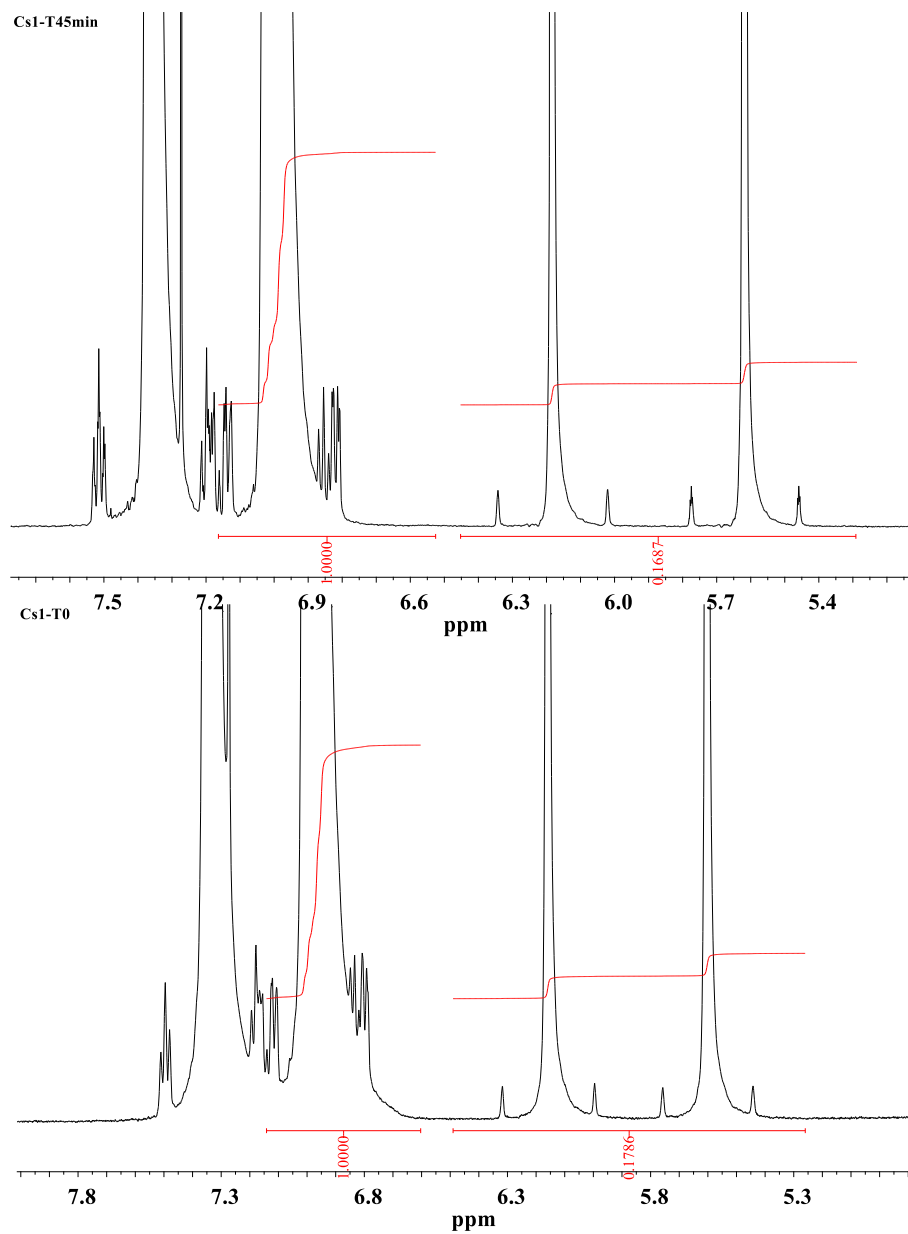
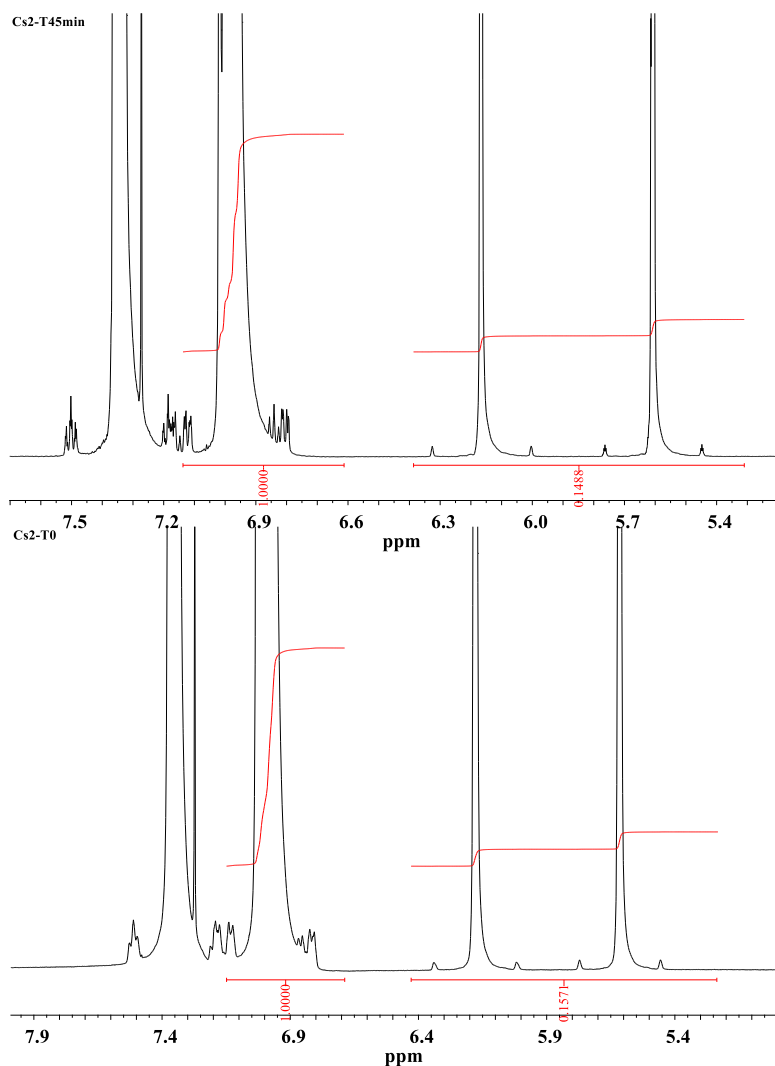


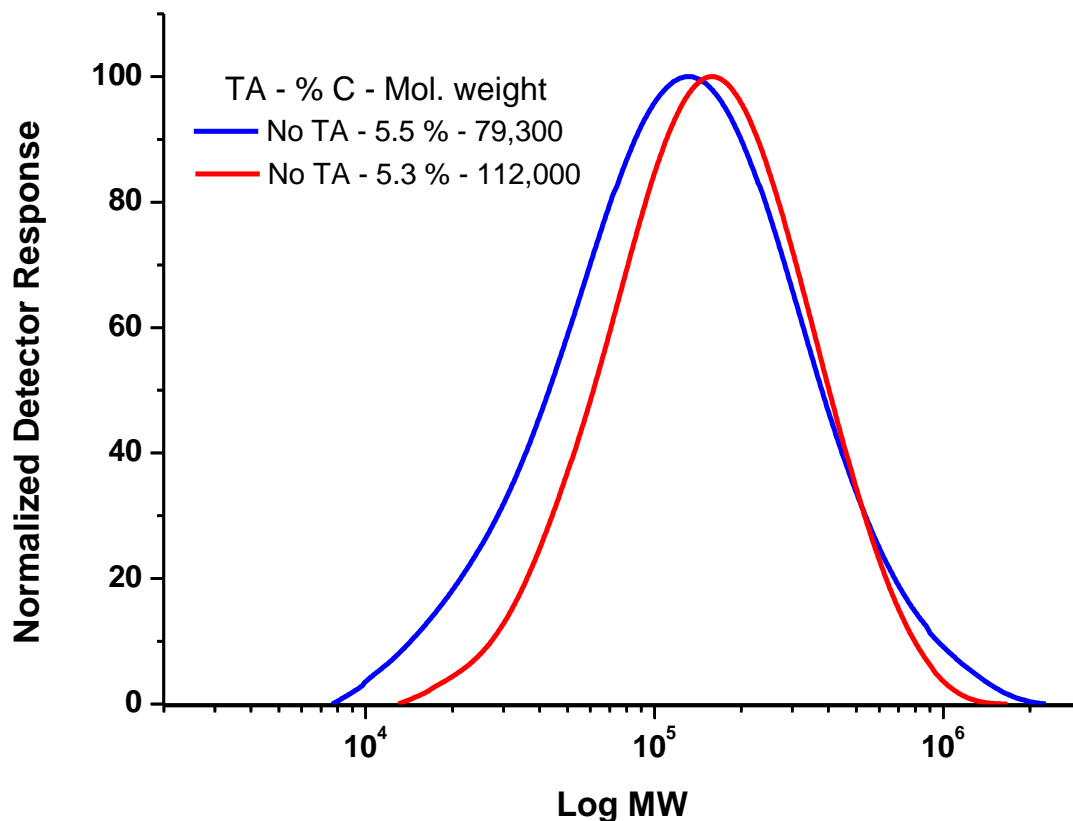
Figure 48 – ^1H NMR for polymerization of MMA by FRP without transfer agent (TA) at $60\text{ }^\circ\text{C}$ for 45 minutes of reaction - Repetition 2.



In repetition 2, the peaks between 5.4 and 6.3 ppm refer to methylene protons ($-\text{CH}_2$) and the peaks between 6.8 and 7.5 ppm refer to the methyl protons of the ester group ($-\text{COOCH}_3$) decreased in intensity compared to experiment 1, due to the fact that in repetition 2, a lower one was used with MMA monomer concentration.

Figure 49 shows the GPC traces for both experiments and the molecular weight, conversion are also indicated in this set of results.

Figure 49 – GPC traces for polymerization of MMA by FRP without transfer agent (TA) at 60 °C for 45 minutes of reaction - Repetitions 1 and 2.

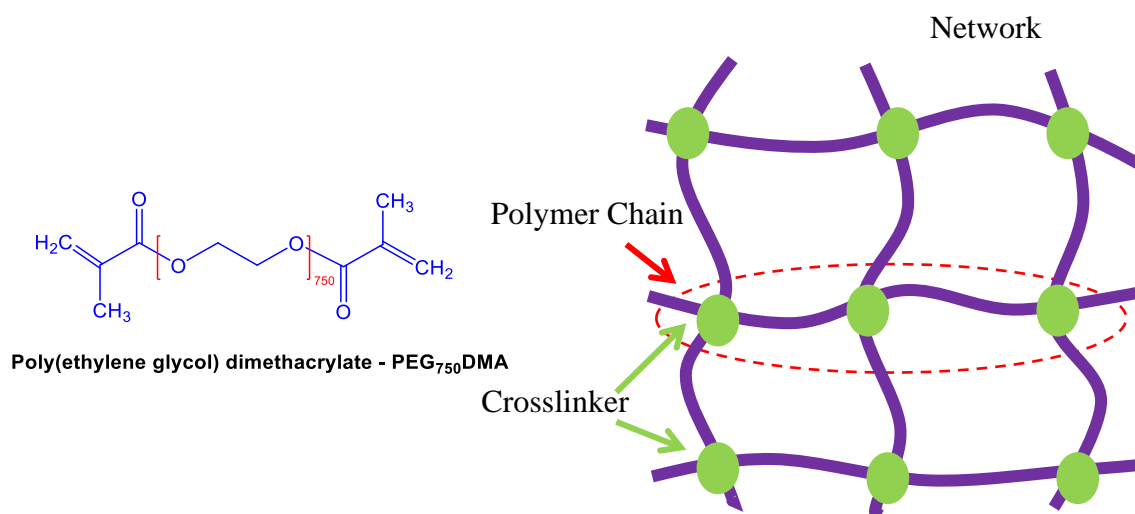


The GPC graph shows that in the experiment that had a conversion rate of 5.3%, it was possible to obtain a polymer with a higher molecular weight of 112.0 g/mol, greater than in experiment 1, in which a conversion of 5.5% and the molecular weight was 79.3 g/mol.

3.3 SYNTHESIS of GS-MATRIX USING PEG₇₅₀DMA by FRP

3.3.1 Experimental Procedures

The structure of PEG₇₅₀DMA as well as example of network are showed below in the Figure 50, this monomer can polymerize on both sides at the ends of the chain and form crosslinks.

Figure 50 – Structure of the monomer PEG₇₅₀DMA and an ideal network.

All conditions used for this experiment are listed in Table 15.

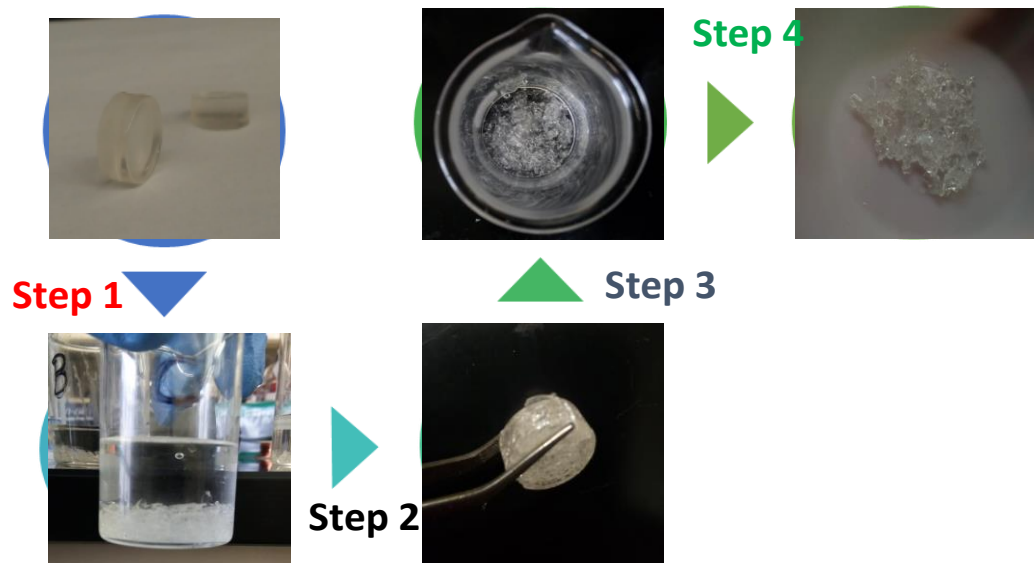
Table 15 – Conditions used for GS-Matrix synthesis.

Materials	ρ (g/mL)	MW(g/mol)	n(mol)	Mass(g)	Vol(mL)	Ratio	Sample
PEO₇₅₀DMA	1.11	750.00	0.00167	1.2497	1.13	50.00	
AIBN		164.21	0.00001	0.0011		0.20	A and B
				0.0055		1	C and D
				0.0088		1.6	E and F
DMF (IS)	0.944	73.09					
Toluene	0.867	92.14			1.13		

The AIBN Ratio for this sequence of experiments was increased: 0.02/1.0/1.6 and a monomer ratio of 50 was used for all samples. The preparation of the gels was carried out in duplicate for each ratio (A/B, C/D and D/C).

After 24 hours of reaction, all gels were put in toluene for 12 hours and then in a methanol/water mixture (50/50%) in order to remove the residual monomer. All steps performed are described in Table 16. Yields were calculated by gravimetry when the polymers were removed from the oven after 24 hours drying and Figure 51 shows all steps for this process of swelling.

Figure 51 – Steps for checking swelling for GS-Matrix



In this case, the steps of the procedure are described below:

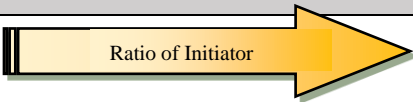
Step 1- Gel preparation.

Step 2- Swelling tests.

Step 3- Gel drying.

Step 4- Weighing the gel after swelling.

Table 16 – Data yields and steps for checking the swelling.

Gels						
						
	A	B	C	D	E	F
All sample run in 60 °C for 24 hours						
Weight (g)	1.1680	1.0401	1.4139	1.1948	1.2363	1.3460
Average Weight (g)	1.1041		1.3044		1.2912	
Step 1 -The gels were put in toluene for 12h						
Weight (g)	1.3846	0.9872	1.5805	1.3369	1.4629	1.5564
Average Weight (g)	1.1859		1.4587		1.5097	
The gels were put in water/methanol (50%/50%) for 12h						
Weight (g)	1.7221	1.4550	1.8319	1.5874	1.8171	1.9145
Average	1.5886		1.7097		1.8658	
Weight (g)						
Step 2 -The gels were dried for 24h in the oven (vacuum system)						
Weight (g)	0.9727	0.7828	1.2866	1.1089	1.1060	1.0610
Dried gels						
Average Weight (g)	0.8778		1.1978		1.0835	
Yield (%)	77.83	63.64	-	88.730	88.50	84.90
Average Yield (%)	70.74		~ 88.73		86.7 %	

The yield for the gels were calculated using the following equation (1).

$$\text{Yields (\%)} = \frac{\text{Weight of Monomer}}{\text{Weight of dried gels}} \times 100 \quad (1)$$

Yield was calculated after removal of the residual monomer, that is, the final mass of each gel was calculated in Step 2.

The Degree of Swelling was calculated using equation (2).

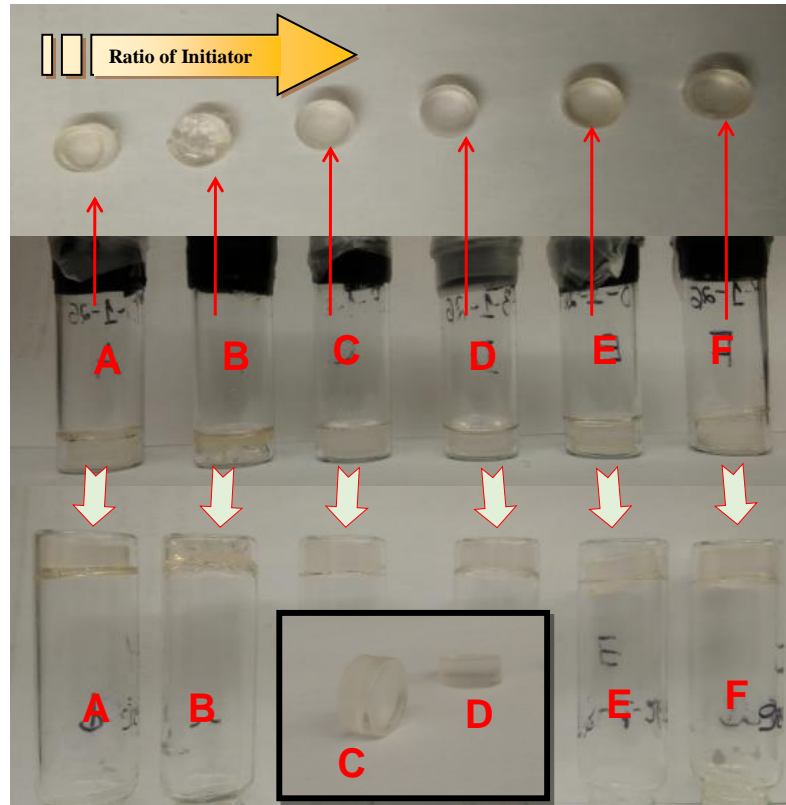
$$\text{Swelling (\%)} = \frac{(W_s - W_d)}{W_d} \times 100 \quad (2)$$

Here: W_s = weight of swollen polymer and W_d = weight of dry polymer.

3.3.2 Results and discussion

Figure 52 shows some pictures of these gels.

Figure 52 – GS-Matrix made by FRP.



3.3.2.1 Swelling Test

Table 17 shows data for swelling.

Table 17 – Data swelling for GS-Matrix.





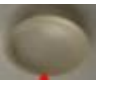







Step 3 -The gels were put in water for 20h - shattered						
Sample	A	B	C	D	E	F
Weight of piece of swollen gel (g)	0.0580	0.0695	0.0728	0.0159	0.1167	0.1601
Average Weight (g)	0.0638		0.0444		0.1384	
Step 4 -The small pieces of gels were put in oven to dry for 24h						
Weight of piece of dry gel (g)	0.0271	0.0373	0.0425	0.0093	0.0571	0.0719
Average Weight (g)	0.0322		0.0259		0.0645	
Degree of Swelling (%)	>100	86.33	71.29	70.97	>100	>100
Average value	98.14		71.43		>100	

Normally hydrogels swell a lot but since these gels were prepared from pure crosslinker, and will be called "GS-Matrix" gels, it would be normal for the swelling to be lower than 100%. Also, a swelling ratio of approximately 100% should be good. According to the theoretical calculations it is expected that the gels should swell around 100%. Thus, PEG has very high crosslinker density so we expect that it can swell very much, when it is dried it is very brittle because crosslinker density is high, because of this after swelling the gels shattered during testing.

The ratio of initiator (AIBN) was increased, because it could favor the formation of crosslinks, but it appears that the amount of AIBN does not affect the swelling ratio.

Final results for swelling and yields are summarized in Table 18.

Table 18 – Data swelling and yields for GS-Matrix.

	Sample					
	A	B	C	D	E	F
Before Swelling						
After Swelling						
Yields (%)	78 %	64 %	100%	89%	89	85
Swelling (%)	100	86	71	71	100	100

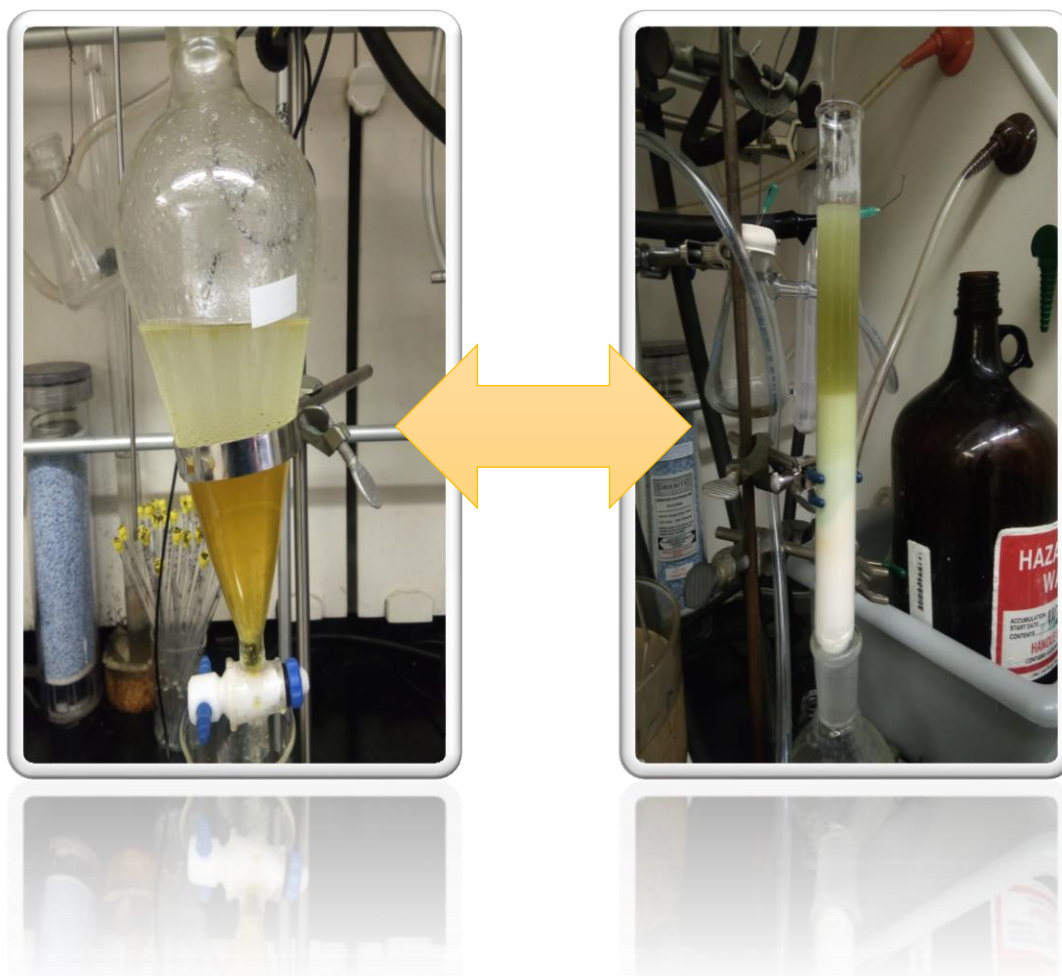
3.4 STEM GELS by RAFT and PHOTO ATRP

3.4.1 Experimental Procedures

3.4.1.1 Synthesis of Inimer

A 250 mL round-bottom flask was loaded with a magnetic stir bar, 2-hydroxyethyl methacrylate, pyridine and 85 mL of dichloromethane (DCM), before being cooled to 0 °C in an ice bath. 2-Bromoisobutyryl bromide was added dropwise to the reaction mixture over ~15 min. The reaction was allowed to come to room temperature overnight. After the reaction, solids were filtered and the solution was washed 3 times with saturated sodium bicarbonate solution and once with water. The mixture was dried over magnesium sulfate, mixed with a few mg. of CuCl₂, then passed through a 50/50% neutral/basic alumina plug. The product was rotovapped, to obtain a slightly yellow oil. The Figure 53 shows the process of synthesis.

Figure 53 – Process of Synthesis of Inimer.



3.4.1.2 Method for purification of HEMA

HEMA was purified by first dissolving the monomer in water (25% by volume). The solution was extracted with hexane to remove diacrylates. The aqueous solution was salted (250 g/ L NaCl) and the monomer was then separated from the aqueous phase by ether extraction (4 times). The organic solvent was removed under reduced pressure. The purified monomer was kept refrigerated and it was passed through a sand/alumina column, in order to remove the radical inhibitor, immediately prior to use. Then, from this purified HEMA, a new (Inimer-Cl) and a new backbone polymer (PB-BB-A) were synthesized.

3.4.1.3 Purification Method of Inimer-Cl

All the conditions used for the purification of the inimer as well as purification of the HEMA are available in the literature [33,34].

For the silica column chromatography, a 4:1 - hexane:ethylacetate mixture was used as solvent. Before using the column, a TLC plate was ran and it was recorded the RF values of all the spots as well as the solvent component. Three compounds were observed in my final product and it was checked the ¹H NMR for all products and from integral values, product 2 was the one that most closely approached of inimer-Cl structure.

3.4.1.4 Synthesis of STEM-0 and STEM-1 by RAFT and ATRP

The synthesis of STEM gels followed the steps below:

- 1) 8 mL vial was rinsed with Rainx and dried.
- 2) MMA monomer, crosslinker PEO750DMA, HEMA-iBBr inimer, the RAFT agent, CPDTA, DMSO, and AIBN were added to the 8 mL vial, DMF was also added as an internal standard.
- 3) The pre-gel solution was mixed.
- 4) A sample is taken for NMR (t=0 h).
- 5) The vial was sealed, placed in an ice bath, and sparged with N₂ for 30 min.
- 6) The vial was further sealed and covered with aluminum foil.
- 7) The vial was placed in an oil bath at 60°C for 48 hours.

After the gel forms, conversion was determined by extraction of the unreacted monomer in DMSO-d₆ and subsequent ¹H NMR. The gel was dried in an oven (50°C) under vacuum, using a high vacuum pump, for 2 days. After drying, the STEM 0 was weighed then put in solvent (DMSO or water) for 48h to check the degree of swelling, the solvent was changed each 12h.

Tables 19 and 20 show the conditions that were used for these experiments and Figure 54 summarizes what has been done.

Figure 54 – Flow chart to exemplify how the STEM -Gels were characterized by swelling ratio.

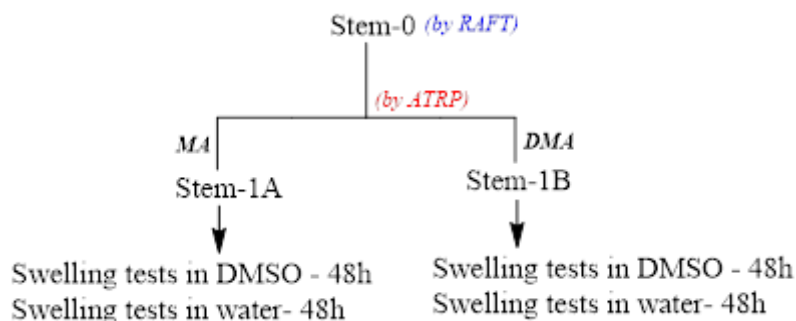


Table 19 – Conditions used for synthesis of STEM -0 by RAFT.

STEM-0 1st by RAFT								
Thermal RAFT	T(°C)	Mn (g/mol)	n(mol)	Mass Theo (g)	Mass actual	Conversion	DP	
	60							
Materials	Density (g/mL)	MW (g/mol)	n (mol)	Mass (g)	Mass act (g)	Vol (mL)	Ratio	[]
MMA	0.94	100.12	0.0050	0.4961		0.47	200.00	4.2671
HEMA-iBBr		279.13	0.0005	0.1383			20.00	
PEG ₇₅₀ DMA	1.1	750.00	0.0000	0.0372		0.034	2.00	
CPDTA		402.67	2.47×10^{-5}	0.0100			1.00	0.0213
AIBN		164.21	4.95×10^{-5}	0.0008			0.20	
DMSO	1.1	78.13		0.6650		0.60		0.0000
DMF (IS)	0.944	73.09		0.0472		0.05		

Table 20 – Conditions used for synthesis of STEM -1 by photo ATRP using UV-Light for 6 hours.

STEM- 1 by Photo ATRP using UV-Light for 6 hours								
Thermal RAFT	T(°C)	Mn (g/mol)	n(mol)	Mass Theo (g)	Mass actual	Conversion	DP	
	60							
Materials	Density (g/mL)	MW (g/mol)	n (mol)	Mass (g)	Mass act (g)	Vol (mL)	Ratio	[M]
MA or DMA	0.95	86.09	0.0110	0.9500		1.00		
STEM -0				0.3655				
CuBr ₂		223.37	5.000E-06	0.0011			1.00	0.0025
Me6TREN		230.39	3.00E-05	0.0069			6.00	
DMSO	1.1	78.13	0.00E+00	1.1000		1.0000		
DMF (from CuBr ₂ /Me6T REN stock solution)								

3.4.1.5 Swelling tests

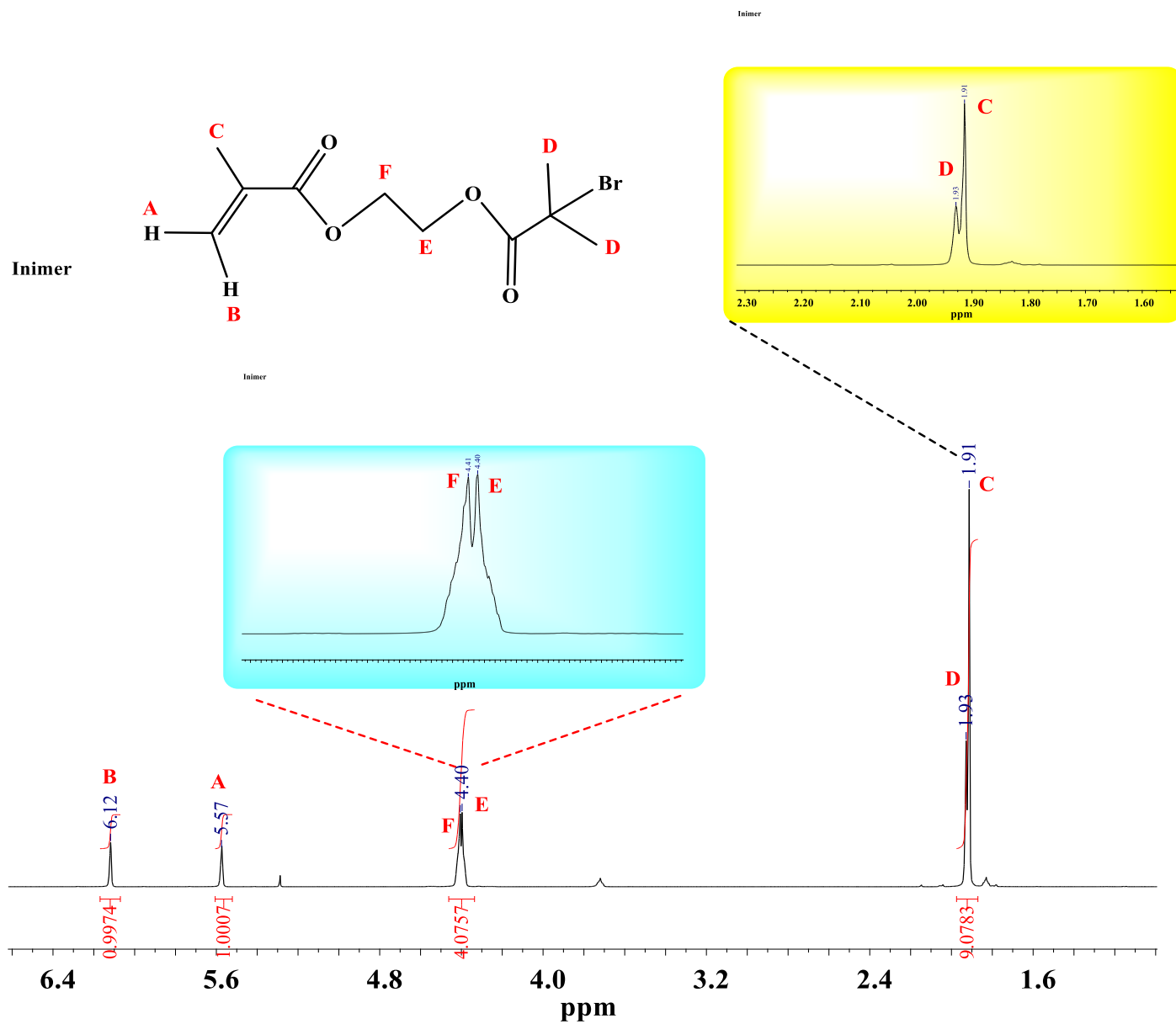
Swelling ratio was calculated using equation 2:

$$\text{Swelling (\%)} = \frac{(W_s - W_d)}{W_d} \times 100$$

3.4.2 Results and discussion

3.4.2.1 Characterization of Inimer-Br by ¹H NMR

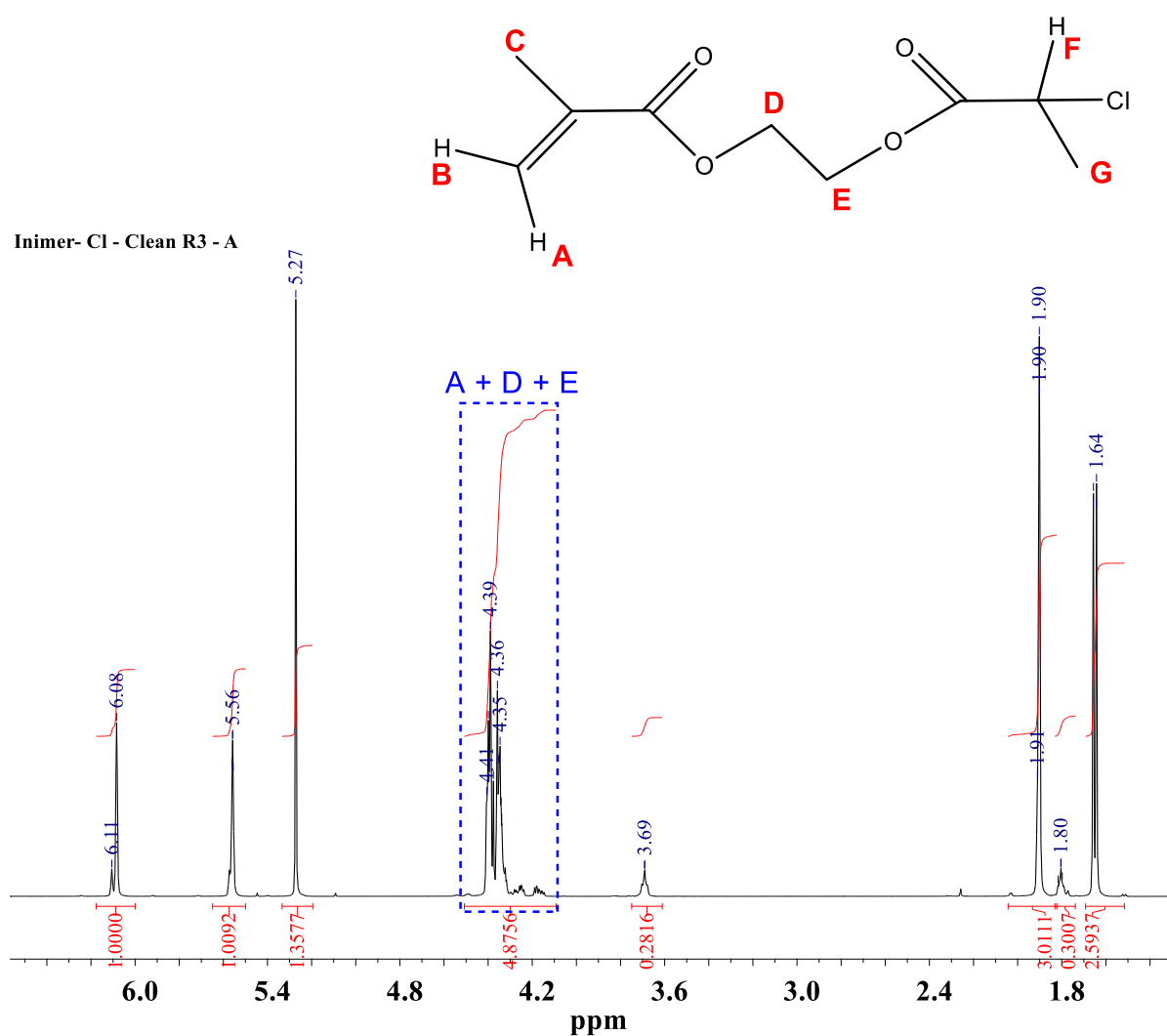
In the ¹H NMR spectrum of the iminer-Br molecule (Figure 55), the most unshielded protons **A** and **B** have a chemical shift of 5.57 and 6.12 ppm, respectively. Protons **F** and **E**, located between the ester group, have a shift of 4.40 ppm, and protons **C** and **D** have a chemical shift of about 1.90 ppm. In the case of **D** protons, the electron-donor mesomeric effect of the Br atom predominated over the inductive effect, so it had a smaller shift.

Figure 55 – Characterization of inimer-Br molecule by ^1H NMR.

3.4.2.2 Characterization of Inimer-Cl by ^1H NMR

The final inimer obtained was characterized accord to literature [34] and it seems better than my previous synthesis.

Figure 56 shows the ^1H NMR spectrum of inimer-Cl before purification and Figure 58 shows ^1H NMR spectrum of inimer-Cl (Compound 2) after purification.

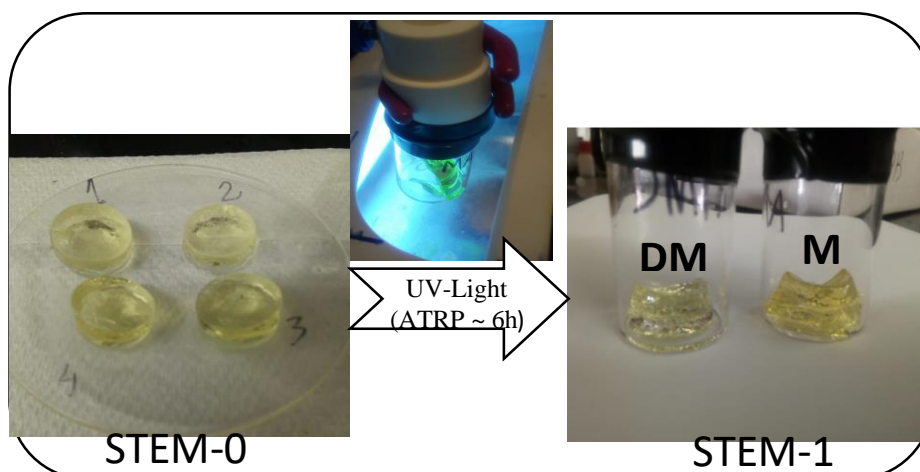
Figure 56 – ^1H NMR spectrum of inimer-Cl before purification

The spectrum of compound 2, after purification of inimer-Cl presented the same peaks referring to Inimer-Cl without purification, indicating the obtaining of a pure compound by the used synthesis procedure.

3.4.2.3 Synthesis of STEM-0 and STEM-1 by RAFT and ATRP

Figure 57 shows the STEM -0 and STEM -1 by RAFT and ATRP.

Figure 57 – STEM -0 and STEM -1 by RAFT and ATRP.



3.4.2.4 Swelling tests

Table 21 shows the degree of swelling calculated for STEM -0 and STEM -1A and Stem-1B after immersion in water and DMSO.

Table 21 – Degree of Swelling calculated for STEM -0 and STEM -1 (A and B)

	STEM -Gels					
	STEM -0		STEM -1A (MA)		STEM -1B (DMA)	
Solvent	Water	DMSO	Water	DMSO	Water	DMSO
Weight: Time 0	0.567 g	0.654 g	0.844 g	0.756 g	0.602 g	0.485 g
Weight: After 48h	0.506 g	1.298 g	0.776 g	1.697 g	0.422 g	0.717 g
Degree of Swelling	<0	98.5 %	<0	124.5 %	<0	47.8 %

All STEM -gels showed no degree of swelling in water, but in DMSO they had a high degree of swelling, the lowest degree being for STEM -1B, in which DMA was used, showing that the use of this monomer caused greater crosslinking, decreasing the space between the chains.

3.5 NEW FUNCTIONALIZED NETWORKS WITH PEG₅₅₀DMA

In this series of experiments, PEG₅₅₀DMA was used as crosslinker monomer in the functionalization of new networks, in addition to MMA as the main chain monomer, AIBN as initiator, pyrene, a fluorophore used as a probe compound as it absorbs at a wavelength in

the visible region and 2-amino as polar monomer and LMA as non-polar monomer, which were used for various molar ratios and the results of this modification on the synthesis of functionalized networks was evaluated.

3.5.1 Experimental Procedures

Table 22 shows the effect of different molar ratios of 2-amino and LMA used to prepare the networks.

Table 22 – Conditions used in functionalized networks with PEG₅₅₀DMA

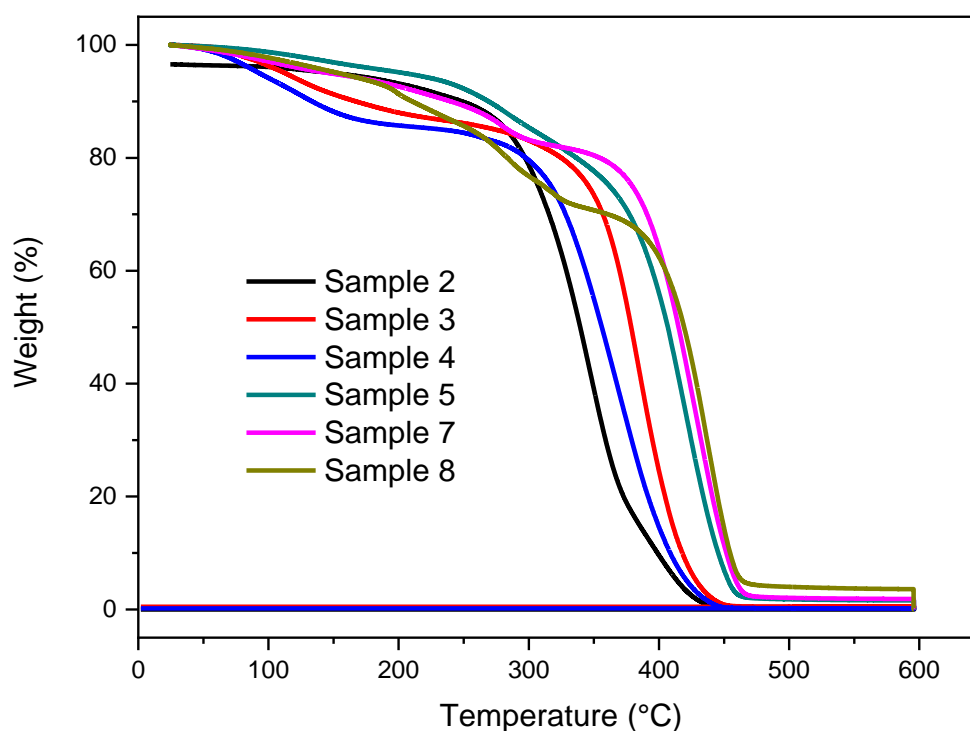
Sample	Monomer ratio				probe compound	initiator
	MMA	PEG	LMA	2-amino	Pyrene	AIBN
1	300	20				1
2	300	20	90		2	1
3	300	20	90	10	2	1
4	300	20	70	30	2	1
5	300	20	50	50	2	1
6	300	20	30	70	2	1
7	300	20	10	90	2	1
8	300	20		90	2	1

3.5.2 Results and discussion

3.5.2.1 Thermogravimetric analysis (TGA)

Figure 58 shows the curves of the thermogravimetric analysis of samples 2, 3, 4, 5, 7 and 8, as described in Table 22.

Figure 58 – TGA curves of samples 2, 3, 4, 5, 7 and 8.



The TGA curves showed that the higher the molar ratio of the 2-amino monomer (sample 8), the more thermally stable the polymeric network, and sample 2, with the higher ratio of the LMA monomer, was less stable compared to the other samples. This profile indicates that the presence of 2-amino causes a higher crosslinking density, thus reducing the mobility of the polymer chains

Table 23 – Quantitative results from TG curves. Including temperature range, mass loss percentages and residues for sample analyzed.

Sample	Temperature range / °C	Mass loss / %
2	23,41 – 241,3	6,44
	241,3 – 396,9	82,10
	369,9 – 465,0	11,04
	residue 465	0,42
3	23,67 – 225,2	13,03
	225,2 – 467,1	86,63
	residue 467,1	0,34
4	25,31 – 212,6	14,22
	212,6 – 271,9	2,76
	271,9 – 464,0	82,77
	residue 464,0	0,25
5	23,30 – 201,1	4,84
	201,1 – 250,9	2,76
	250,9 – 317,3	9,38
	317,3 – 507,0	81,11
	residue 507,0	1,91
7	23,30 – 153,7	5,05
	153,7 – 239,0	4,97
	239,0 – 322,1	7,73
	322,1 – 507,4	80,01
	residue 507,4	2,24
8	24,76 – 233,4	12,52
	233,4 – 311,7	2,69
	311,7 – 344,9	3,87
	344,9 – 506,1	66,76
	residue 506,1	4,16
	residue 591,5	3,61

3.5.2.2 Rheology

Rheology analysis allows determination of the elastic modulus or storage modulus (G'), viscous modulus or loss modulus (G'') and the glass transition temperature through change in the $\tan \delta$ peak as a function of temperature.

Figure 59 and 60 shows the curves obtained from G' and G'' and $\tan \delta$, respectively, of samples 1, 2, 3, 4, 5 and 7, as described in table 22.

Figure 59 – Storage modulus (G') and loss modulus (G'') of samples 1, 2, 3, 4, 5 and 7.

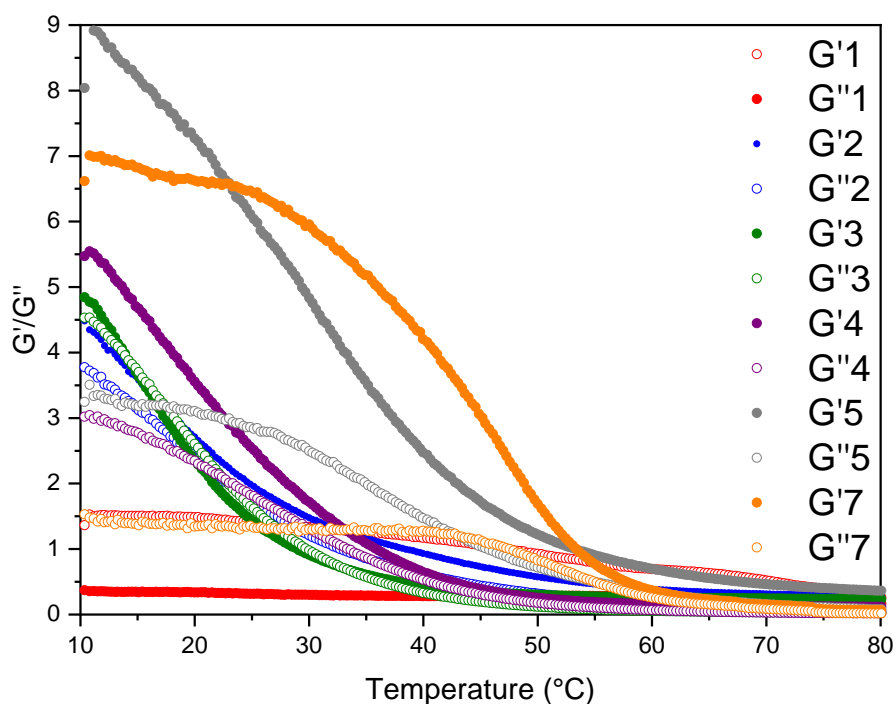
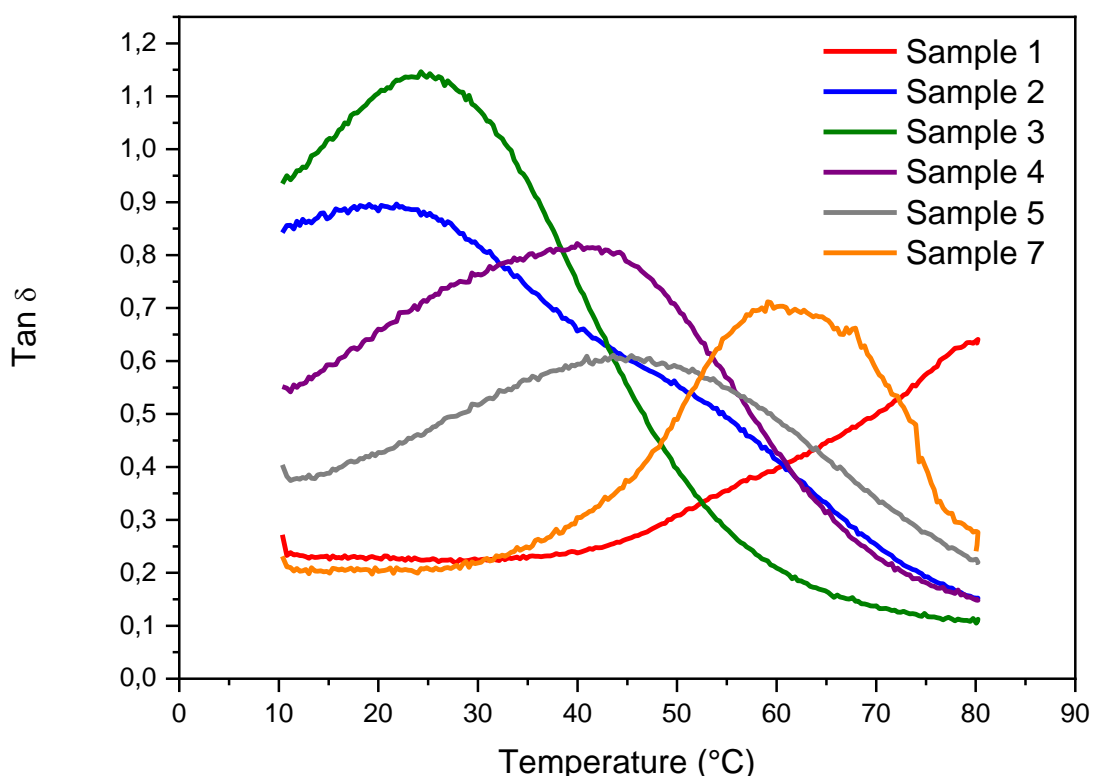


Figure 59 compares the variation of G' and G'' as a function of temperature. In all samples, G' and G'' decrease with increasing temperature, indicating fewer non-crosslinked chains in the polymer, with the exception of sample 1, in which the modulus did not vary with temperature, that is, this sample formed a fully cross-linked network. Sample 5 had a higher storage modulus (G') compared to the other samples, up to 25°C, and from then on, sample 7 had the highest G' up to a temperature of 53°C. This profile shows that when equal ratios of both polar (2-amino) and non-polar (LMA) monomer were used, there was a higher crosslink

density up to room temperature, and after that temperature, a higher ratio of polar monomer favors the crosslinking. In these samples, in addition to samples 2 and 4, $G' > G''$, but for sample 1, in which there is no presence of LMA and 2-amino monomers, $G'' > G'$, in the case of sample 3, that there is greater LMA ratio, $G' = G''$.

Figure 60 – Tan δ of samples 1, 2, 3, 4, 5 and 7.

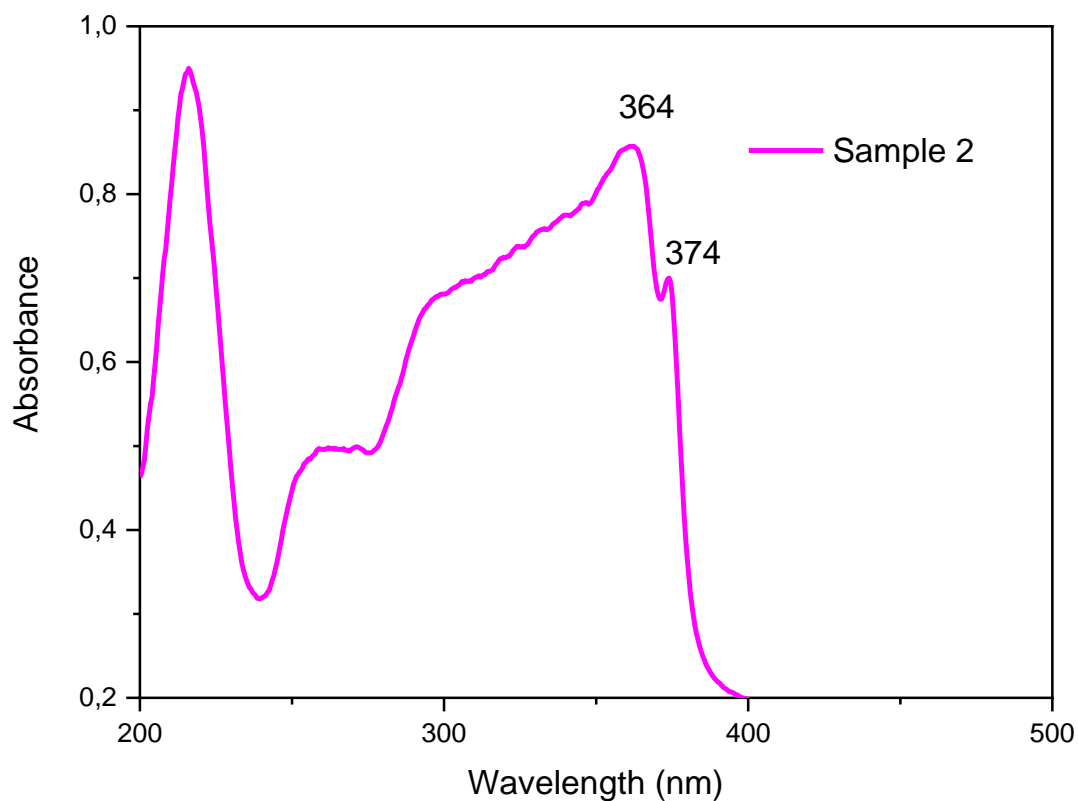


The Tan δ peak could not be observed in Sample 1 in the temperature range studied (Figure 60), but it has a higher T_g compared to the other samples. Sample 7, which has a higher polar monomer (2-amino) ratio, had a higher T_g compared to the other samples, that is, this monomer increased the crosslinking density and, consequently, the sample presented a higher activation energy. On the other hand, sample 2, without the presence of the 2-amino monomer and with a high ratio of the apolar LMA monomer, had a lower T_g , indicating a free volume between the chains due to the formation of non-reactive pendant ends in the networking.

3.5.2.3 UV-vis

Figure 61 shows the UV-vis absorption spectrum of sample 2.

Figure 61 – UV-vis absorption spectra of sample 2

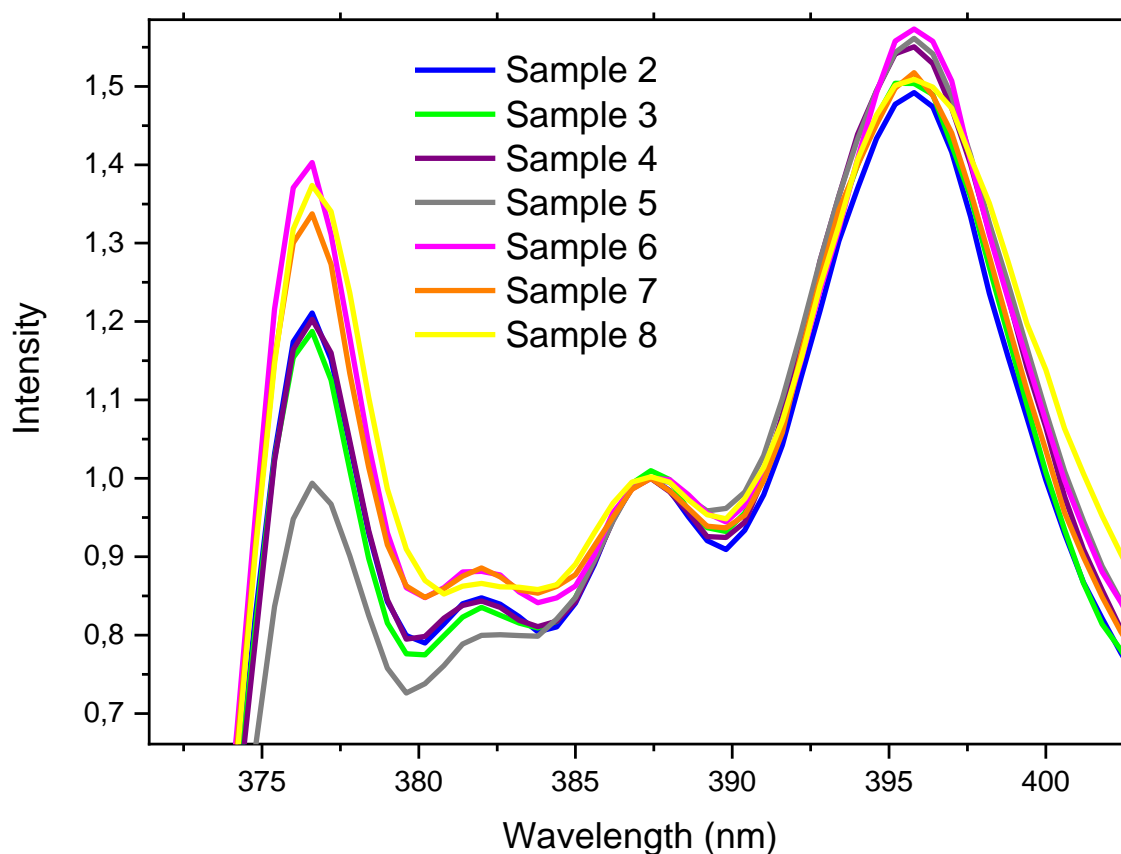


As can be seen in Figure 61, sample 2, with the highest ratio of non-polar LMA monomer and without the presence of the polar 2-amino monomer, exhibits two bands at 364 and 374 nm, and the low degree of crosslinking of this sample, verified by the low t_g (Figure 61). Pyrene has S_0 transitions to S_2 and S_0 to S_3 that are allowed the transition S_0 to S_1 in pyrene is prohibited by spin.

3.5.2.4 Fluorescence

The fluorescence analyzes were performed for the samples 2, 3, 4, 5, 6, 7 and 8 using pyrene as a probe and the spectra are presented in the Figure 62.

Figure 62 – Fluorescence spectra of samples 2, 3, 4, 5, 6, 7 and 8.



Pyrene is sensitive to the polarity of the environment (35) and presents the characteristic peaks I at 377 nm and III at 388 nm. The polarity scale of the pyrene solvent is defined as the ratio of the emission intensity of these two peaks I_I/I_{III} , where band I corresponds to transition $S_1 (\nu = 0) \rightarrow$ transition $S_0 (\nu = 0)$ and band III is the $S_1 (\nu = 0) \rightarrow S_0 (\nu = 1)$ transition (36.37).

The emission intensity ratio I_I/I_{III} increases with increasing solvent polarity. This justifies the results obtained because, from the graph (Figure 64), it is obtained that the ratio of peaks I_I/I_{III} is 0.91 for the sample with the highest molar ratio of the 2-amino monomer (sample 8), which presented the highest value among the other samples analyzed, with the

value of I_I/I_{III} being 0.80 for sample 2, with the highest molar ratio of the non-polar monomer LMA.

4 CHAPTER 4 - CONCLUSION

RAFT photopolymerization of poly(ethylene glycol) methyl ether methacrylate (PEG₃₀₀MA and PEG₅₀₀MA), poly(dimethylsiloxane) methacrylate (PDMSMA) and 2-(dimethylamino)ethyl methacrylate (DMAA) monomers showed that these reactions were difficult to control. As for the butyl methacrylate (BMA) and lauryl methacrylate (LMA) monomers, a high conversion and low dispersity of 95% were obtained; 1.31 and 80%; 1.35, respectively.

Transfer agents were added to Free Radical Polymerizations (FRP) to calculate the transfer coefficient from halogen to the propagation chain and determine how quickly it occurs and also to find a good molecule to make bottle brush structures. The best results were obtained with ethyl-bromo- α -isobutyrate (EBiB) where we found a transfer coefficient (Cs) equal to 0.0162.

The “GS-matrix” gels, as they were synthesized with a pure crosslinker, in this case PEG₇₅₀DMA, had a high degree of swelling, which made the gels brittle, indicating that the use of this crosslinker did not favor the formation of crosslinks.

The HEMA purification method is effective and must be used before synthesizing the inimer molecule. While the purification of pure inimer-Cl was not as efficient as an impure product was obtained, analyzed by ¹H NMR.

STEM-gels showed a high degree of swelling in DMSO, with the lowest degree being for STEM-1B, in which DMA was used as monomer, indicating greater crosslinking.

In the functionalization of new networks with PEG₅₅₀MMA, the highest values of tg obtained both by DSC analysis and by rheology, showed that the use of the 2-amino polar monomer led to networks with higher crosslink density in detriment to the use of the nonpolar LMA monomer.

5 REFERENCES

- 1 PAN, X.; FANTIN, M.; YUAN, F.; MATYJASZEWSKI, K. Externally controlled atom transfer radical polymerization. **Chemical Society Reviews**, Cambridge, v. 47, n. 14, p. 5457-5490, 2018.
- 2 SHANMUGAM, S.; CUTHBERT, J.; FLUM, J.; FANTIN, M.; BOYER, C.; KOWALEWSKI, T.; MATYJASZEWSKI, K. Transformation of gels via catalyst-free selective RAFT photoactivation. **Polymer Chemistry**, Cambridge, v. 10, n. 19, p. 2477-2483, 2019.
- 3 TAMATE, R.; UEKI, T.; KITAZAWA, Y.; KUUUNUKI, M.; WATANABE, M.; AKIMOTO, A. M.; YOSHIDA, R. Photo-dimerization induced dynamic viscoelastic changes in ABA triblock copolymer-based hydrogels for 3D cell culture. **Chemistry of Materials**, Washington, v. 28, n. 17, p. 6401-6408, 2016.
- 4 RANGANATHAN, K.; DENG, R.; KAINTHAN, R. K.; WU, C.; BROOKS, D. E.; KIZHAKKEDATHU, J. N. Synthesis of thermoresponsive mixed arm star polymers by combination of RAFT and ATRP from a multifunctional core and its self-assembly in water. **Macromolecules**, Washington, v. 41, n. 12, p. 4226-4234, 2008.
- 5 THERIOT, J. C.; MIYAKE, G. M.; BOYER, C. A. N. N-diaryl dihydrophenazines as photoredox catalysts for pet-raft and sequential pet-raft/o-atrp. **ACS Macro Letters**, Washington, v. 7, n. 6, p. 662-666, 2018.
- 6 CUTHBERT, J.; BEZIAU, A.; GOTTLIEB, E.; FU, L.; YUAN, R.; BALAZS, A. C.; KOWALEWSKI, T.; MATYJASZEWSKI, K. Transformable materials: structurally tailored and engineered macromolecular (STEM) gels by controlled radical polymerization. **Macromolecules**, Washington, v. 51, n. 10, p. 3808-3817, 2018.
- 7 SHANMUGAM, S.; CUTHBERT, J.; FLUM, J.; FANTIN, M.; BOYER, C.; KOWALEWSKI, T.; MATYJASZEWSKI, K. Transformation of gels via catalyst-free selective RAFT photoactivation. **Polymer Chemistry**, Cambridge, v. 10, n. 19, p. 2477-2483, 2019.
- 8 SUN, H.; KABB, C. P.; DAI, Y.; HILL, M. R.; GHIVIRIGA, I.; BAPAT, A. P.; SUMERLIN, B. S. Macromolecular metamorphosis via stimulus-induced transformations of polymer architecture. **Nature chemistry**, Berlin, v. 9, n. 8, p. 817, 2017.
- 9 ROCHA, Beatriz. Aline. Riga. **Síntese de ligantes diimínicos para obtenção de complexos organocobalto (iii) para polimerização radicalar mediada por cobalto**. 2017. 175 f. Dissertação (mestrado em Química) - Unesp, São José do Rio Preto, 2017.
- 10 SZWARC, M. 'Living' polymers. **Nature**, Berlin, v. 178, n. 4543, p. 1168-1169, 1956.
- 11 SZWARC, M. Shelftime of living polymers. some comments on living cationic polymerization of vinyl monomers. **Die Makromolekulare Chemie, Rapid Communications**, United Kingdom, v. 13, n. 3, p. 141-145, 1992.

- 12 FISCHER, H. The persistent radical effect: a principle for selective radical reactions and living radical polymerizations. **Chemical Reviews**, Washington, v. 101, n. 12, p. 3581-3610, 2001.
- 13 OUCHI, M.; TERASHIMA, T.; SAWAMOTO, M. Transition metal-catalyzed living radical polymerization: toward perfection in catalysis and precision polymer synthesis. **Chemical Reviews**, Washington, v. 109, n. 11, p. 4963-5050, 2009.
- 14 MATYJASZEWSKI, K.; XIA, J. Atom transfer radical polymerization. **Chemical Reviews**, Washington, v. 101, n. 9, p. 2921-2990, 2001.
- 15 MATYJASZEWSKI, K. Macromolecular engineering: from rational design through precise macromolecular synthesis and processing to targeted macroscopic material properties. **Progress in Polymer Science**, Oxford, v. 30, n. 8-9, p. 858-875, 2005.
- 16 MATYJASZEWSKI, K. Atom transfer radical polymerization (ATRP): current status and future perspectives. **Macromolecules**, Washington, v. 45, n. 10, p. 4015-4039, 2012.
- 17 BORIM, Patrícia. **Dimetilsulfóxidos como ligantes ancilares em complexos de rutênio: catalisadores duais para a combinação da ROMP de norborneno e ATRP de metacrilato de metila**, 2016.89f. Dissertação (Mestrado em Química) - Unesp, São José do Rio Preto, 2016.
- 18 BERGENUDD, Helena. **Understanding the mechanisms behind atom transfer radical polymerization: exploring the limit of control**, 2011. 64f. Thesis (Polymer Chemistry PhD) - Royal Institute of Technology, Stockholm, 2011.
- 19 AKEROYD, N.; KLUMPERMAN, B. The combination of living radical polymerization and click chemistry for the synthesis of advanced macromolecular architectures. **European Polymer Journal**, Oxford, v. 47, n. 6, p. 1207-1231, 2011.
- 20 CHIEFARI, Y. K.; CHONG, J.; ERCOLE, F. Living free-radical polymerization by reversible addition-fragmentation chain transfer: the RAFT process. **Macromolecules**, Washington, v. 31, n. 16, p. 5559-5562, 1998.
- 21 SOLOMON, D. H.; RIZZARDO, E.; CACIOLI P. **Polymerization process and polymers produced thereby**. U.S. Patent 4,581,429A, March 27, 1985.
- 22 QUINN, J. F.; BARNER, L.; RIZZARDO, E.; DAVIS, T. P. Living free-radical polymerization of styrene under a constant source of γ radiation. **Journal of Polymer Science Part A: polymer chemistry**, Hoboken, v. 40, n. 1, p. 19-25, 2002.
- 23 MUTHUKRISHNAN, S.; PAN, E. H.; STENZEL, M. H.; BARNER-KOWOLLIK, C.; DAVIS, T. P.; LEWIS, D. ; BARNER, L.. Ambient temperature RAFT polymerization of acrylic acid initiated with ultraviolet radiation in aqueous solution. **Macromolecules**, Washington, v. 40, n. 9, p. 2978-2980, 2007.
- 24 MOAD, G.; RIZZARDO, E.; SOLOMON, D. H. Selectivity of the reaction of free radicals with styrene. **Macromolecules**, Washington, v. 15, p. 909, 1982.

- 25 BRAUNECKER, W. A.; MATYJASZEWSKI, K. Controlled/living radical polymerization: Features, developments, and perspectives. **Progress in Polymer Science**, Oxford, v. 32, n. 1, p. 93-146, 2007.
- 26 IDE, N.; FUKUDA, T. Nitroxide-controlled free-radical copolymerization of vinyl and divinyl monomers. Evaluation of pendant-vinyl reactivity. **Macromolecules**, Washington, v. 30, n. 15, p. 4268-4271, 1997.
- 27 TSAREVSKY, N. V.; MATYJASZEWSKI, K. Reversible redox cleavage/coupling of polystyrene with disulfide or thiol groups prepared by atom transfer radical polymerization. **Macromolecules**, Washington, v. 35, n. 24, p. 9009-9014, 2002.
- 28 OH, J. K. TANG, C.; GAO, H.; TSAREVSKY, N. V.; MATYJASZEWSKI, K. Inverse miniemulsion ATRP: a new method for synthesis and functionalization of well-defined water-soluble/cross-linked polymeric particles. **Journal of the American Chemical Society**, v. 128, n. 16, p. 5578-5584, 2006.
- 29 BEERS, K. L.; GAYNOR, S. G.; MATYJASZEWSKI, K.; SHEIKO, S. S.; MOLLER, M. The synthesis of densely grafted copolymers by atom transfer radical polymerization. **Macromolecules**, Washington, v. 31, n. 26, p. 9413-9415, 1998.
- 30 ODIAN, G. **Principles of polymerization**. 4.ed. Hoboken: John Wiley, 2004.
- 31 JONES, R. A. L. *et al.* **Soft condensed matter**. Oxford University Press, 2002.
- 32 HEIDENREICH, A. J.; PUSKAS, J.; ALB, A. M.; REED, W. "Online monitoring of the raft polymerization of styrene mediated by vinybenzyl dithiobenzoate." **Abstracts of papers of the american chemical society**. vol. 237. 1155, 2009.
- 33 MENDONÇA, P. V.; OLIVEIRA, A. S.; RIBEIRO, J. P., CASTILHO, A.; SERRA, A. C., COELHO, J. F. Pushing the limits of robust and eco-friendly ATRP processes: untreated water as the solvent. **Polymer Chemistry**, Cambridge, v. 10, n. 8, p. 938-944, 2019.
- 34 GRAFF, R. W.; WANG, X.; GAO, H. Exploring self-condensing vinyl polymerization of inimers in microemulsion to regulate the structures of hyperbranched polymers. **Macromolecules**, Washington, v. 48, n. 7, p. 2118-2126, 2015.
- 35 GODDARD, E. D.; TURRO, N. J.; KUO, P. L.; ANANTHAPADMANABHAN, K. P. Fluorescence probes for critical micelle concentration determination. **Langmuir**, Washington, v. 1, n. 3, p. 352-355, 1985.
- 36 HARA, K.; WARE, W. R. Influence of solvent perturbation on the radiative transition probability from the 1B_{1u} state of pyrene. **Chemical Physics**, Amsterdam, v. 51, n. 1-2, p. 61-68, 1980.

37. KARPOVICH, D. S.; BLANCHARD, G. J. Relating the polarity-dependent fluorescence response of pyrene to vibronic coupling. Achieving a fundamental understanding of the py polarity scale. **The Journal of physical chemistry**, Washington, v. 99, n. 12, p. 3951-3958, 1995.

6 Curriculum vitae

Name:

Patricia Borim

Email address:

borim.patricia@gmail.com

Personal Data:

Born: January 11, 1989 - São Carlos/SP – Brazil.

Citizen of Brazil

Description / Practice areas:

Patricia Borim graduated in Chemistry from the State University of São Paulo (UNESP), Presidente Prudente and during graduation did an exchange internship at the University of Santiago of Compostela, Spain. She did her Master's degree in Inorganic Chemistry at the State University of São Paulo (UNESP), São José do Rio Preto- SP – Brazil. She started her doctorate in 2016 in the area of Analytical and Inorganic Chemistry and in 2018 moved to the area of Physics-Chemistry at the University of São Paulo (USP), São Carlos. She did a doctoral internship at the Carnegie Mellon University (CMU), Pittsburgh (USA) em 2019. She is currently a PhD student in the graduate program in Chemistry of the Institute of Chemistry of the Universidade de São Paulo (Brazil) under the supervision of Profa.Carla Cristina Schmitt Cavalheiro. Her area of research have focused on radical polymerization.

Current Position:

Industrial Chemist: 01/2020 to present

PhD student in Physics-Chemistry: 01/2018 – 12/2019
University of São Paulo (USP), São Carlos - SP - Brazil.

PhD student in Inorganic and Analytic Chemistry: 03/2016 – 12/2017
University of São Paulo (USP), São Carlos - SP - Brazil.

Visiting Researcher in Matyjaszewski's Material Science Lab: 11/2018 - 04/2019
Carnegie Mellon University (CMU) - Pittsburgh - PA - USA.

Website: <https://www.cmu.edu/maty/members/Patricia.html>

Education and Training:

Masters in Inorganic Chemistry 02/2014 - 02/2016

State University of São Paulo(UNESP), São José do Rio Preto- SP – Brazil.

Experience:

Graduate in Chemistry, Fellowship of Brazil 09/2010 - 02/2011

University of Santiago of Compostela, Spain

Graduate in Chemistry 02/2008 - 08/2010 *and* 03/2011- 01/2014

State University of São Paulo, Presidente Prudente - SP – Brazil.

Publications:

- <https://doi.org/10.1016/j.ica.2016.10.044>
- <https://doi.org/10.1007/s10965-017-1354-9>
- <https://doi.org/10.1007/s10562-017-2003-y>
- <https://doi.org/10.21577/0103-5053.20160314>
- <https://doi.org/10.1016/j.inoche.2019.107749>
- DOI:10.5935/0104-8899.20140036

Additional Information:

[Technical Skills] Material Science directed at development & characterization of new materials by Reversible Deactivation Radical Polymerization techniques. Synthesis and characterization of new molecules. Spectrometric Scientific Instrumentation (FTIR, NMR, UV-Vis), GC-MS instrument. Microsoft Office, ChemDraw, Mestre Nova, Top Spin Software.

- Progress:

- Spanish Course at University of Santiago de Compostela, Spain.

-Basic operation and maintenance of the HPLC system at UNESP – Presidente Prudente, SP, Brazil.

- POTENCIOSTATOPGSTAT204 With Impedance Module. Metrohm Pensalab.

Analytical Instrumentation, METROHM, Brazil.

➤ Idioms:

- Portuguese, English and Spanish.